Astroparticle Physics

Lectures:

05.02.2019 1. Historical introduction, basic properties of cosmic rays
07.02.2019 2. Hadronic interactions and accelerator data
19.02.2019 3. Cascade equations
21.02.2019 4. Electromagnetic cascades
26.02.2019 5. Extensive air showers
28.02.2019 6. Detectors for extensive air showers
09.04.2019 7. High energy cosmic rays and the knee in the energy spectrum of cosmic rays
16.04.2019 8. Radio detection of extensive air showers
23.04.2019 9. Acceleration, astrophysical accelerators and beam dumps
07.05.2019 10. Extragalactic propagation of cosmic rays
14.05.2019 11. Ultra high energy cosmic rays
21.05.2019 12. Astrophysical gamma rays and neutrinos
28.05.2019 13. Neutrino astronomy
04.06.2019 14. Gamma-ray astronomy

http://particle.astro.ru.nl/goto.html?astropart1819

lecture 8
Radio detection of extensive air showers

Gaisser chapter 16

First radio detection of air showers 1965

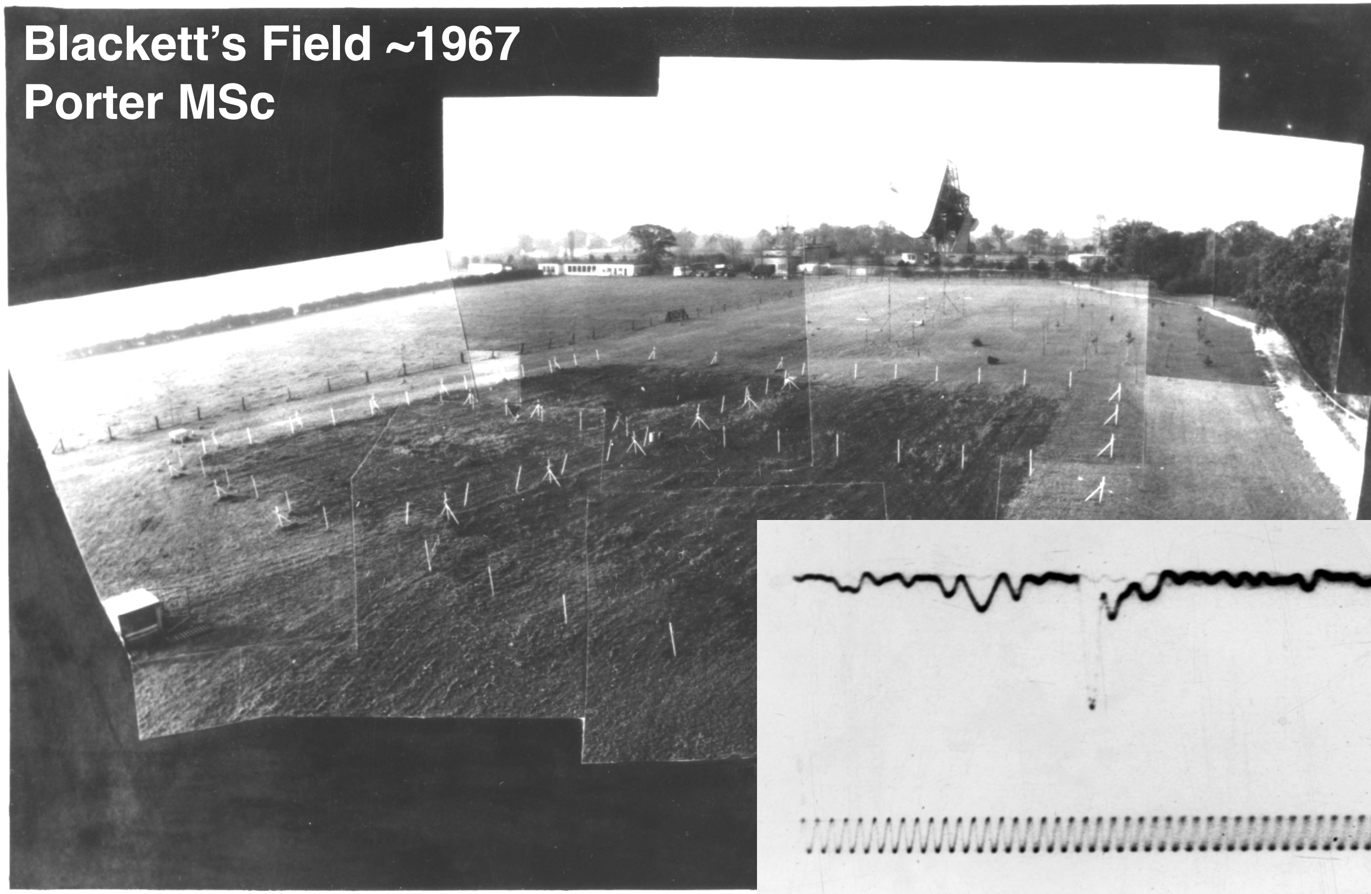

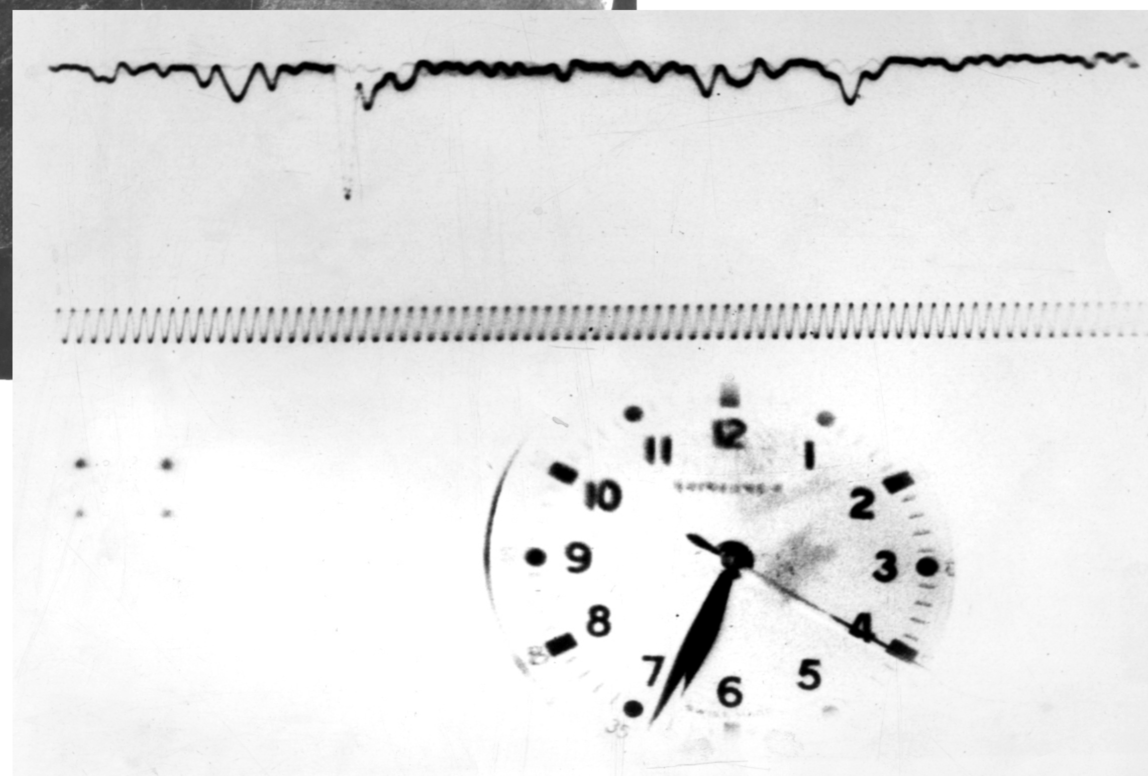

Jelley et al Nature 1965
R. A. Porter MSc Thesis 1967

Haverah Park (Leeds) Allan 1971

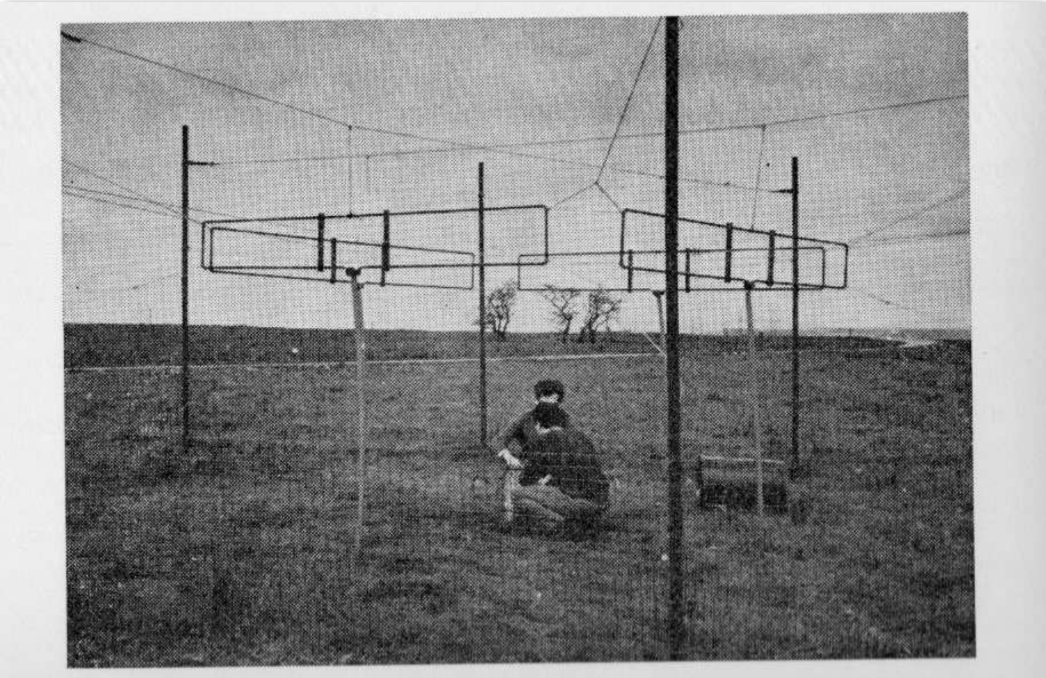

Recent receiving antennas (44 MHz) forming part of the Haverah Park Extensive Air Shower Array.

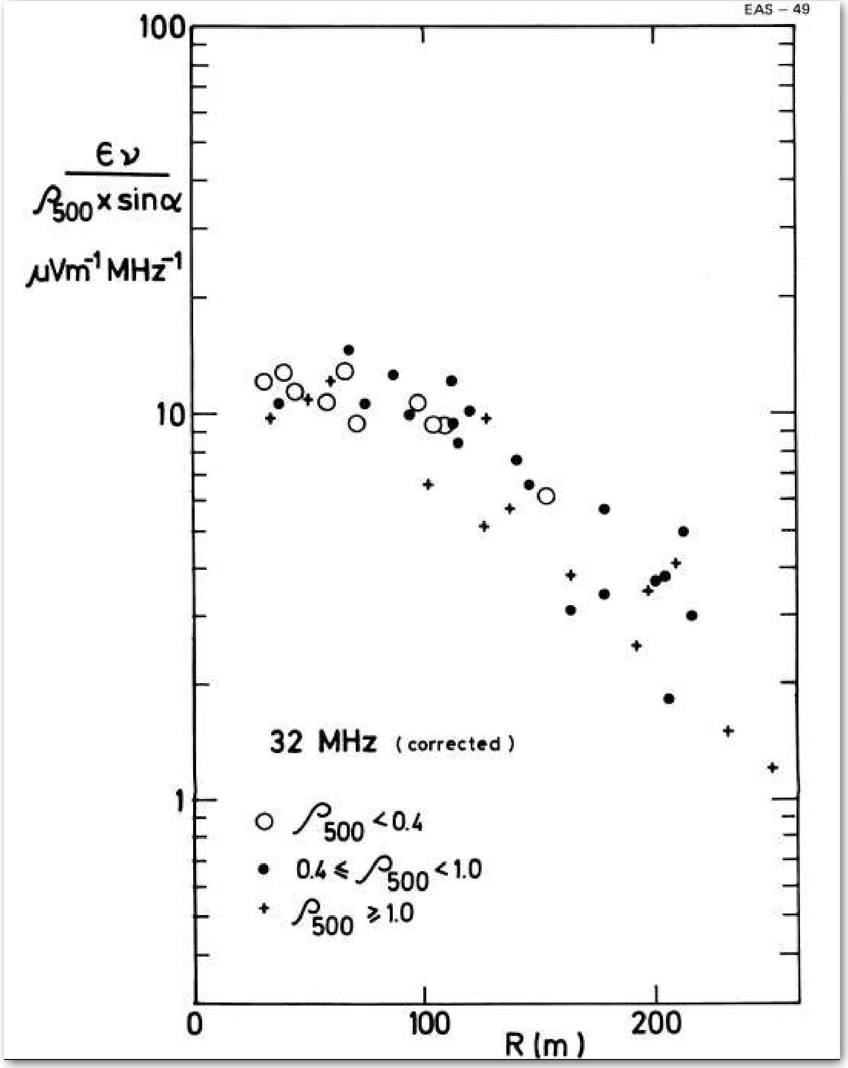

$$\varepsilon_\nu = 2\left(\frac{E_p}{10^{17}}\right)\left(\frac{\sin\alpha\cos\theta}{\sin 45\cos 30}\right)\exp\left(\frac{-r}{r_0}\right)\left(\frac{\nu}{50}\right)^{-1} \quad \mu\text{V/m/MHz}$$

$r_0 = 110$ m at ν=55 MHz. α=angle to B, θ=Zenith angle

H.R. Allan, Prog. Element. Part. Cosmic Ray Phys (1971) 169

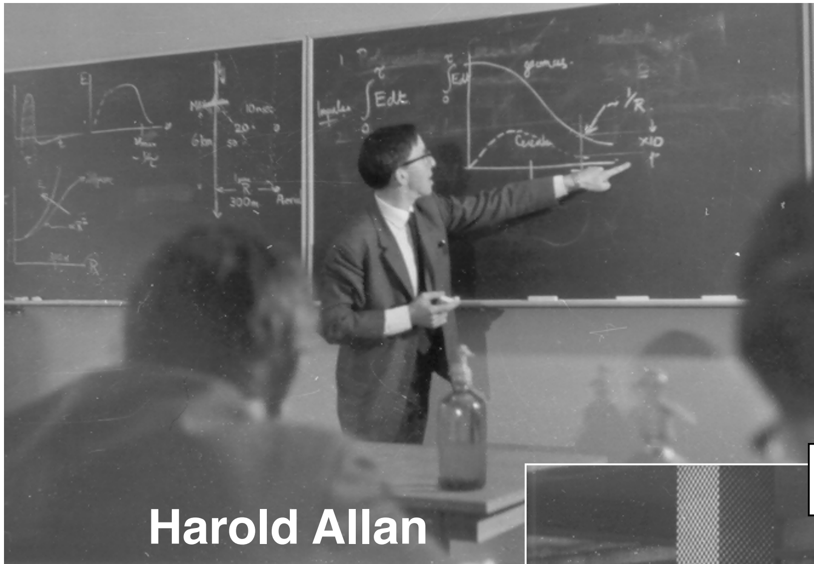

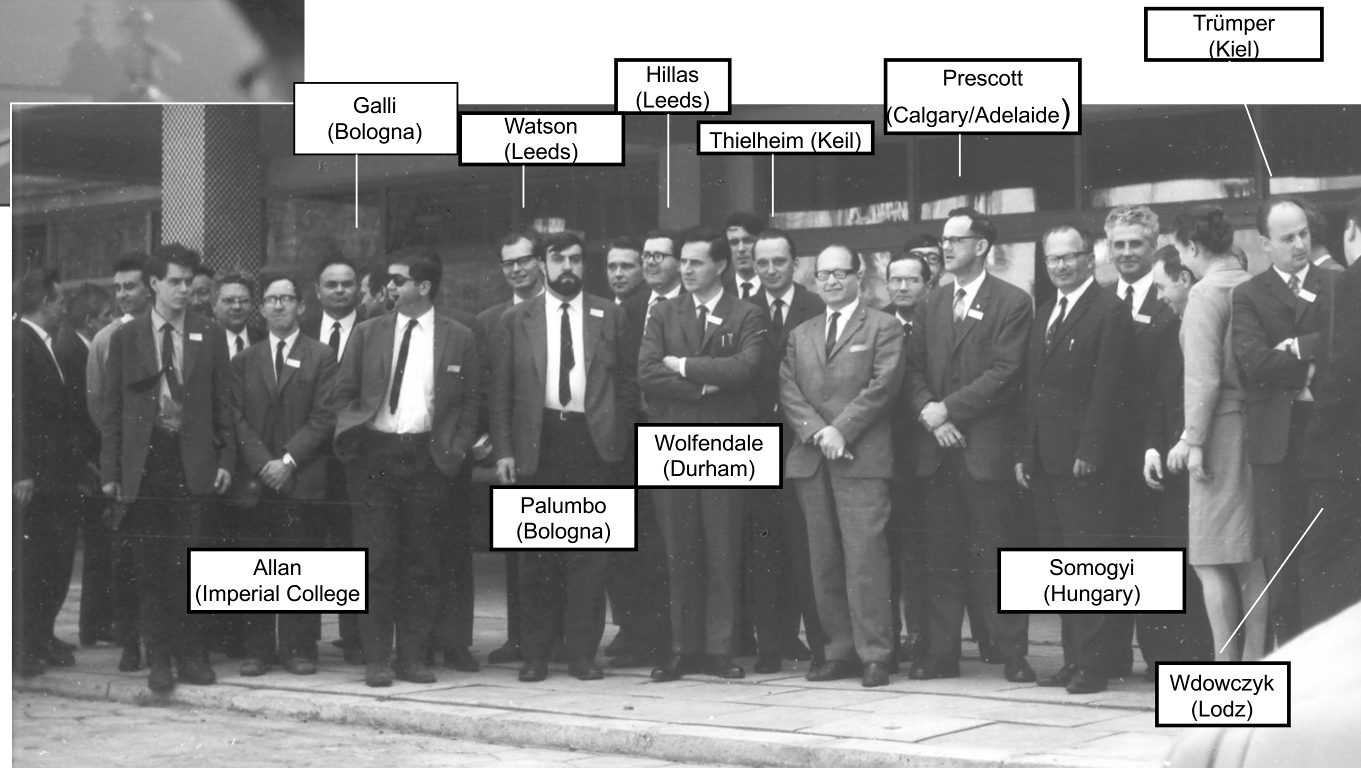

First European Symposium on High Energy Interactions and Extensive Air Shower: Lodz, Poland April 1968

33RD INTERNATIONAL COSMIC RAY CONFERENCE, RIO DE JANEIRO 2013
THE ASTROPARTICLE PHYSICS CONFERENCE

ICRC 2013

The renaissance of radio detection of cosmic rays

TIM HUEGE[1]

2018: beyond capabilities of standard installations

2016: radio technique mature: properties of cosmic rays

2014: understanding the emission processes

2005: understanding the signal

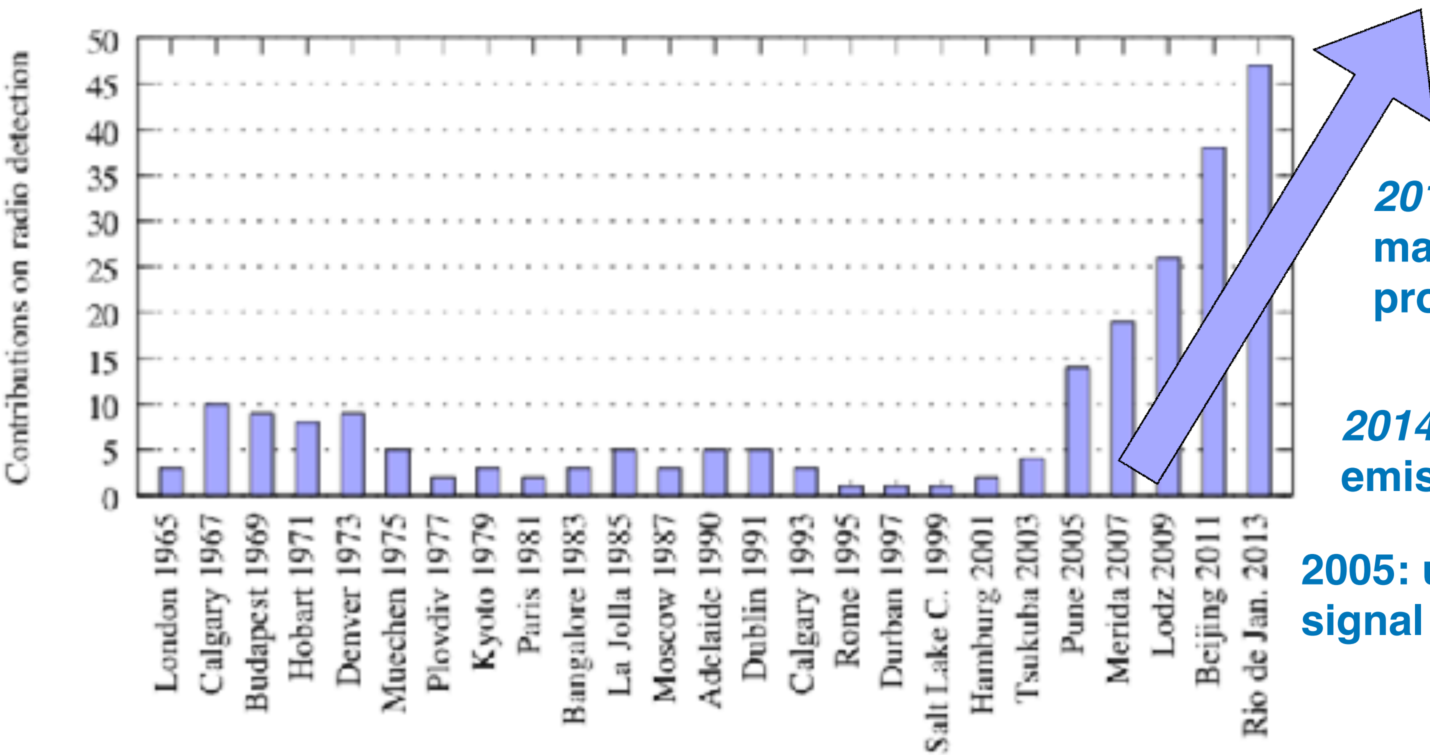

Figure 1: Number of contributions related to radio detection of cosmic rays or neutrinos to the ICRCs since 1965. The field has grown very impressively since the modern activities started around 2003. Data up to 2007 were taken from [11].

Radio Detectors

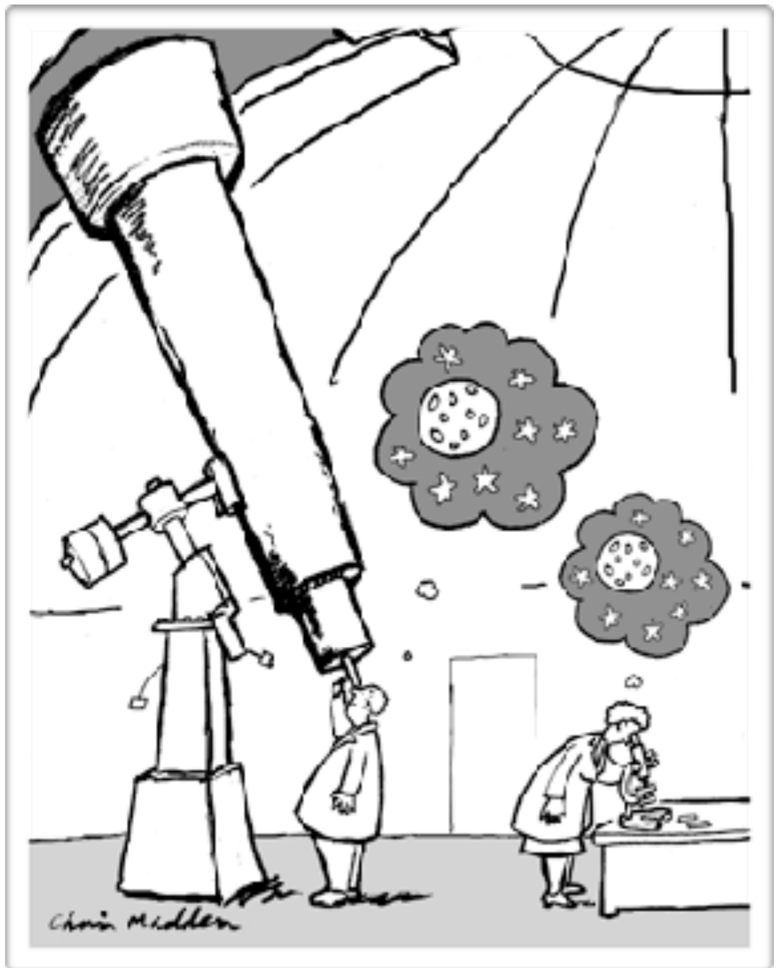

Radio detection of extensive air showers around the world

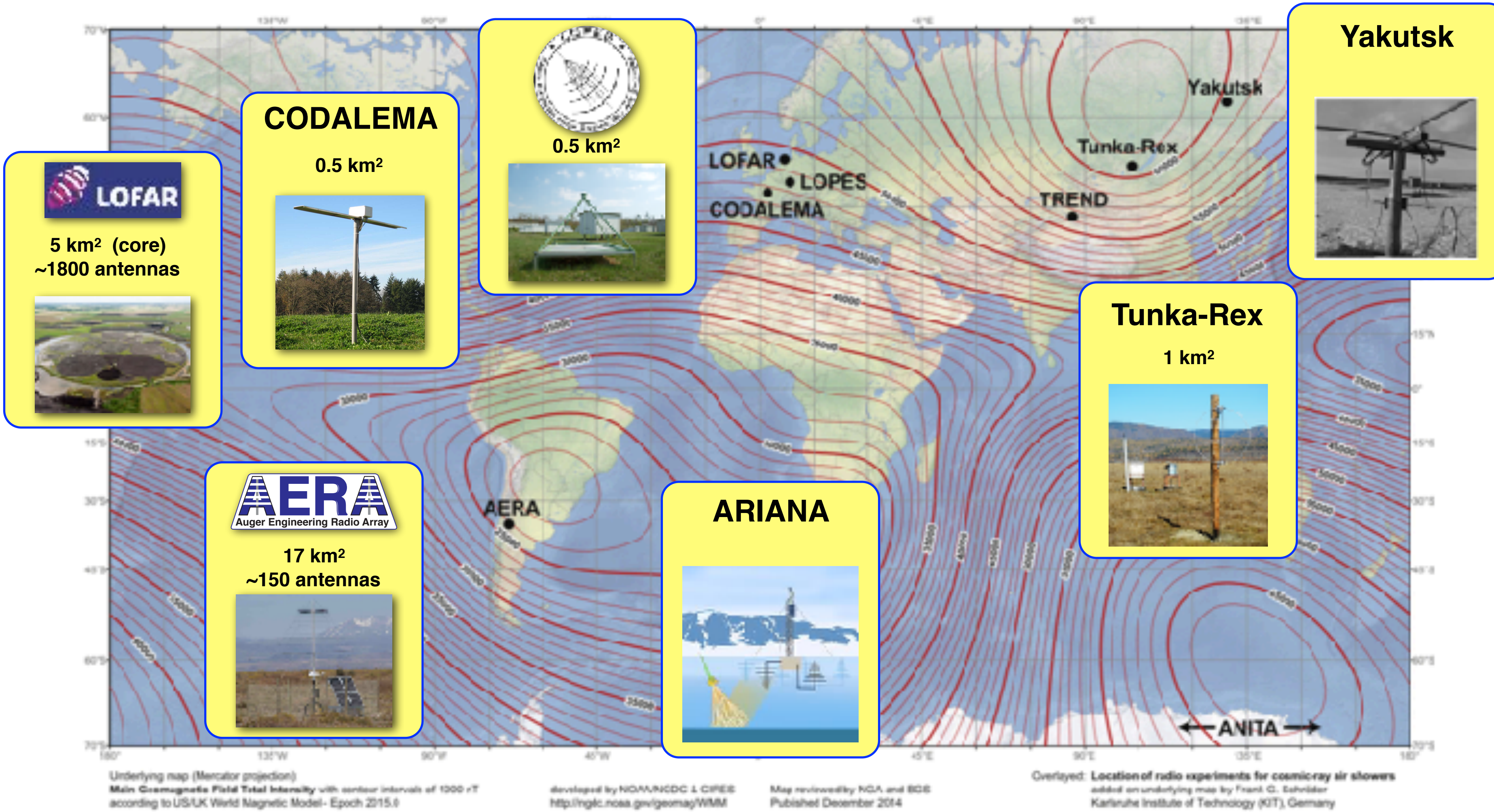

Fig. 21. Map of the total geomagnetic field strengths (world magnetic model [207]) and the location of various radio experiments detecting cosmic-ray air showers.

F.G. Schröder, Prog. Part. Nucl. Phys. 92 (17) 1

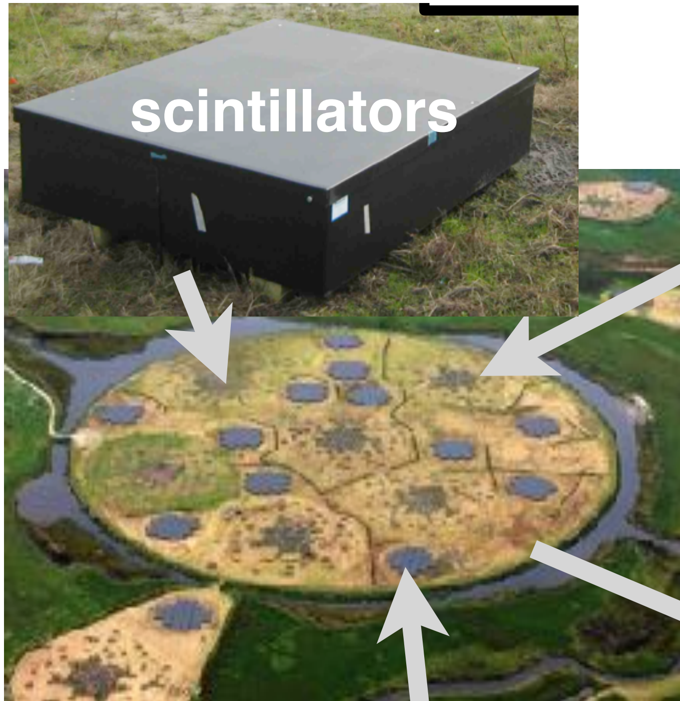

LOFAR

core
23 stations ~5 km²

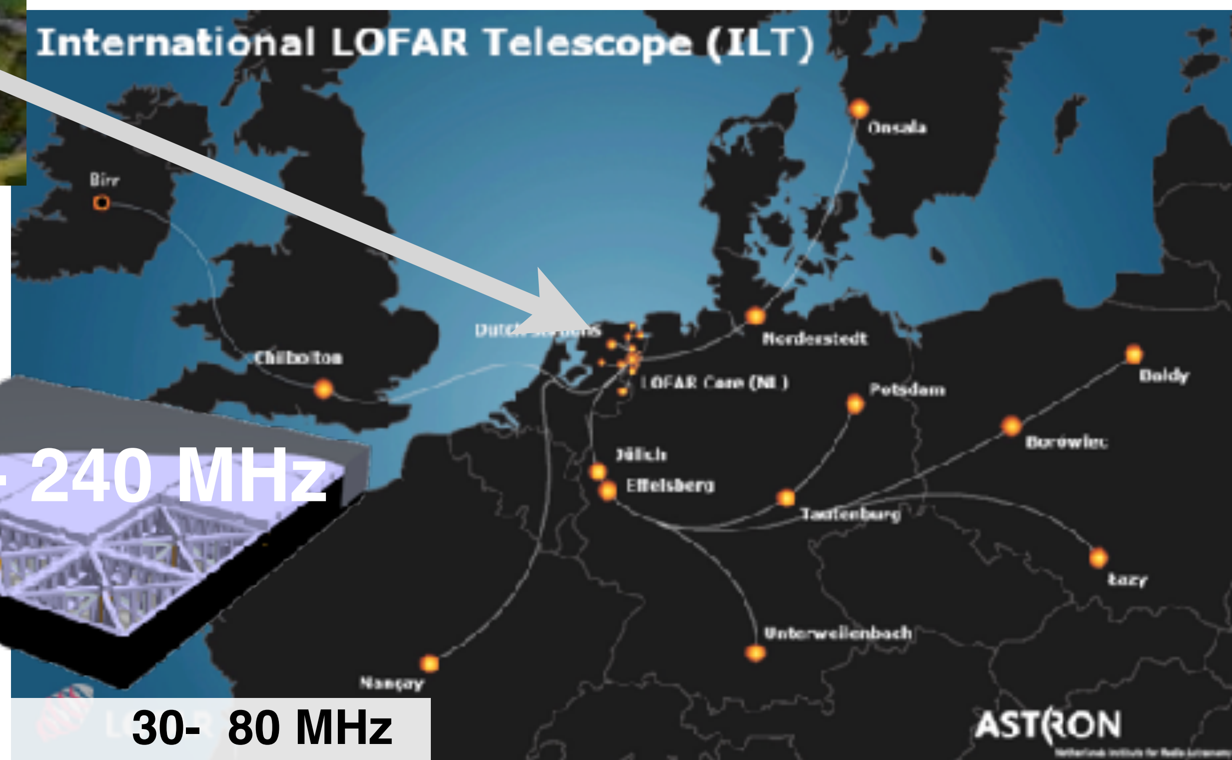

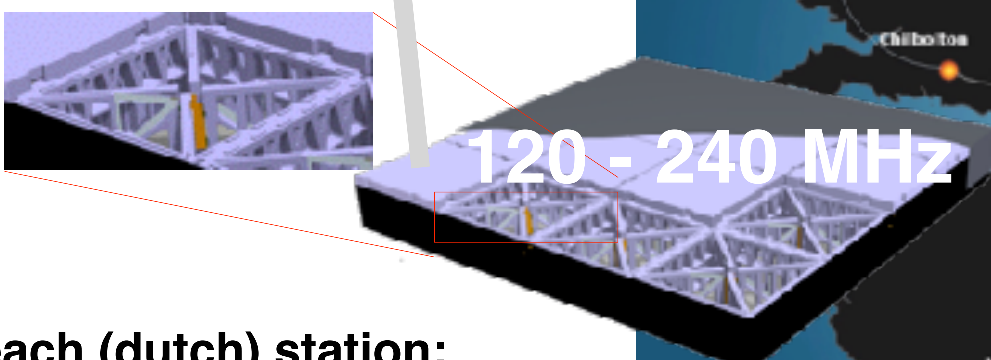

each (dutch) station:
96 low-band antennas 30- 80 MHz
high-band antennas (2x24 tiles) 120-240 MHz

M. van Haarlem et al., A&A 556 (2013) A2

S. Thoudam et al., Nucl. Instr. Meth. A 767 (2014) 339

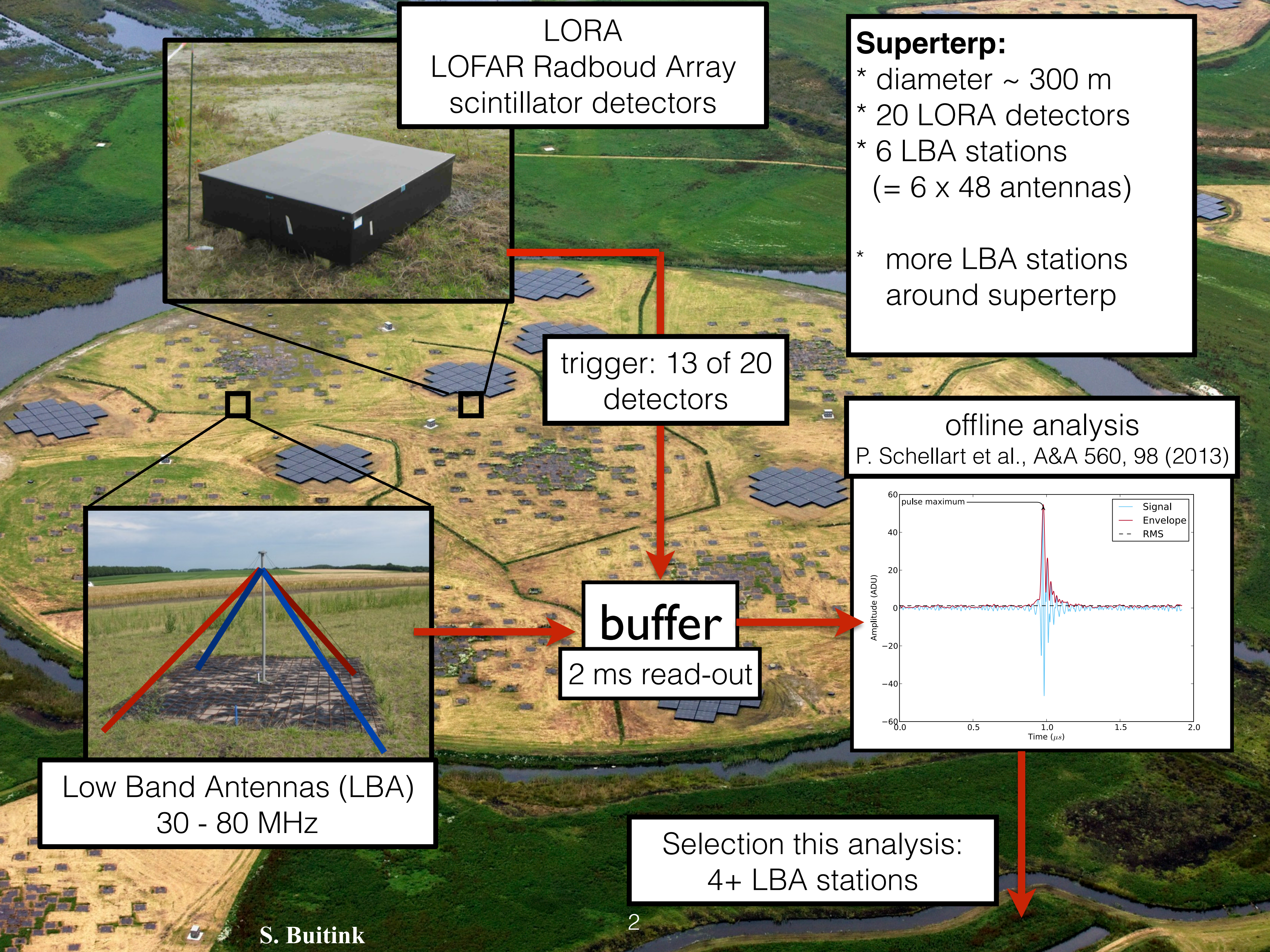
LORA
LOFAR Radboud Array
scintillator detectors
Superterp:
* diameter ~ 300 m
* 20 LORA detectors
* 6 LBA stations
(= 6 x 48 antennas)
* more LBA stations
around superterp
trigger: 13 of 20
detectors
offline analysis
P. Schellart et al., A&A 560, 98 (2013)
pulse maximum
Signal
Envelope
RMS
Amplitude (ADU)
Time (μs)
buffer
2 ms read-out
Low Band Antennas (LBA)
30 - 80 MHz
Selection this analysis:
4+ LBA stations
2
S. Buitink

PIERRE AUGER

AERA
Auger Engineering Radio Array

~150 antennas
~17 km^2
30-80 MHz

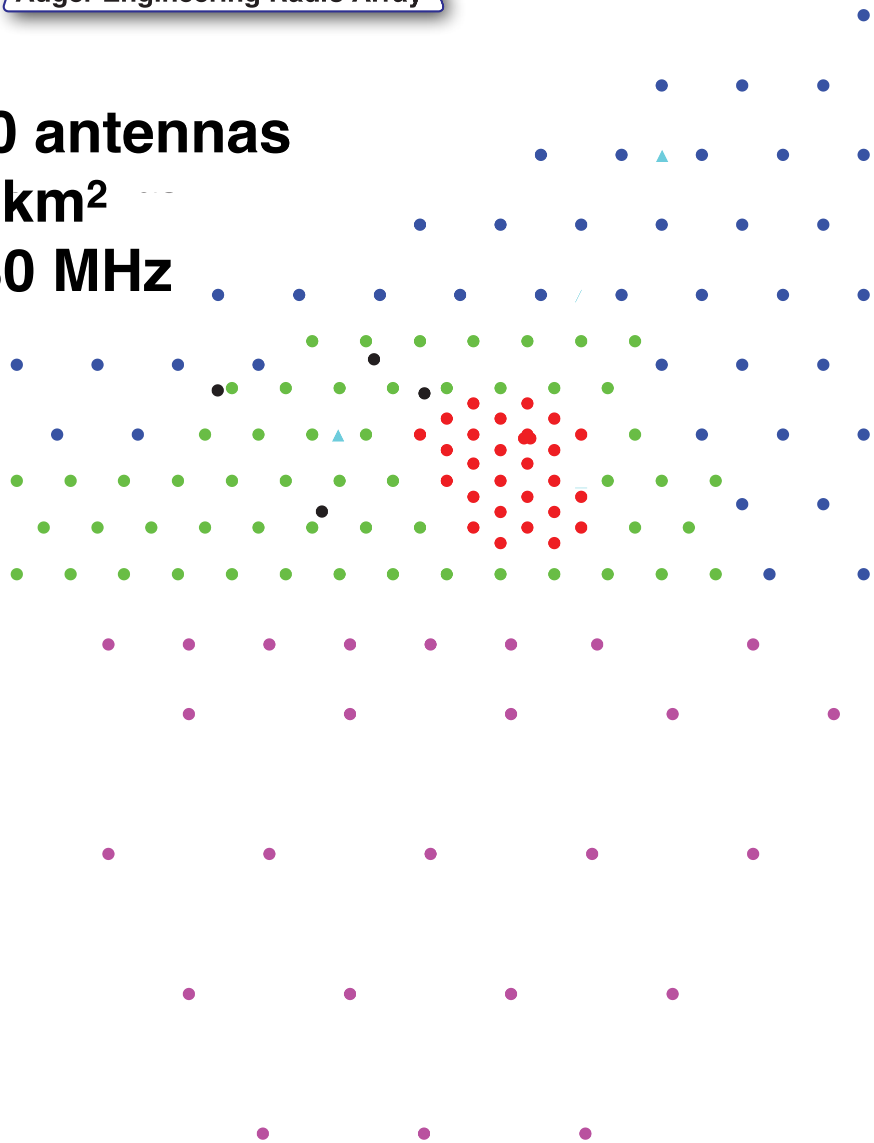

LOFAR core
23 stations ~5 km^2

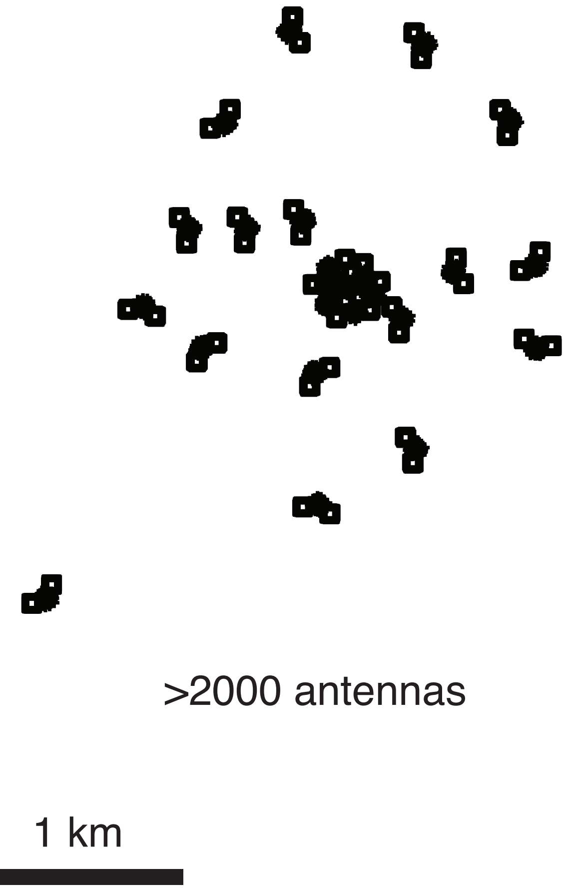

Auger Engineering Radio Array

~150 antennas
~17 km²
30-80 MHz

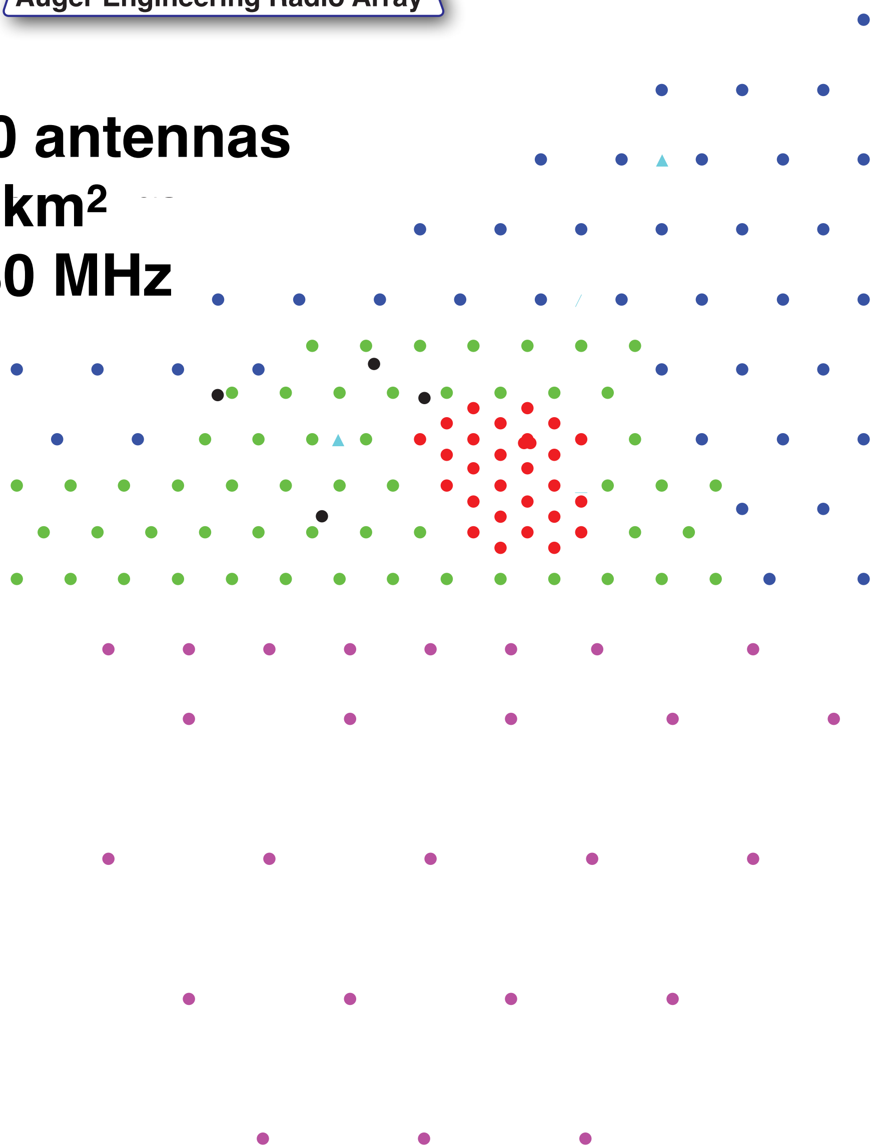

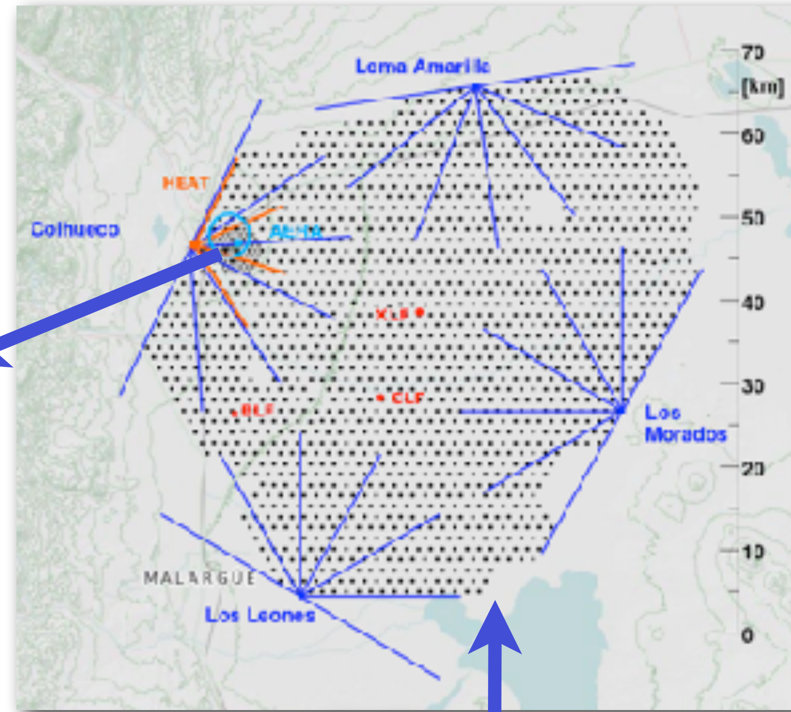

PIERRE AUGER

AERA
Auger Engineering Radio Array

~150 antennas
~17 km²
30-80 MHz

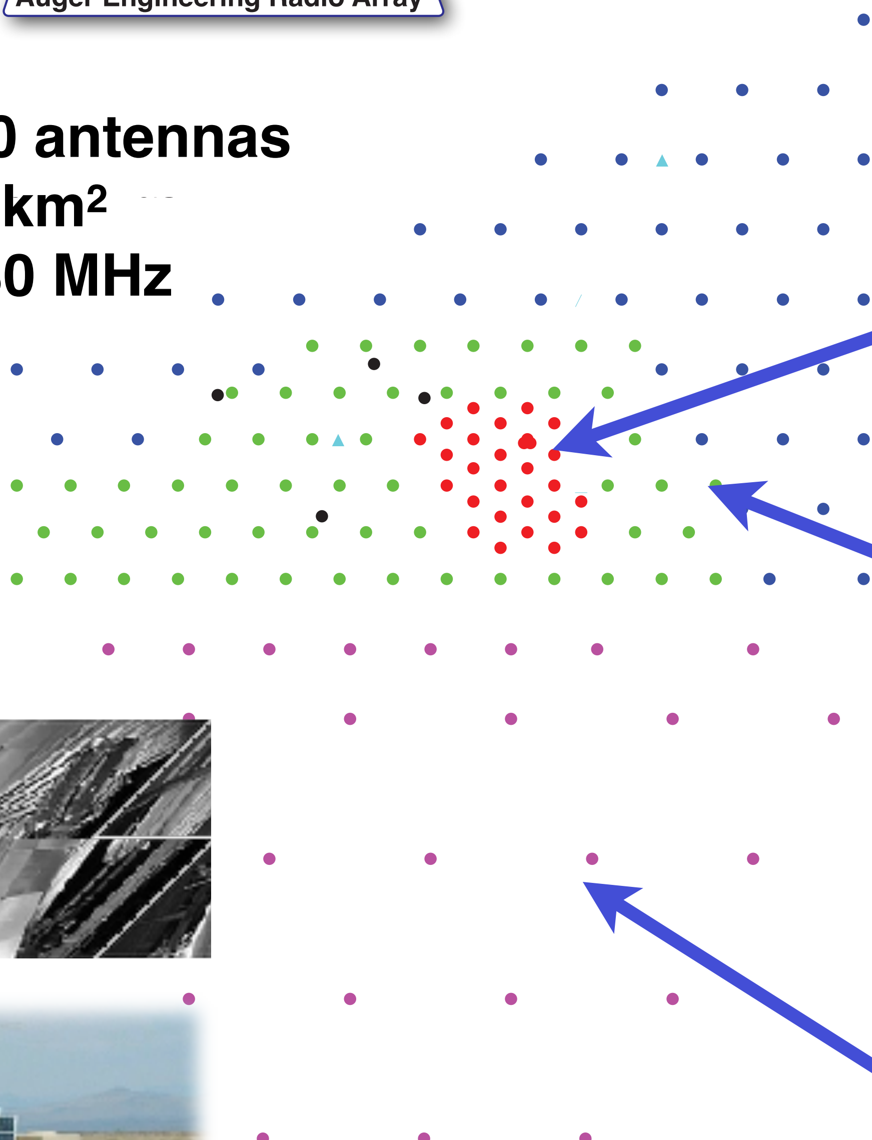

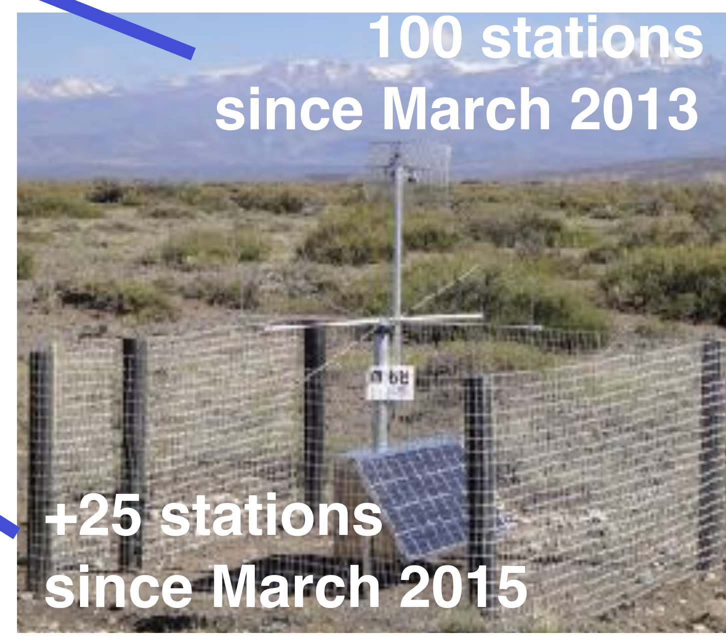

A measured air shower

angular difference particles - radio

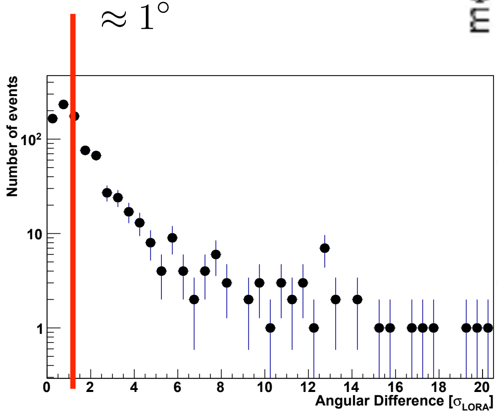

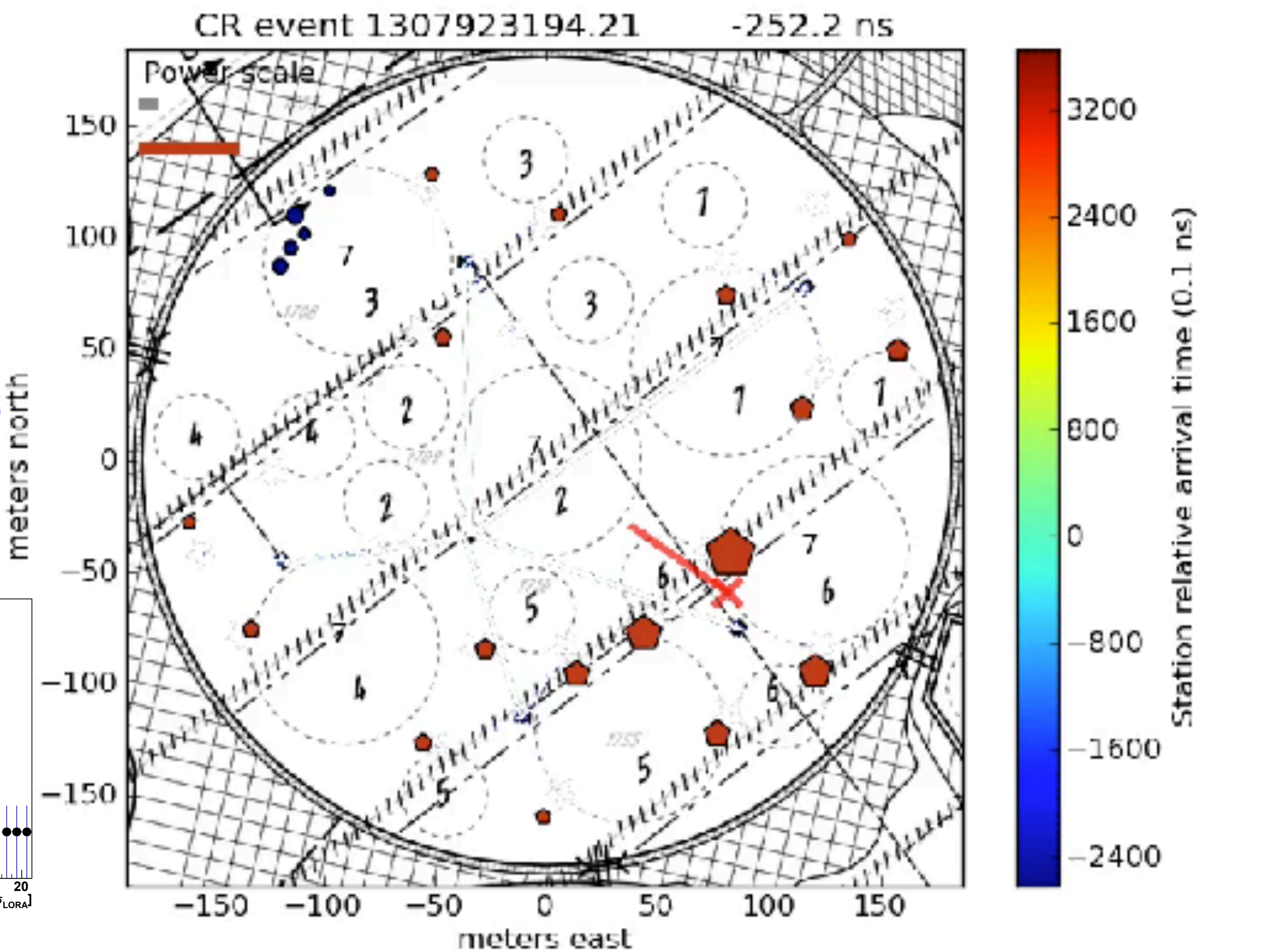

Circles: LOFAR antennas, Pentagons: LORA particle detectors, size denotes signal strength

LOFAR

LOFAR Signal Chain

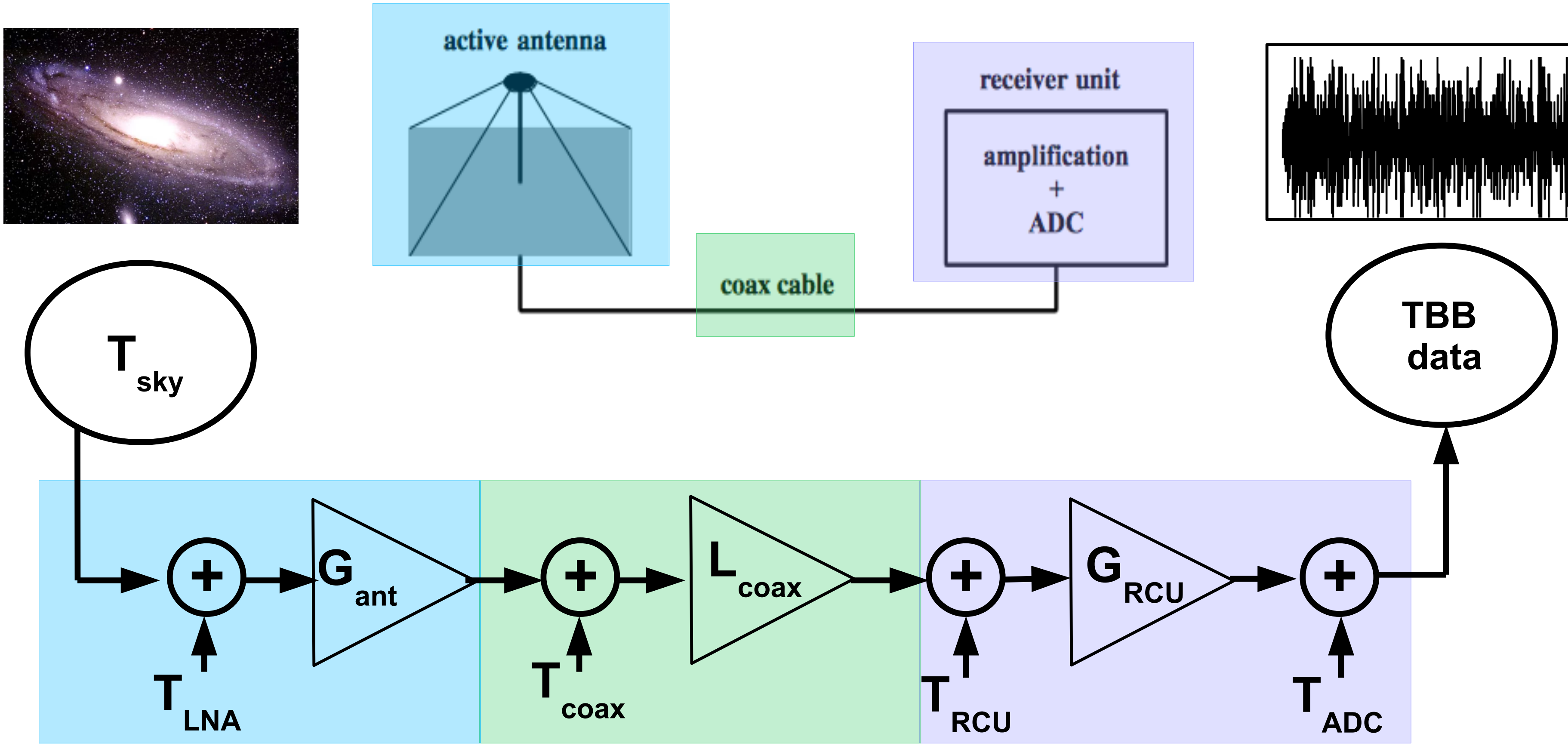

G_{ant} , L_{coax} , G_{RCU} → **Freq. Dependent losses and gains**

T_{LNA} , T_{coax} , T_{RCU} , T_{ADC} → **Constant noise values**

7

K. Mulrey, ARENA 2018

Calibration Results

LOFAR

$$\mathbf{C^2}(\nu) = \mathbf{A}(\nu)\mathbf{L}_{\rm coax}(\nu)\mathbf{G}_{\rm RCU}(\nu)\mathbf{S}$$

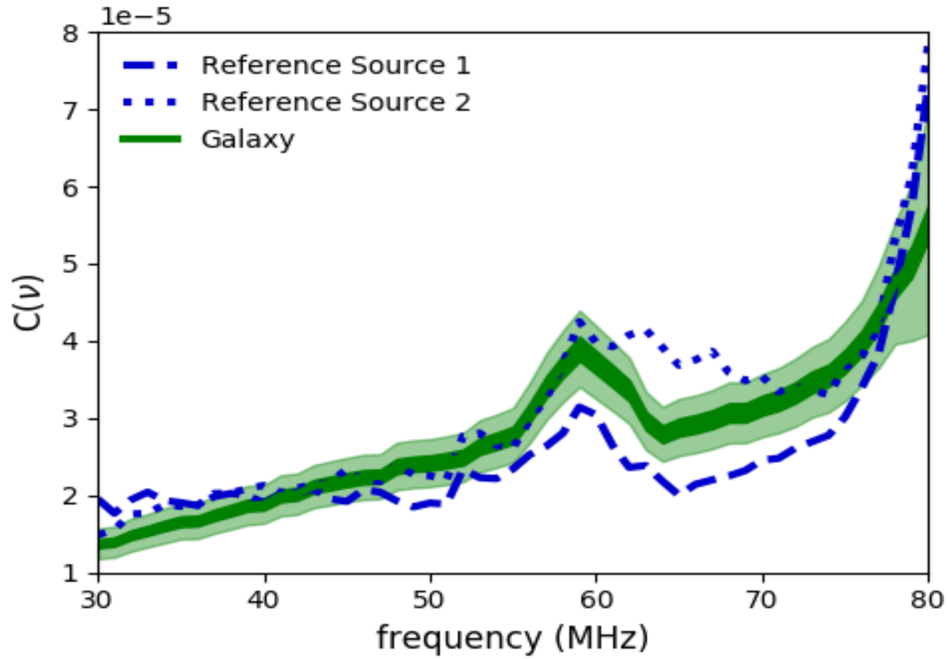

Uncertainty	Percentage
event-to-event fluctuation	4
galaxy model	12
electronic noise < 77 MHz	5-6
electronic noise > 77 MHz	10-20
total < 77 MHz	**14**

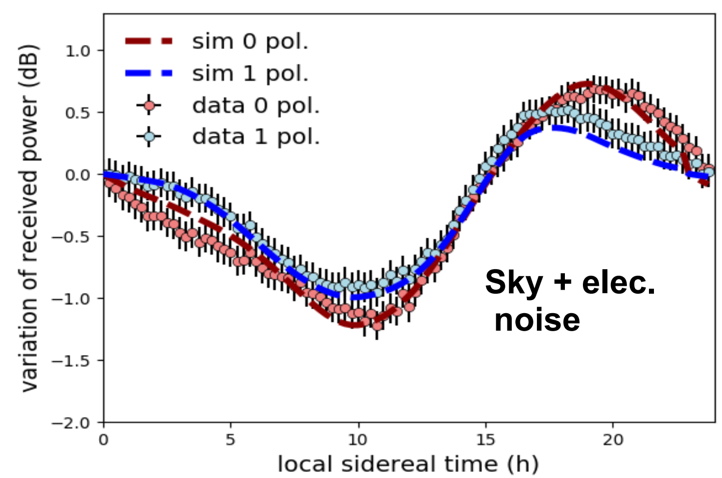

- Galaxy model now limits systematic uncertainties
- Uncertainties from electronic noise are found by comparing resulting calibration constants for different antennas

12

K. Mulrey, ARENA 2018

Timing calibration

Use beacon broadcasting at 4 different frequencies to measure relative time shifts

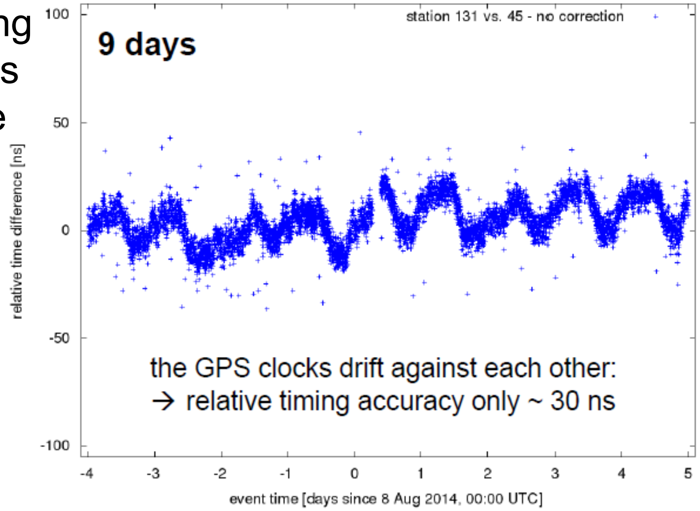

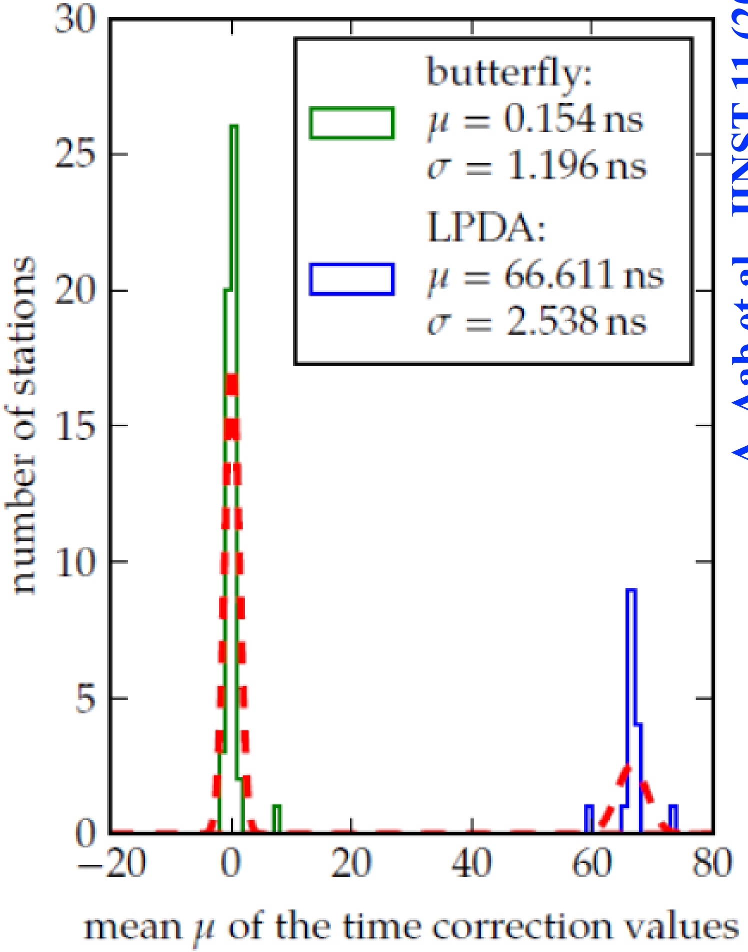

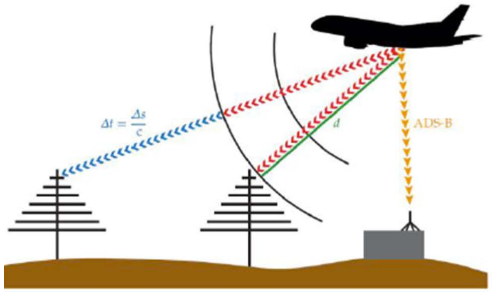

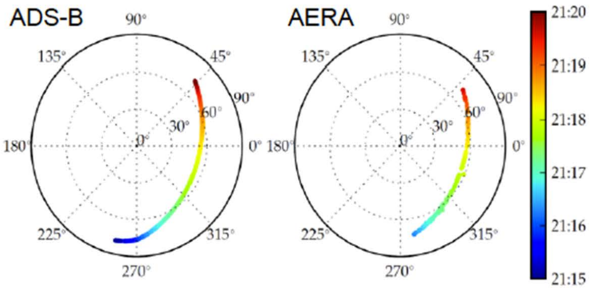

A. Aab et al., JINST 11 (2016) no.01, P01018

Radiation Processes

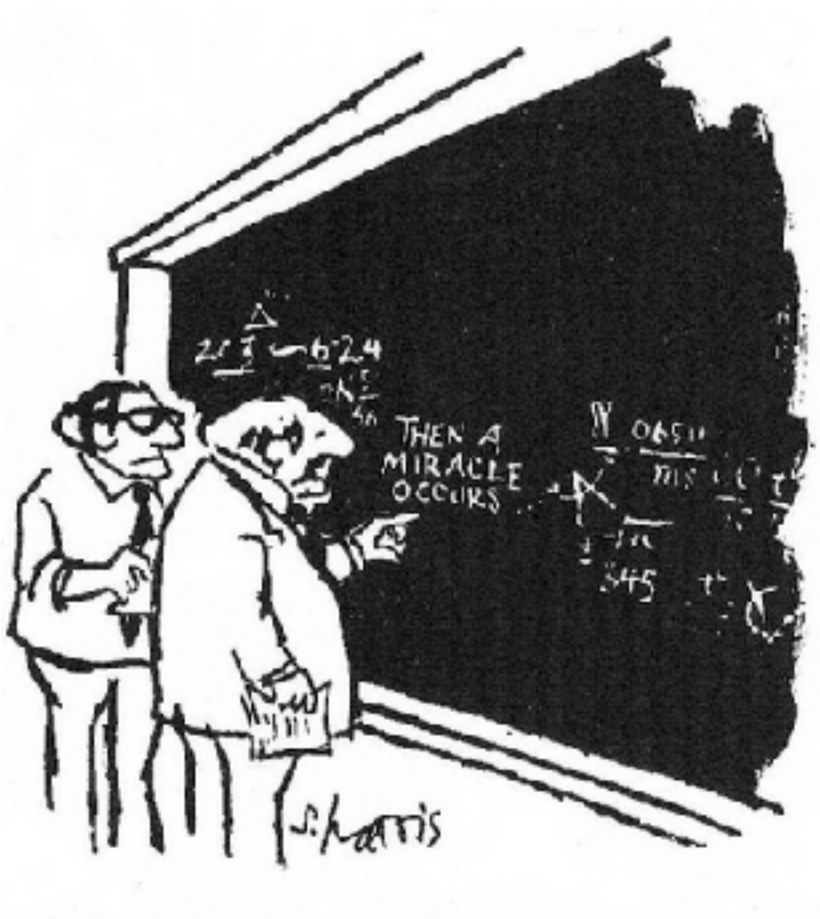

"I think you should be more explicit here in step two."

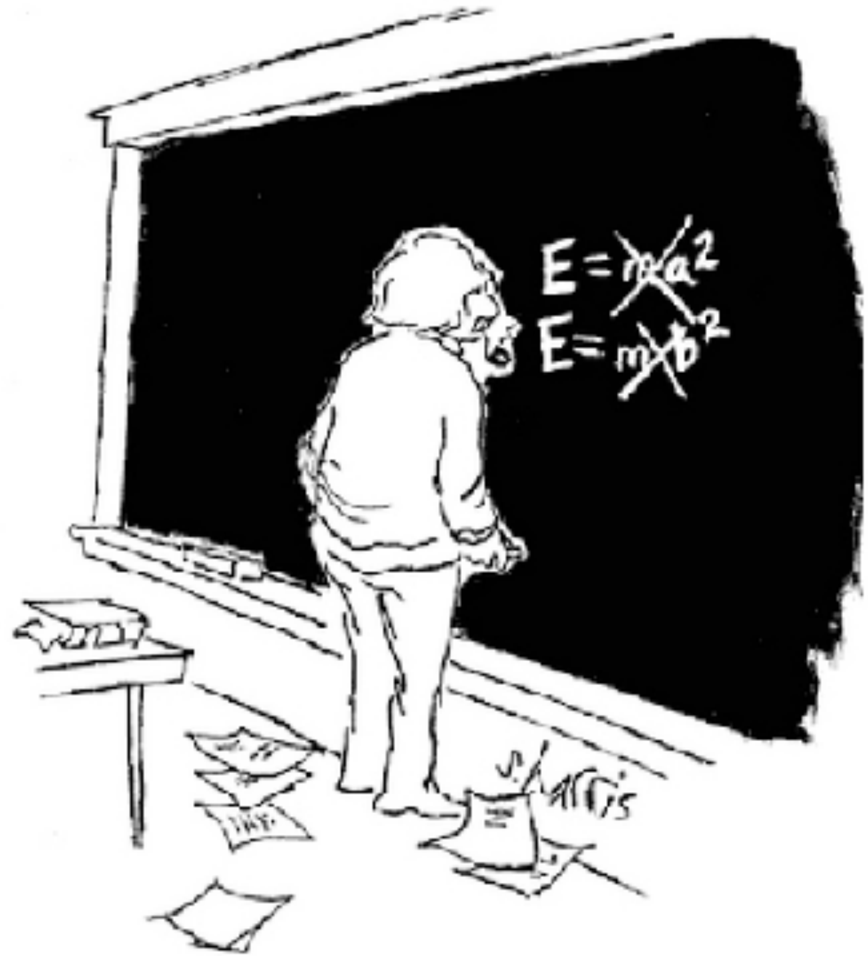

Radio Emission in Air Showers

Mainly: Charge separation in geomagnetic field

$$\vec{E} \propto \vec{v} \times \vec{B}$$

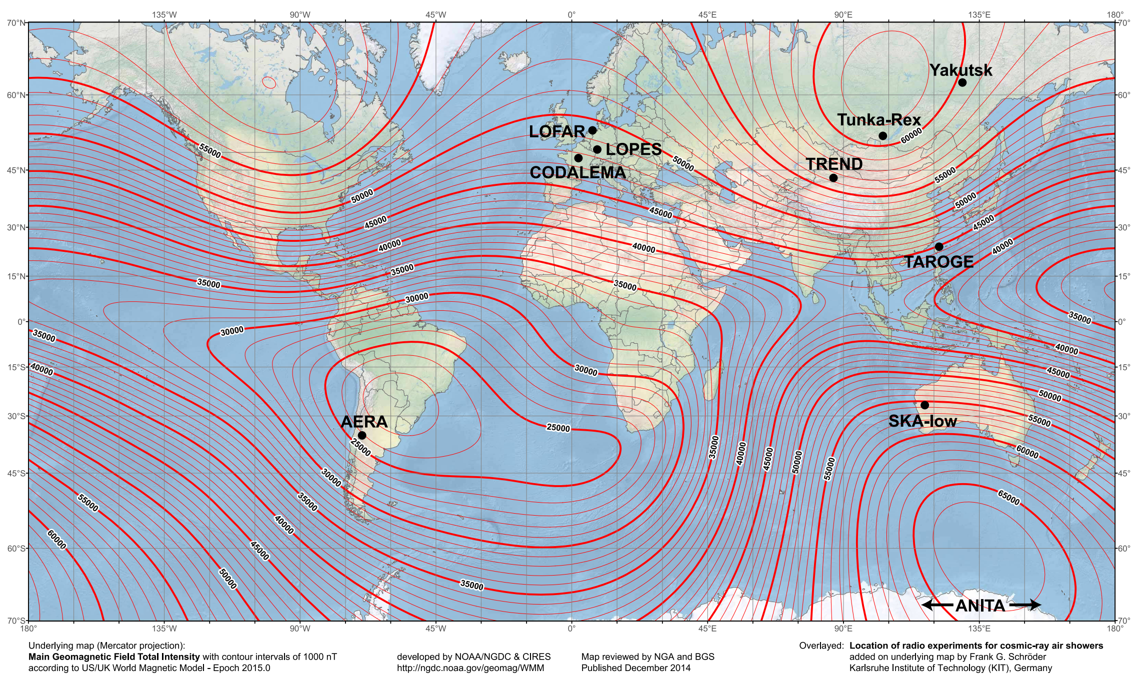

F. Schröder, Prog. Part. Nucl. Phys. 93 (2017) 1

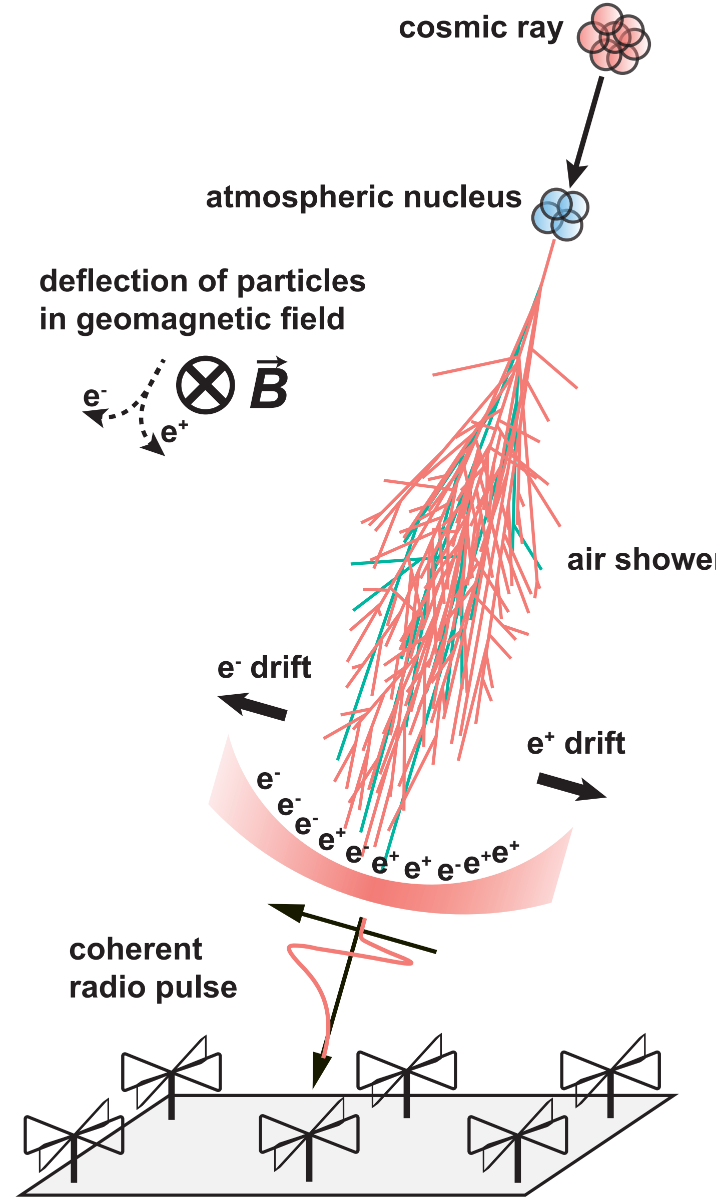

Arrival direction of showers with strong radio signals

north-south asymmetry
v x B effect

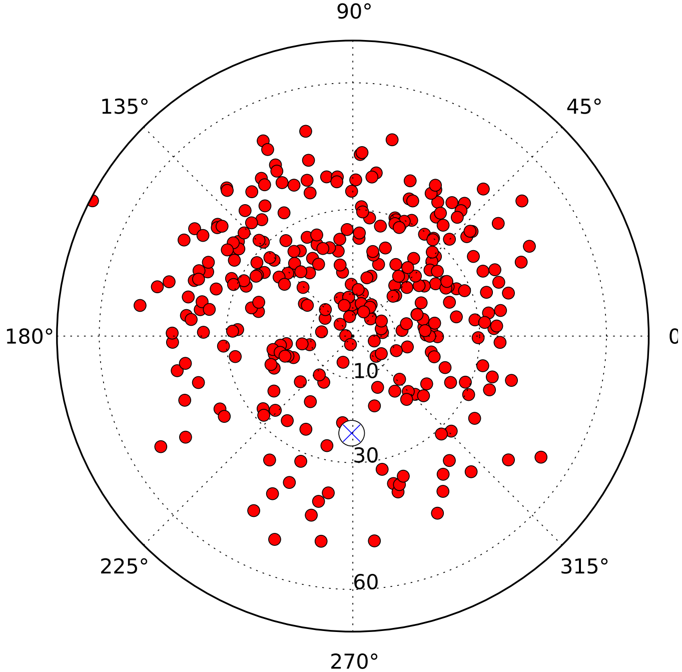

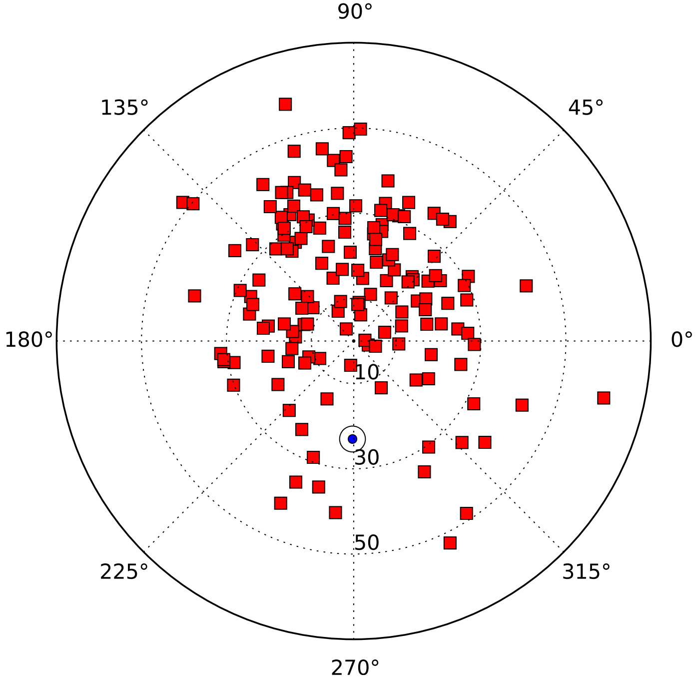

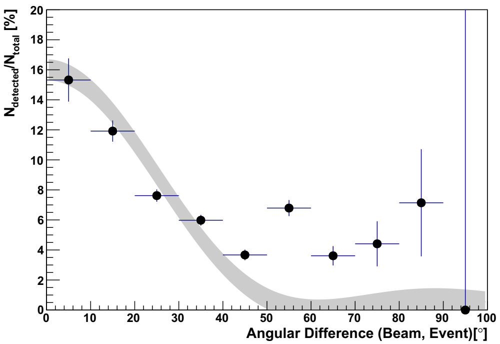

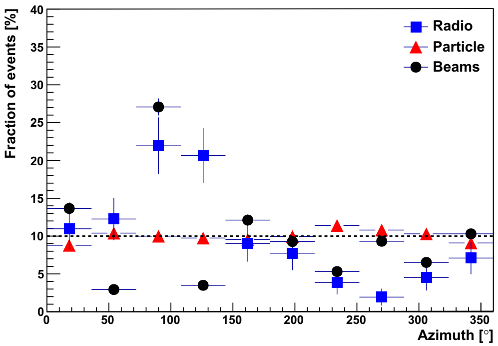

LOFAR

30 - 80 MHz

110 - 190 MHz

A. Nelles et al., Astroparticle Physics 65 (2015) 11

P. Schellart et al., A&A 560 (2013) A98

Arrival direction of showers with strong radio signals

north-south asymmetry
v x B effect

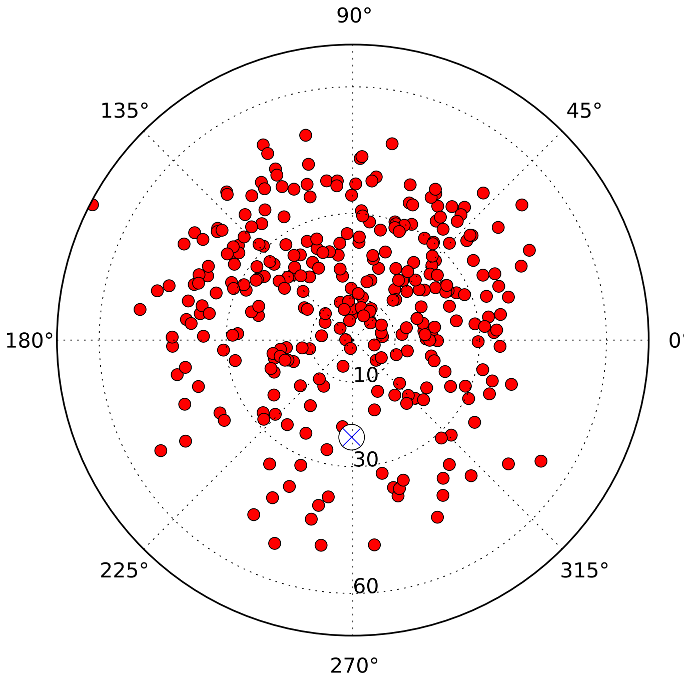

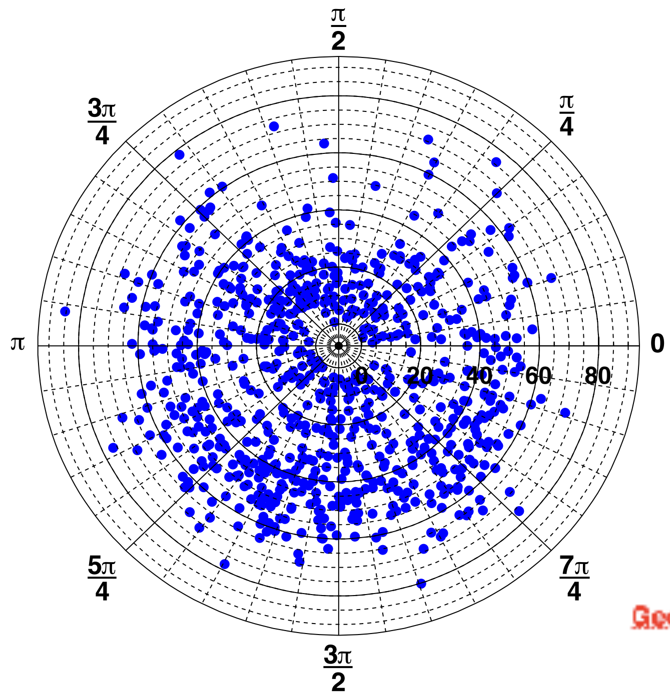

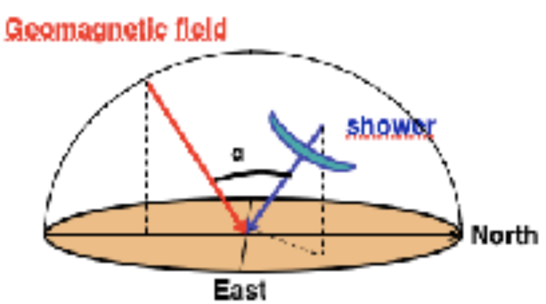

LOFAR

AERA Auger Engineering Radio Array

30 - 80 MHz

P. Schellart et al., A&A 560 (2013) A98

Geomagnetic effect

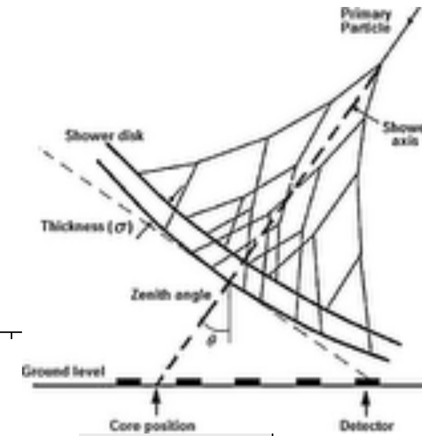

T. Huege / Physics Reports 620 (2016) 1–52

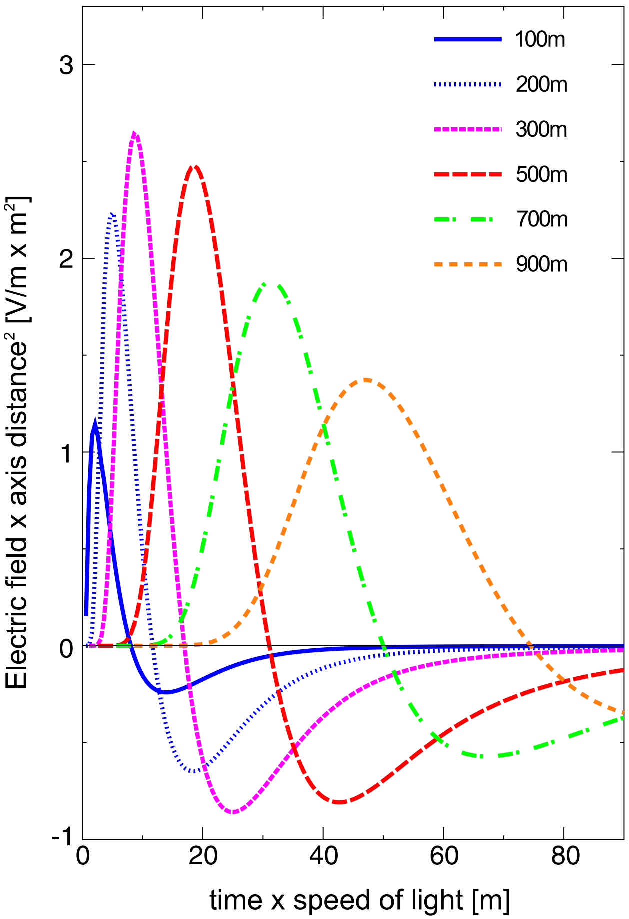

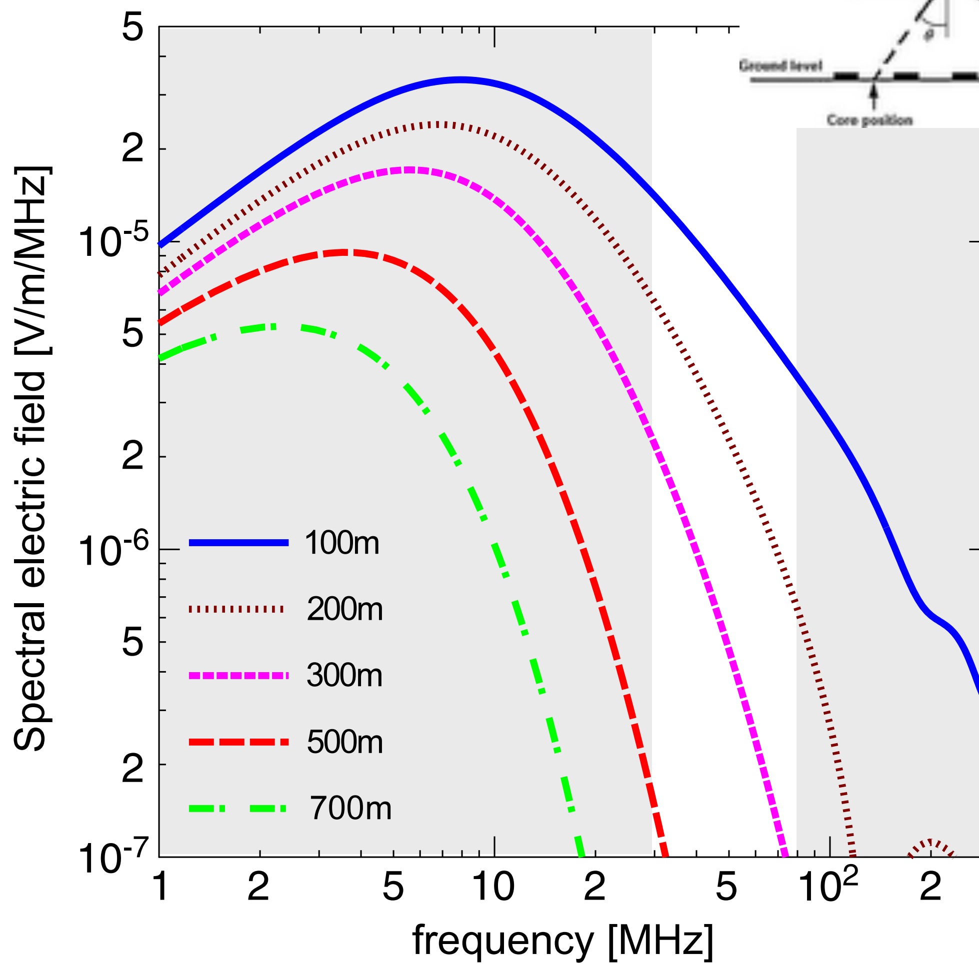

Fig. 4. Radio pulses (top) arising from the time-variation of the geomagnetically induced transverse currents in a 10^{17} eV air shower as observed at various observer distances from the shower axis and their corresponding frequency spectra (bottom). Refractive index effects are not included.
Source: Adapted from [18].

Radio Emission in Air Showers

- Mainly: Charge separation in geomagnetic field

  $\vec{E} \propto \vec{v} \times \vec{B}$

  Theory predicts additional mechanisms:
- excess of electrons in shower: charge excess
- superposition of emission due to Cherenkov effects in atmosphere

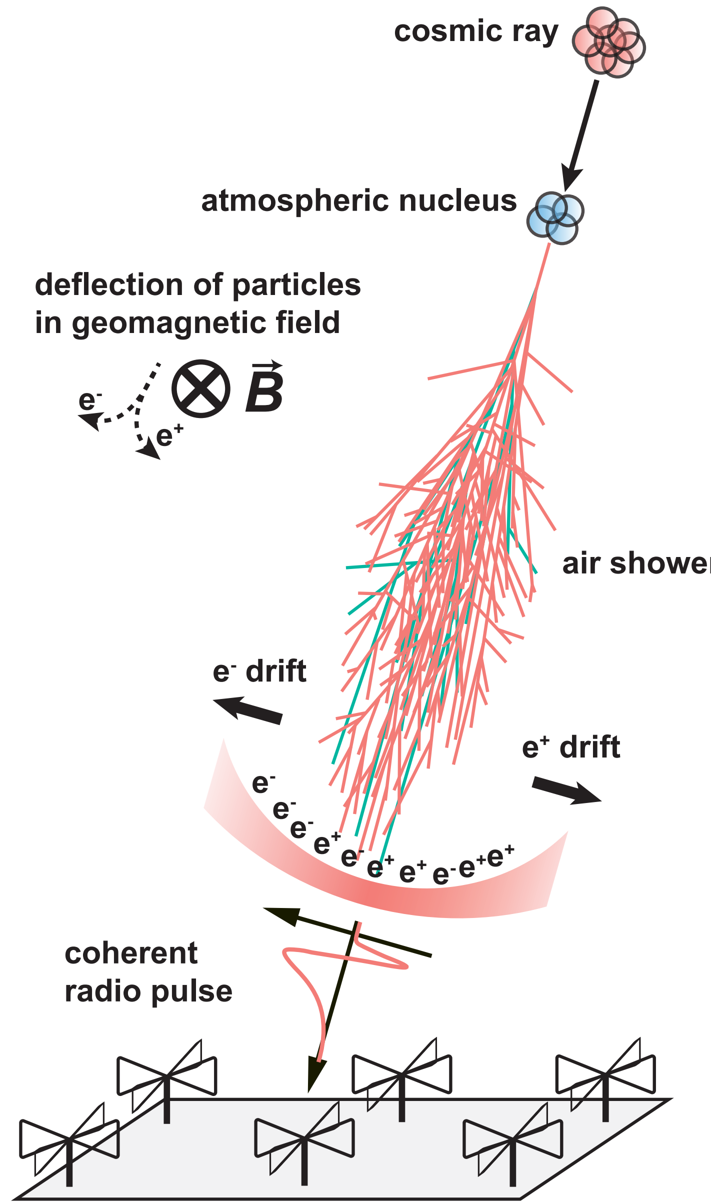

polarization of radio signal

geomagnetic

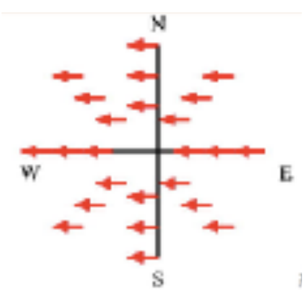

Askaryan

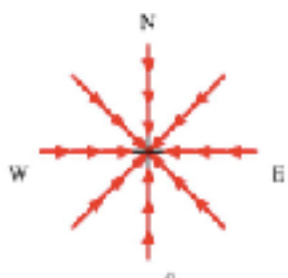

Polarization footprint
of an individual air shower

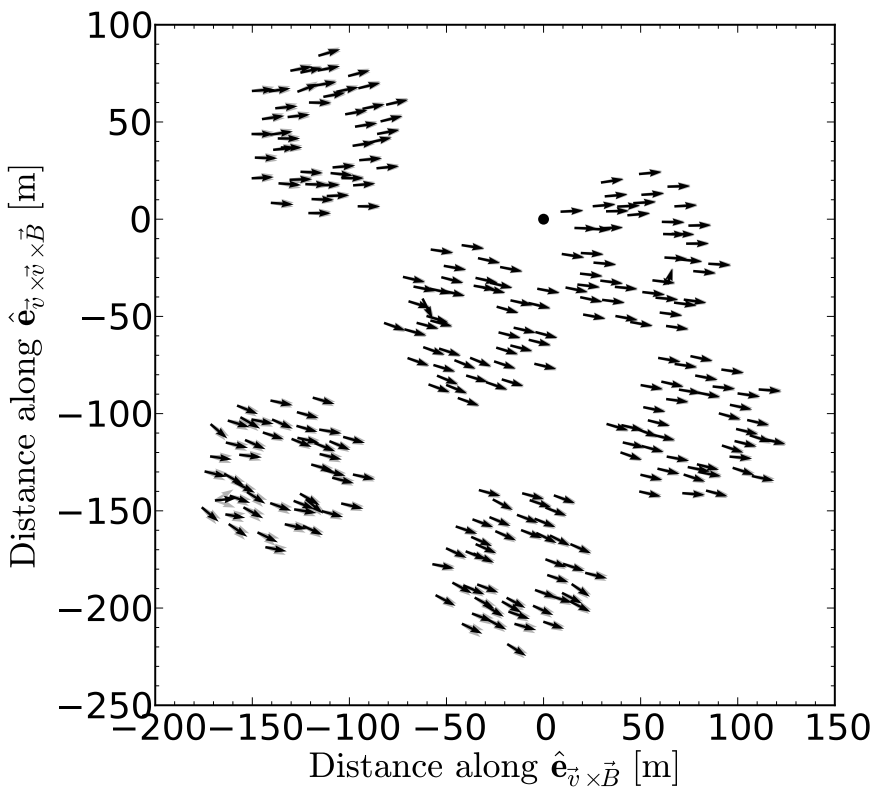

geomagnetic

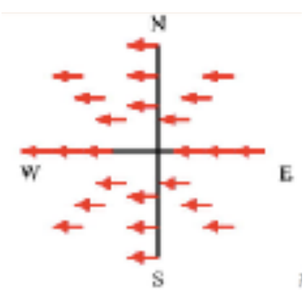

Askaryan

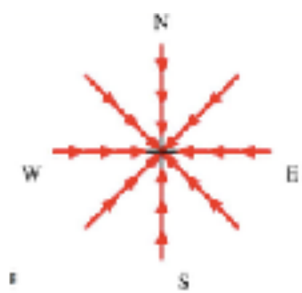

LOFAR

P. Schellart et al., JCAP 10 (2014) 014

Charge excess fraction

$\frac{\text{Askaryan}}{\text{geomagnetic}}$

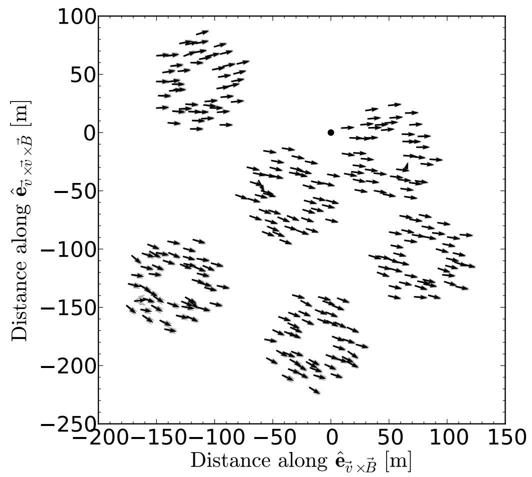

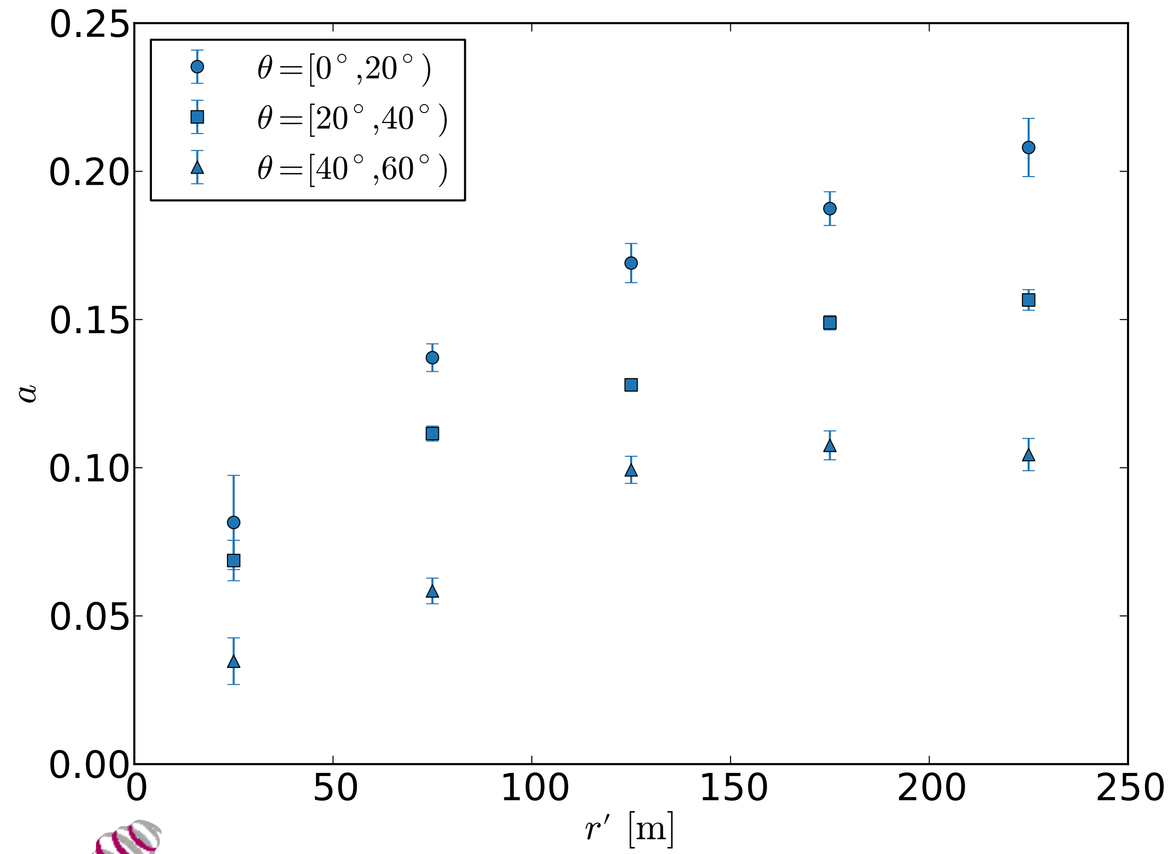

LOFAR

geomagnetic

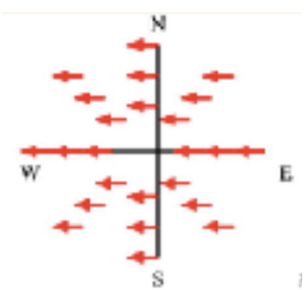

Askaryan

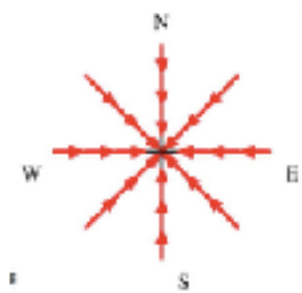

P. Schellart et al., JCAP 10 (2014) 014

Charge excess fraction

Auger Engineering Radio Array

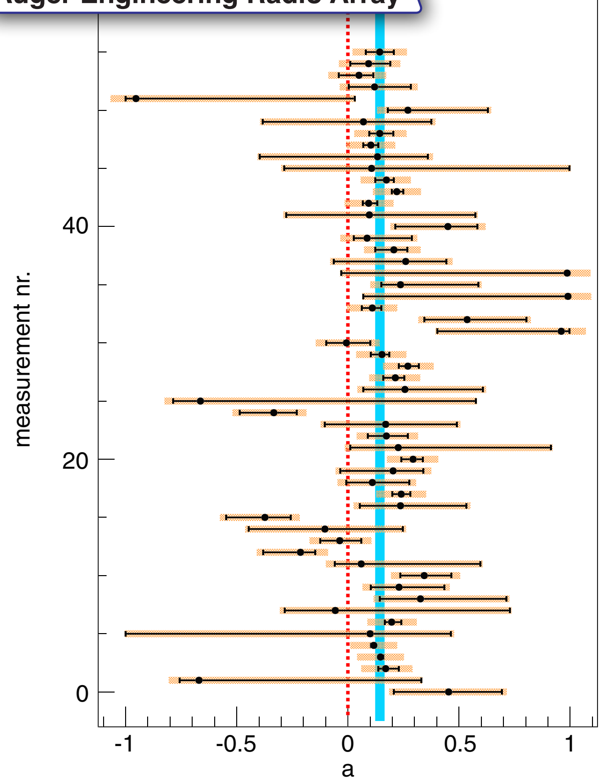

$\frac{\text{Askaryan}}{\text{geomagnetic}}$

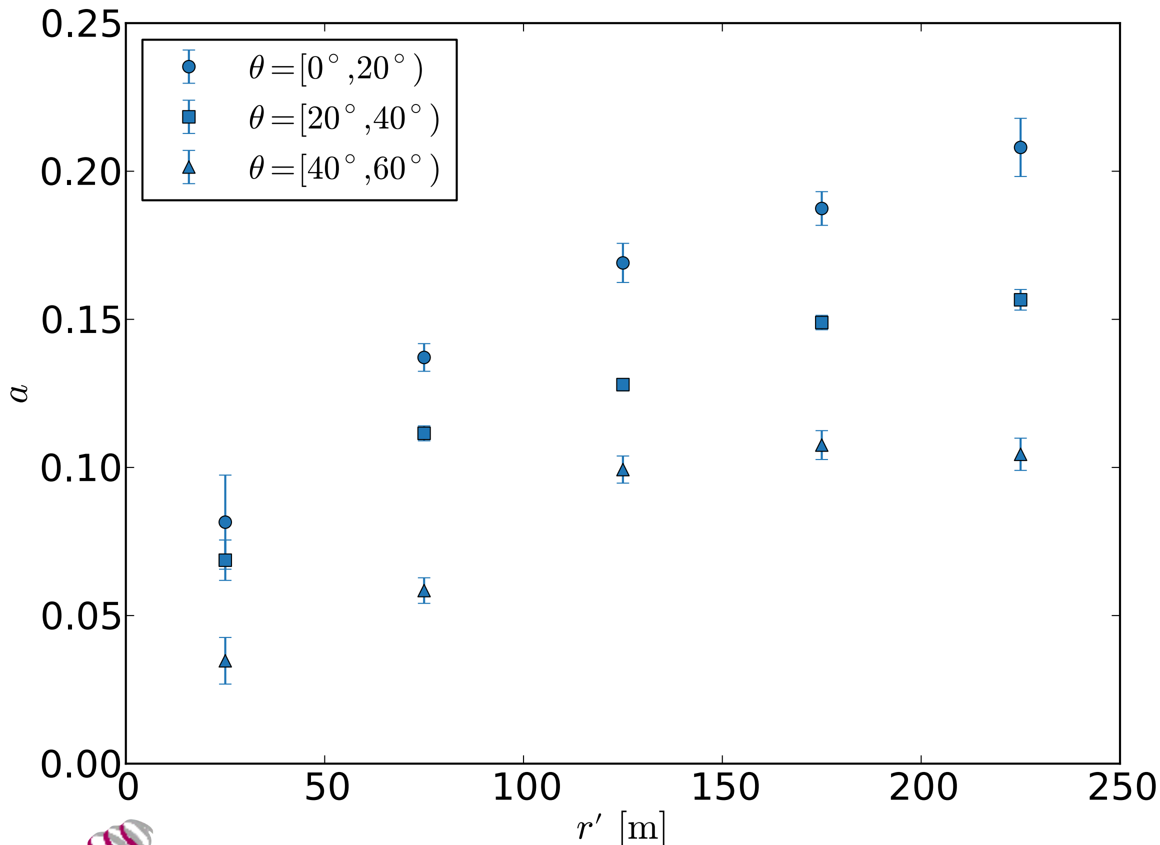

LOFAR

A. Aab, PRD 89 (2014) 052002

P. Schellart et al., JCAP 10 (2014) 014

Footprint of radio emission on the ground

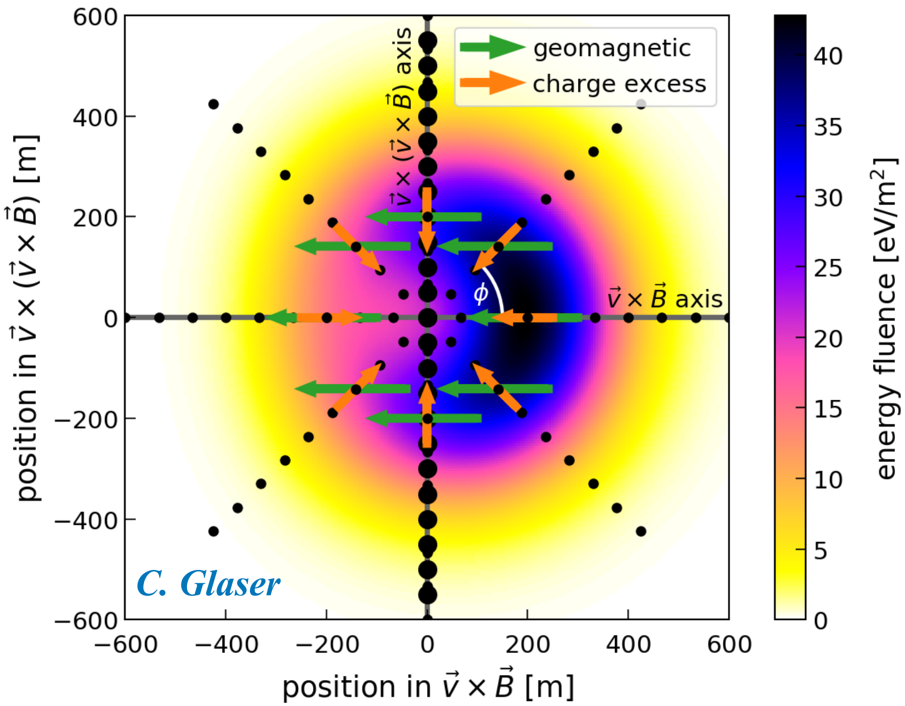

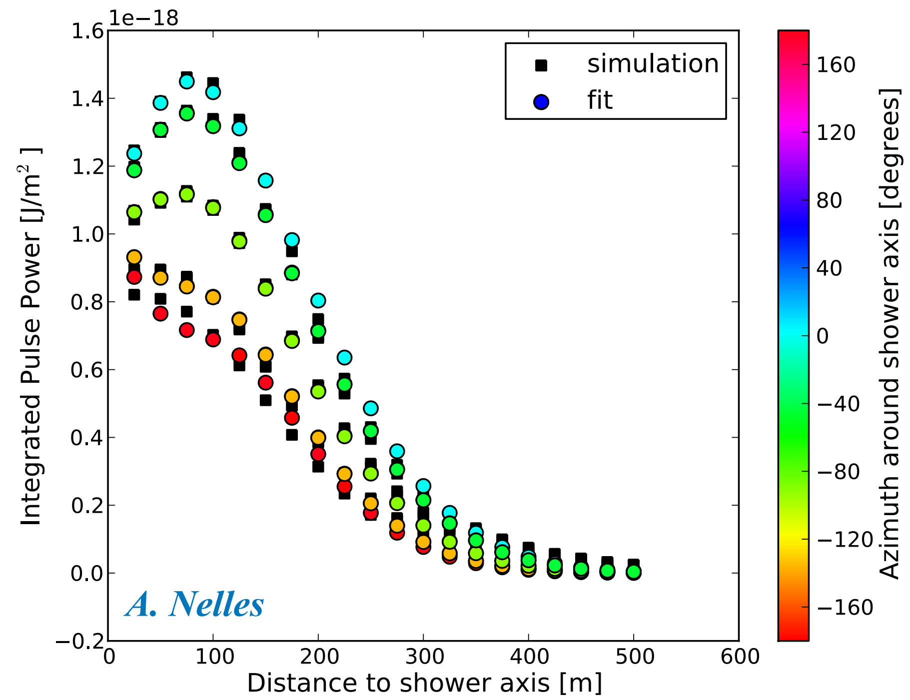

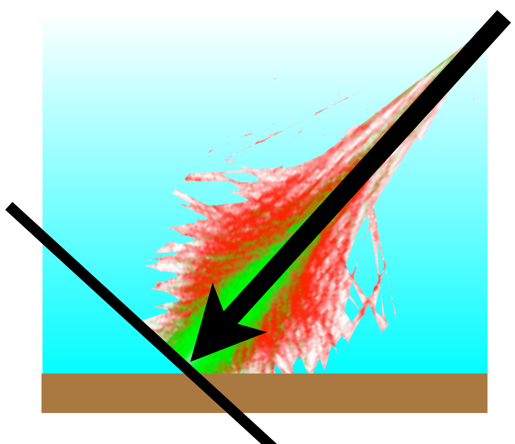

Lateral distribution of radio signals

not rotationally symmetric —> fit two Gaussian functions

v x (v x B)

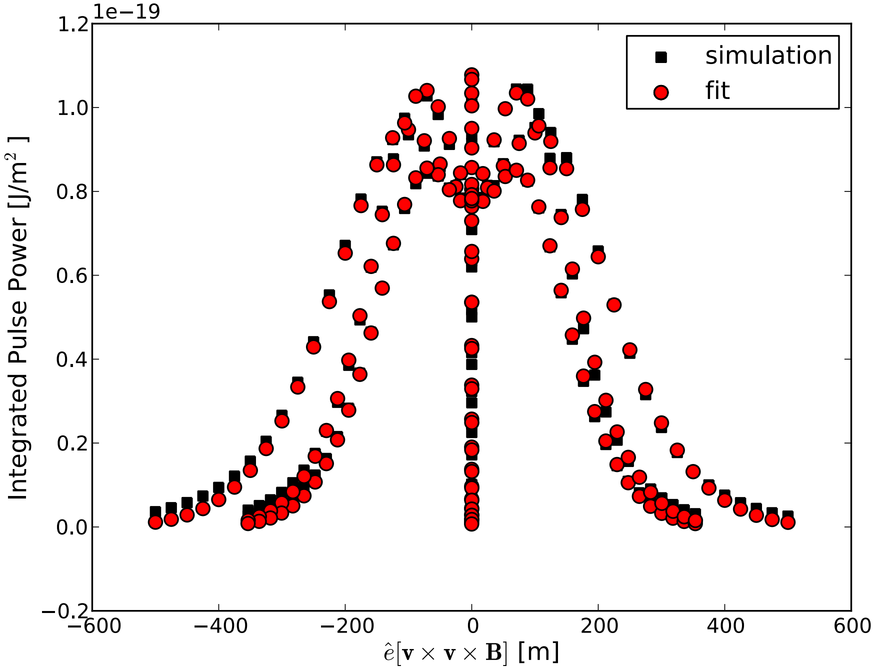

v x B

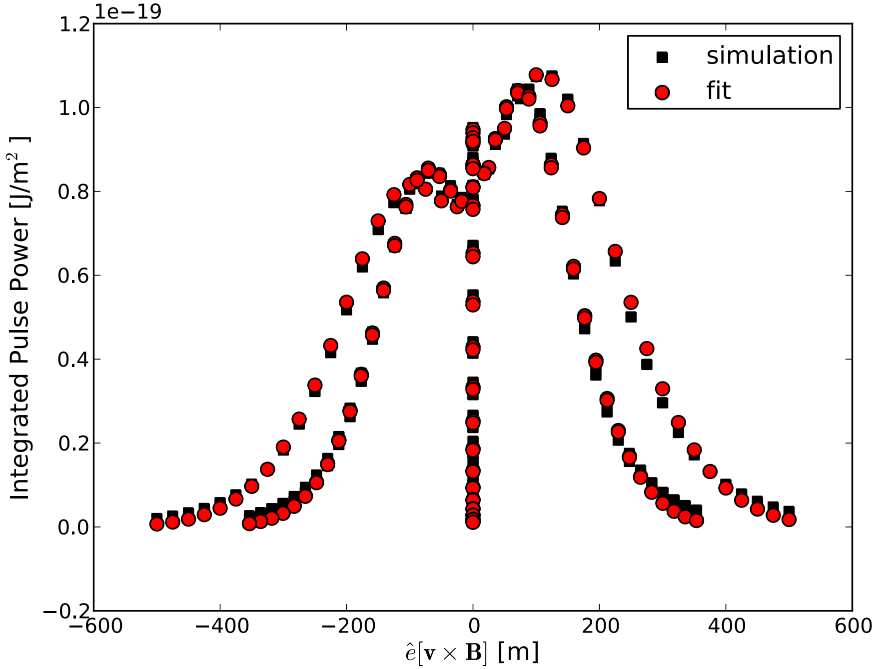

$$P(x',y') = A_+ \cdot \exp\left(\frac{-[(x'-X_+)^2 + (y'-Y_+)^2]}{\sigma_+^2}\right) - A_- \cdot \exp\left(\frac{-[(x'-X_-)^2 + (y'-Y_-)^2]}{\sigma_-^2}\right) + O$$

A. Nelles et al., Astropart. Phys. 60 (2015) 13

Properties of incoming cosmic ray

- direction
- energy
- type

Direction

Shape of Shower Front

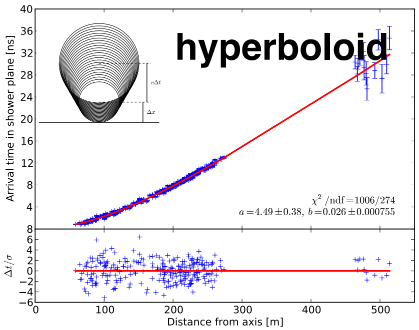

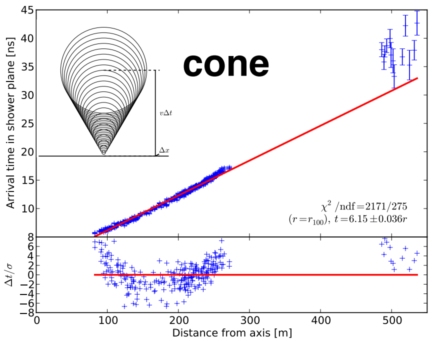

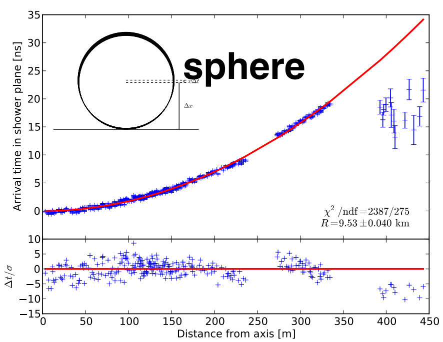

fit quality

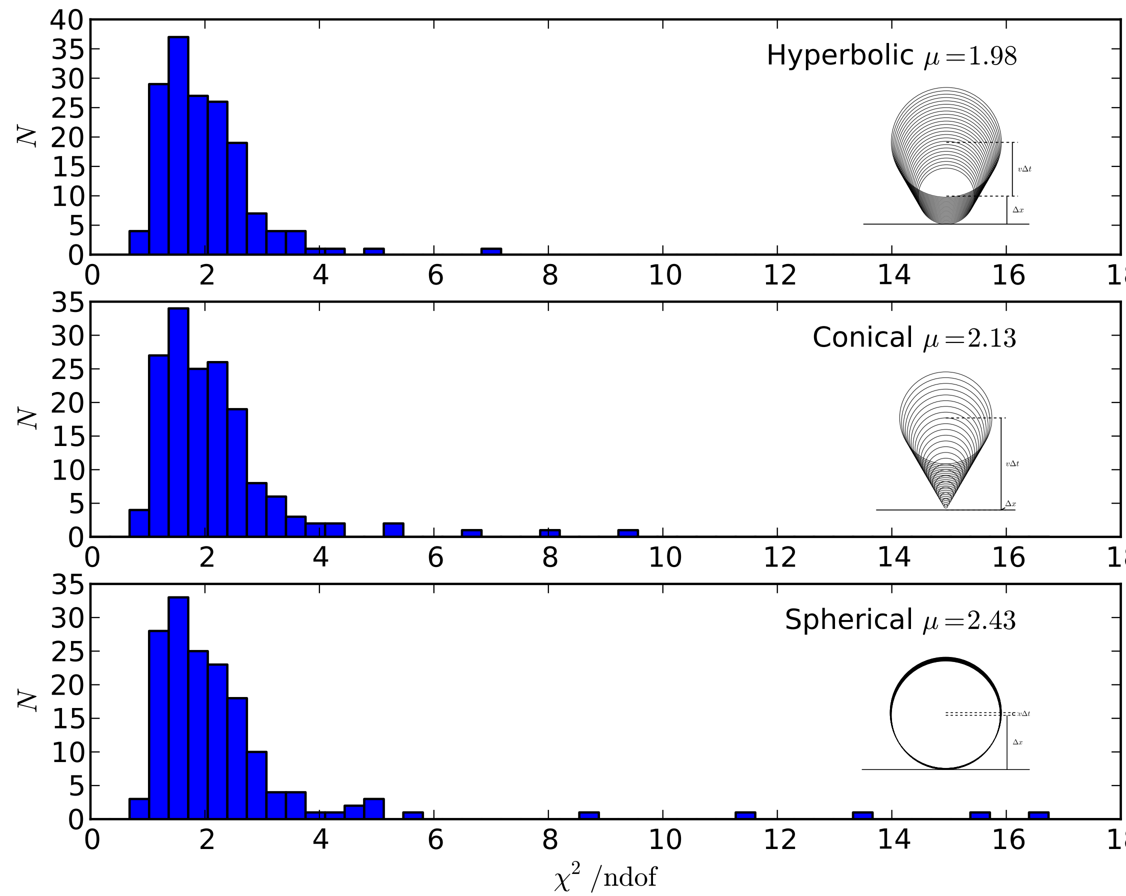

A. Corstanje et al., Astropart. Phys. 61 (2015) 22

Shape of Shower Front

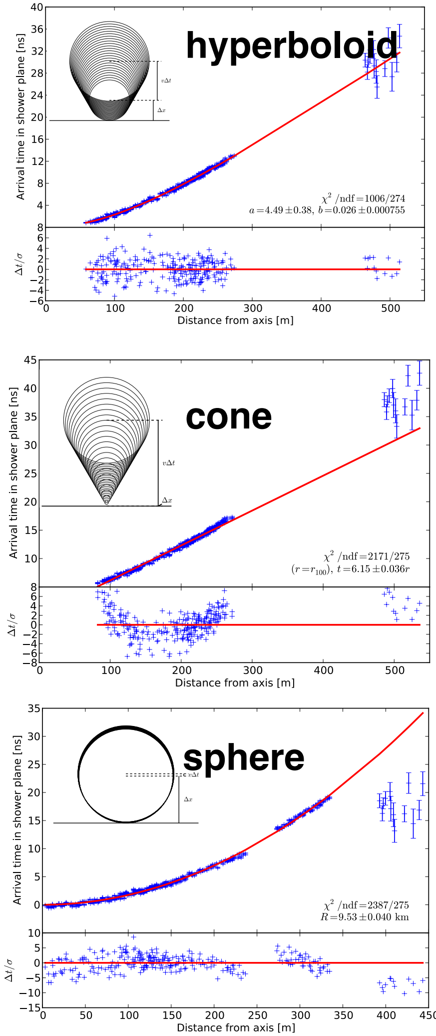

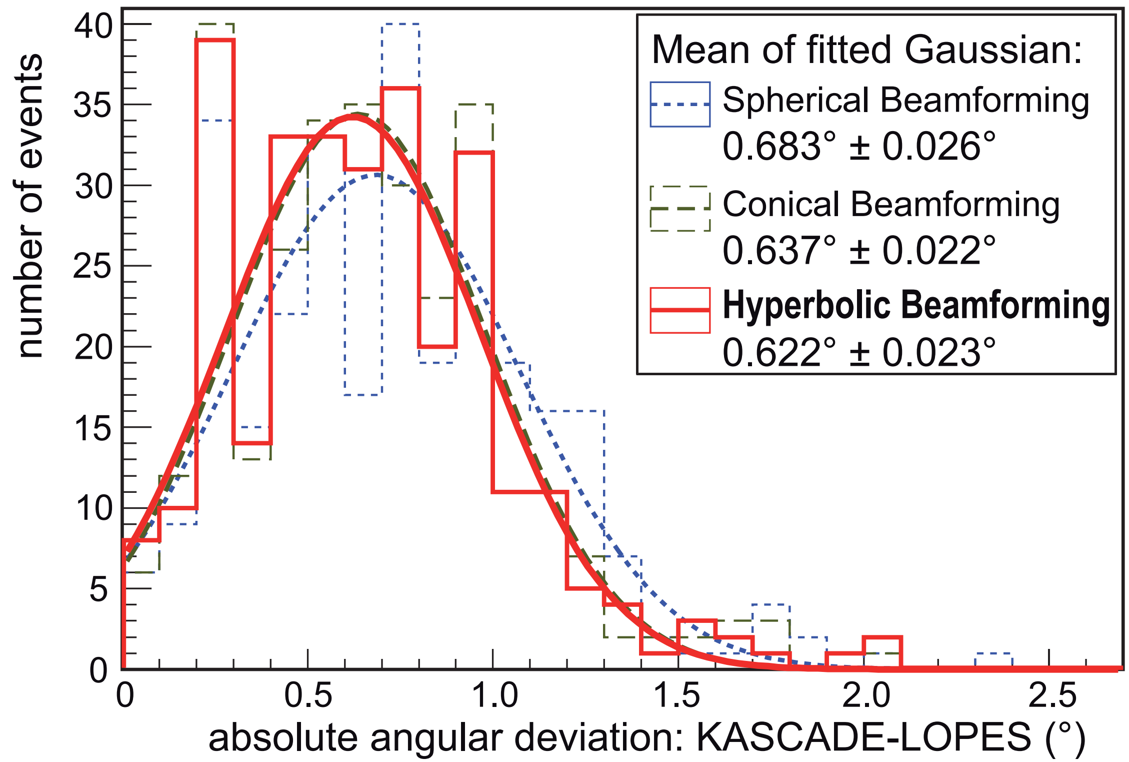

W.D. Apel et al., JCAP 1409 (2014) no.09, 025

A. Corstanje et al., Astropart. Phys. 61 (2015) 22

Accuracy of Shower Direction

angular difference between..

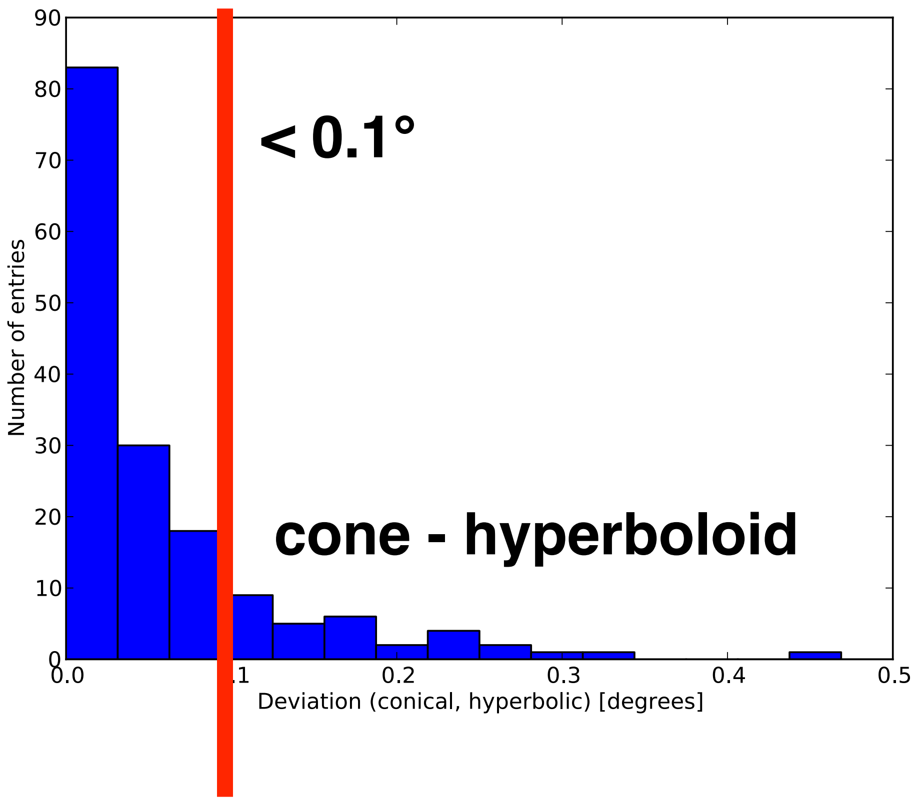

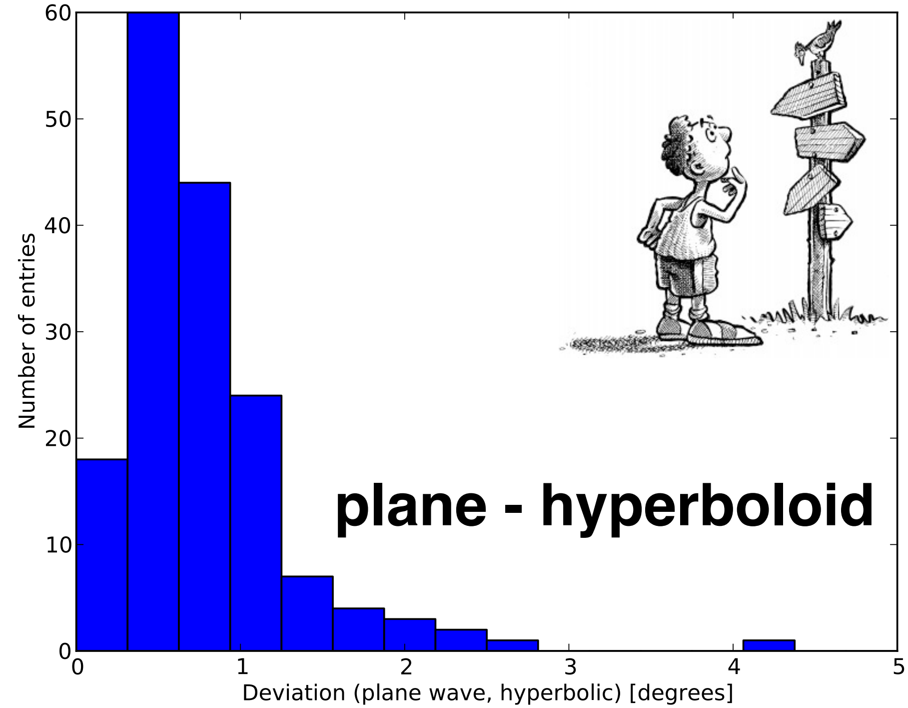

LOFAR

A. Corstanje et al., Astropart. Phys. 61 (2015) 22

Energy

Energy of primary particle

LOFAR

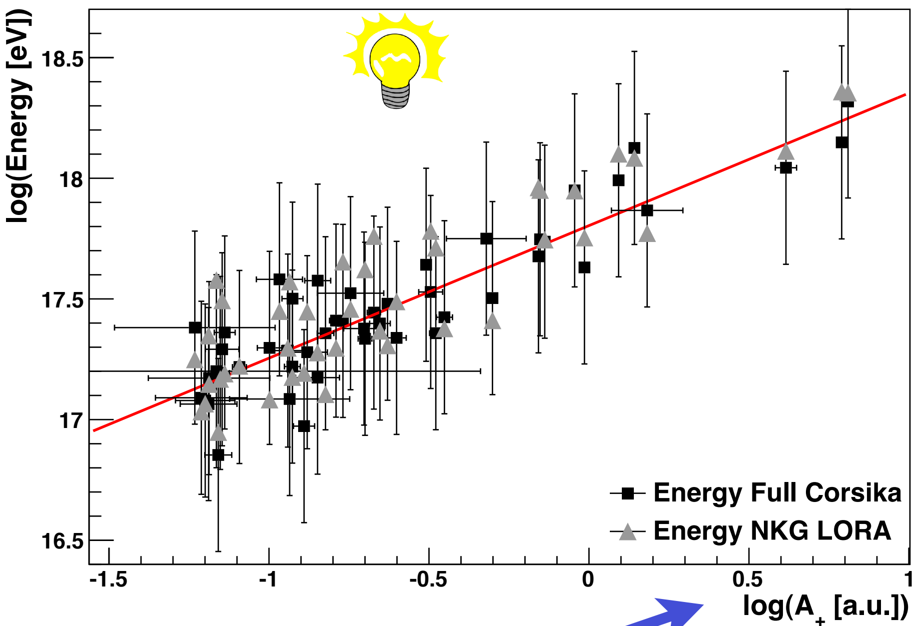

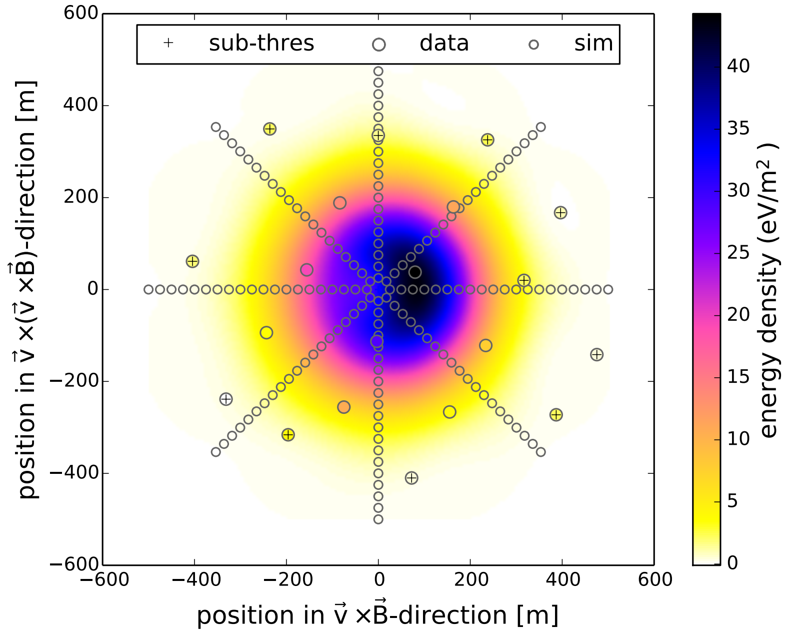

$$P(x',y') = A_+ \cdot \exp\left(\frac{-[(x'-X_+)^2+(y'-Y_+)^2]}{\sigma_+^2}\right) - A_- \cdot \exp\left(\frac{-[(x'-X_-)^2+(y'-Y_-)^2]}{\sigma_-^2}\right) + O$$

A. Nelles et al., JCAP 05 (2015) 018

Measurement of the Radiation Energy in the Radio Signal of Extensive Air Showers as a Universal Estimator of Cosmic-Ray Energy

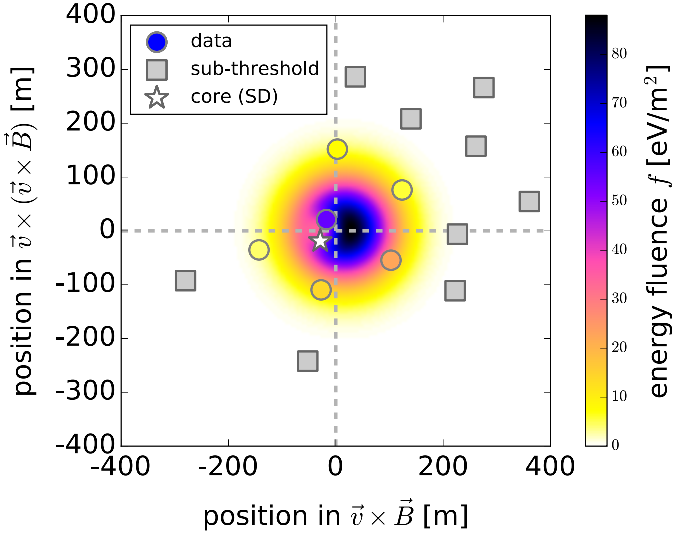

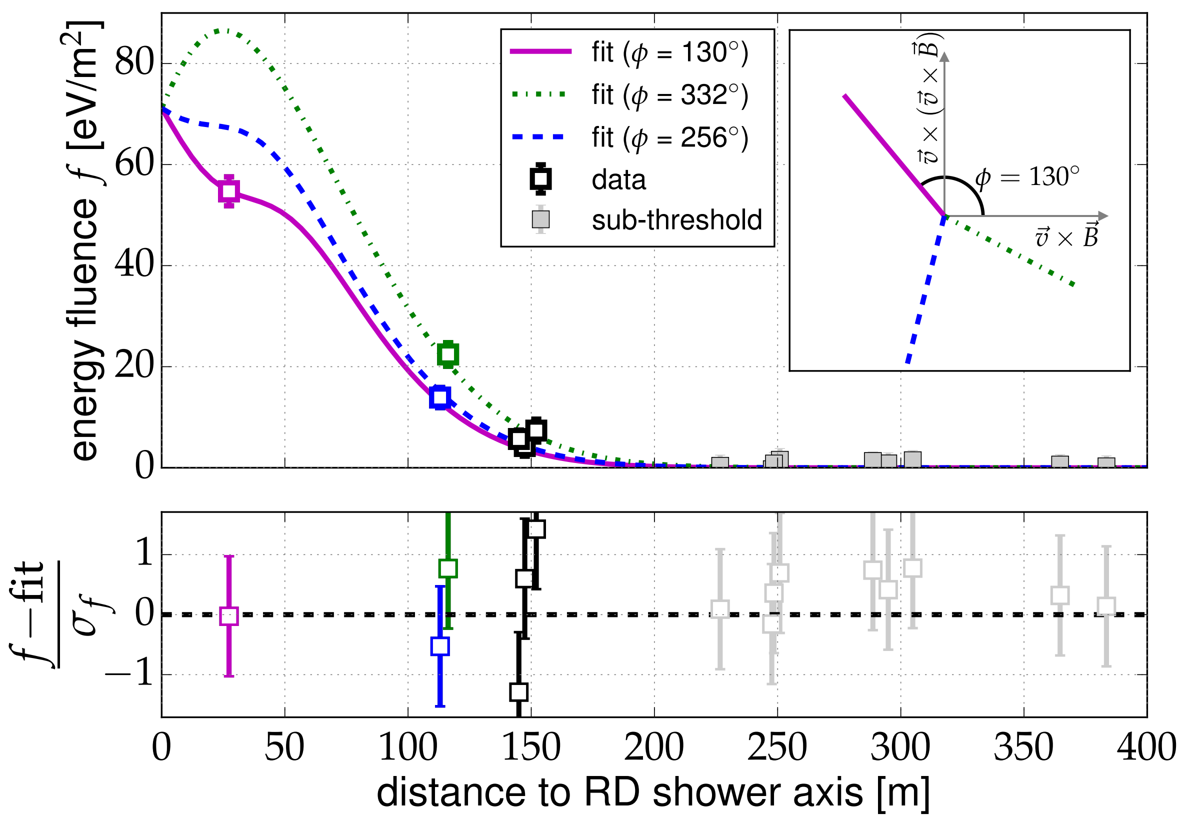

A. Aab et al., PRL 116 (2016) no.24, 241101

Measurement of the Radiation Energy in the Radio Signal of Extensive Air Showers as a Universal Estimator of Cosmic-Ray Energy

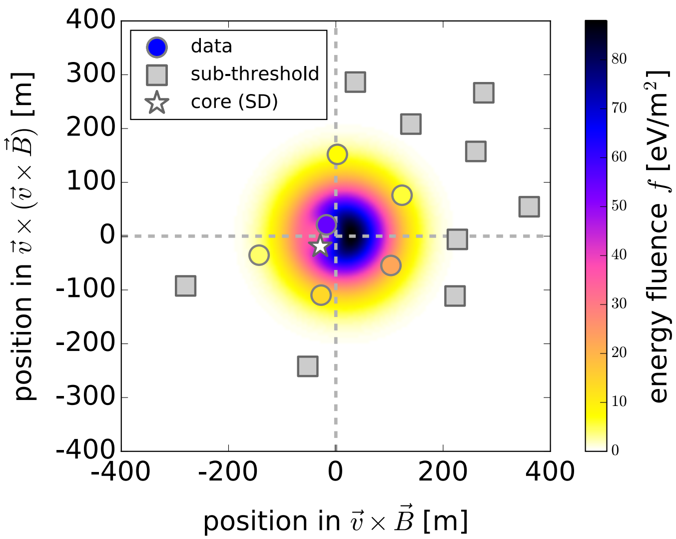

$E_{30\text{-}80}$ MHz = 15.8 MeV @ 10^{18} eV

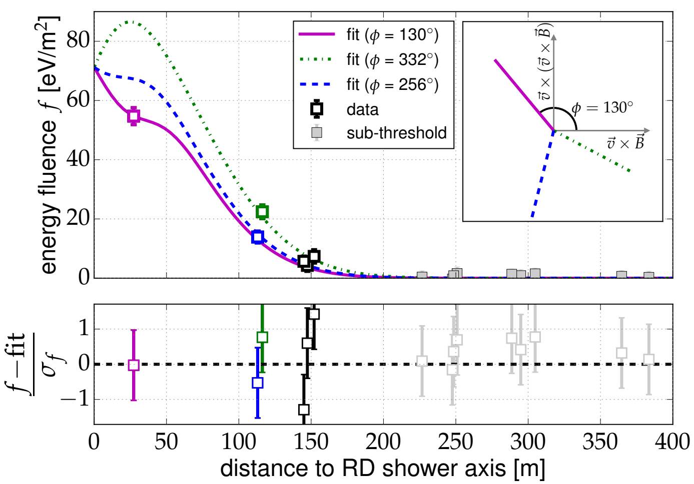

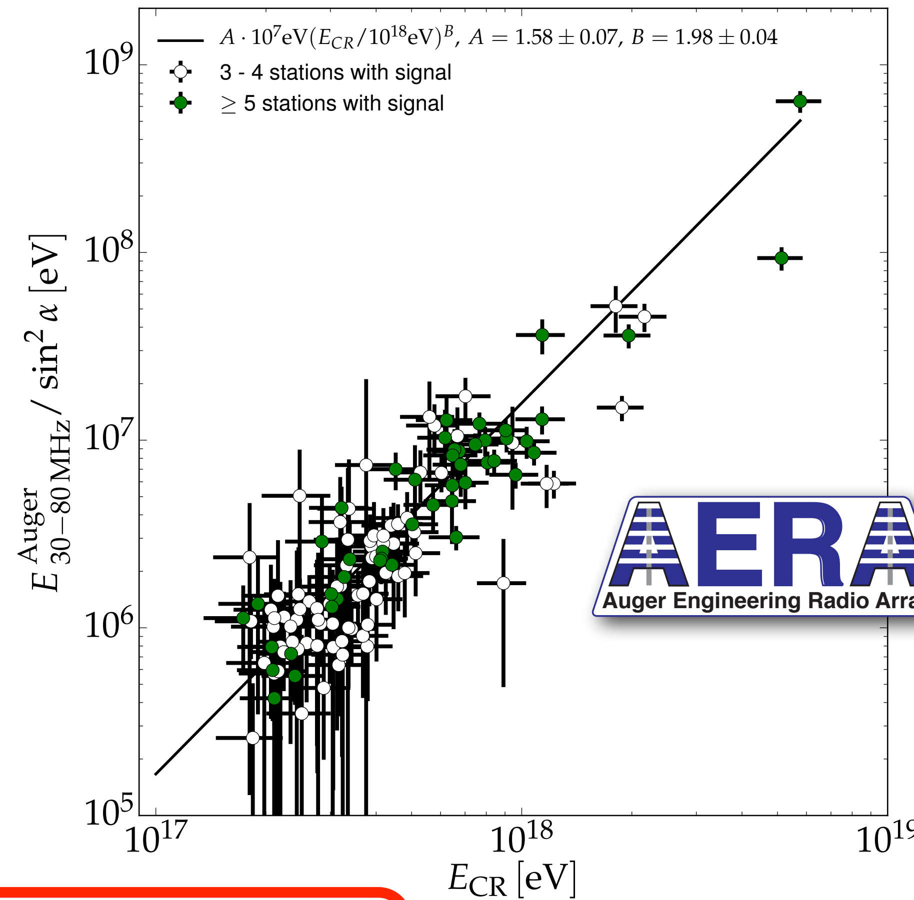

Auger Engineering Radio Array

$$E_{30\text{-}80\ \text{MHz}} = (15.8 \pm 0.7(\text{stat}) \pm 6.7(\text{syst})\ \text{MeV}) \times \left(\sin\alpha \frac{E_{CR}}{10^{18}\ \text{eV}} \frac{B_{Earth}}{0.24\ \text{G}}\right)^2$$

A. Aab et al., PRL 116 (2016) no.24, 241101

Energy Estimation of Cosmic Rays with the Engineering Radio Array of the Pierre Auger Observatory

$E_{30\text{-}80}$ MHz = 15.8 MeV @ 10^{18} eV

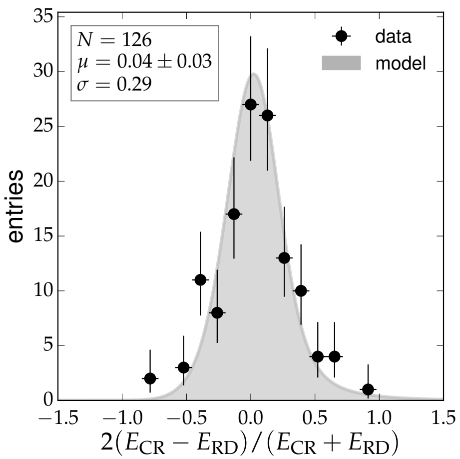

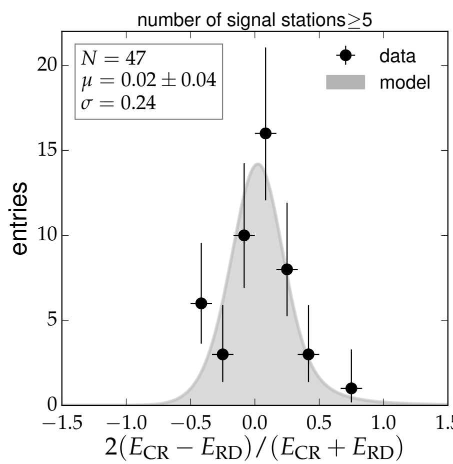

$$\sigma \approx 24\%$$

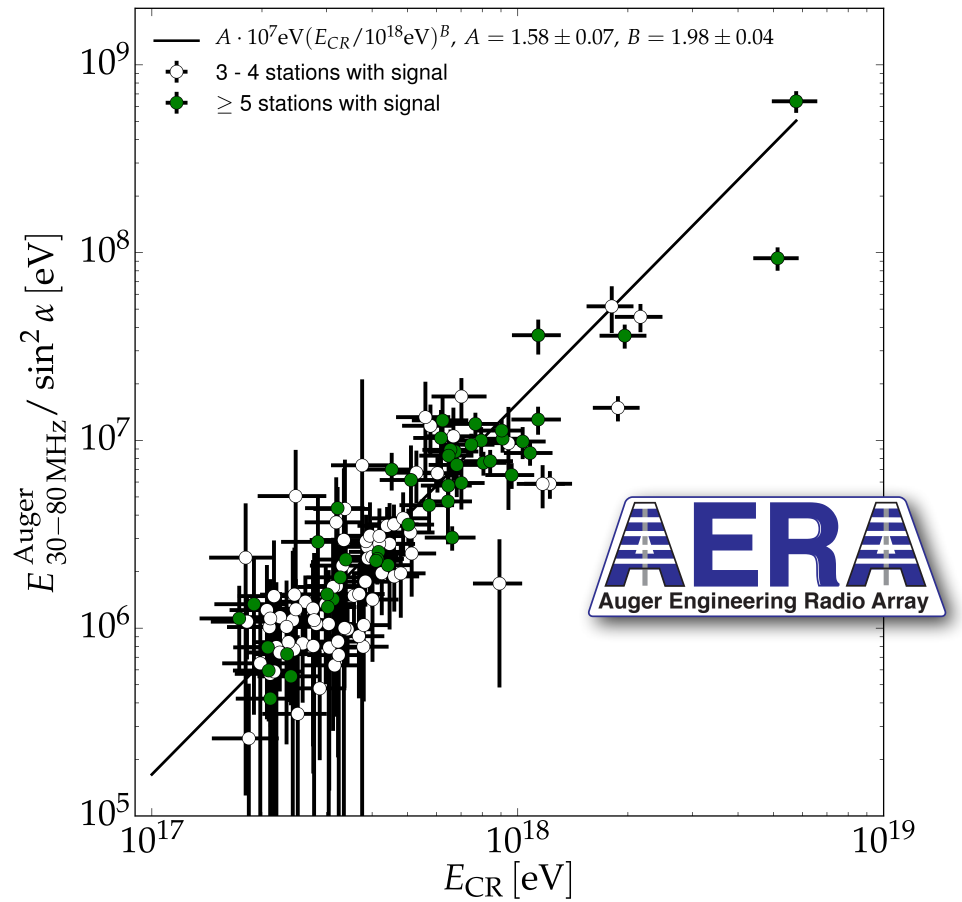

A. Aab et al., PRD 93 (2016) no.12, 122005
A. Aab et al., PRL 116 (2016) no.24, 241101

Cosmic-ray energy (Cherenkov) vs radio signal

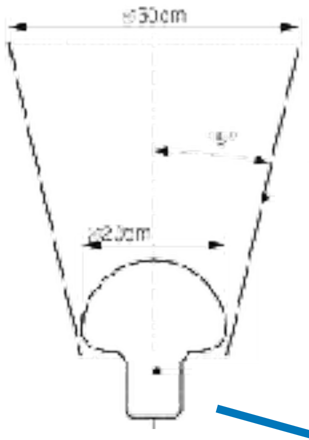

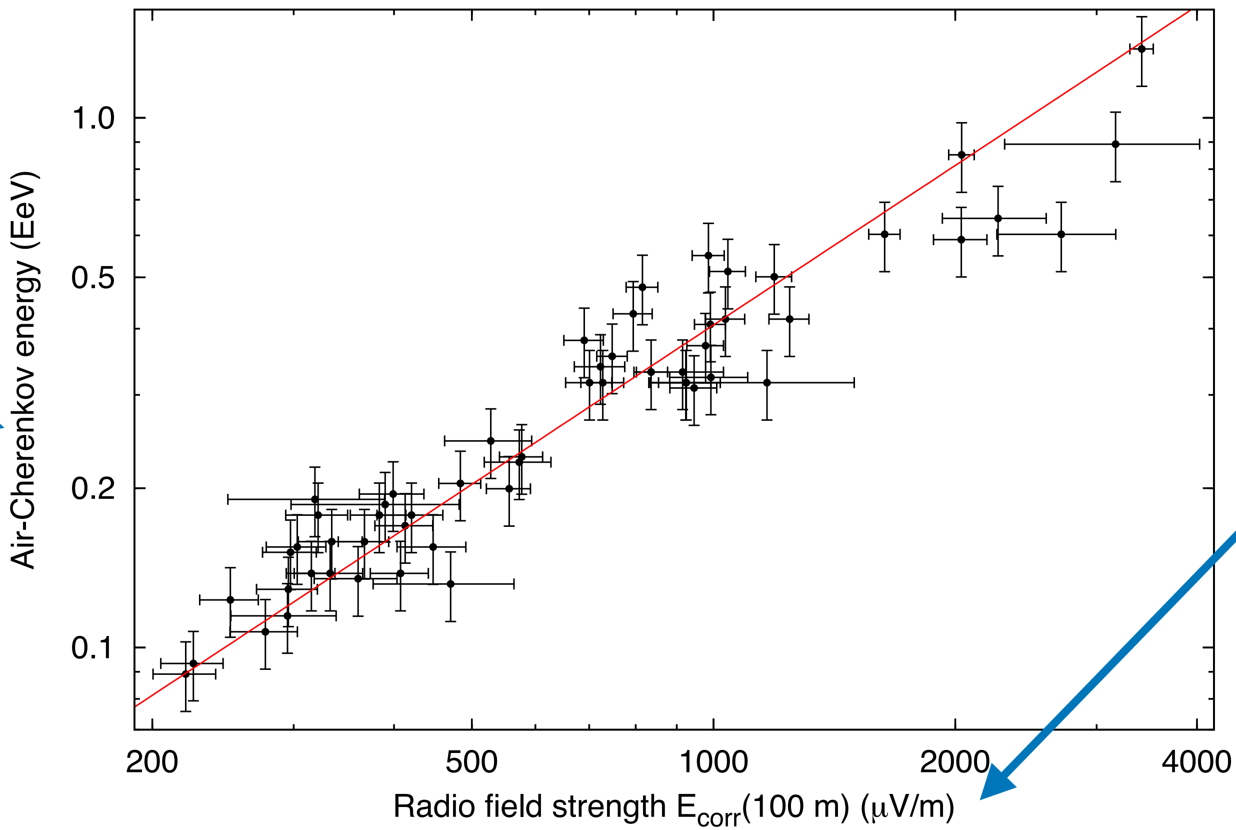

Fig. 3. Correlation of the energy measured with the air-Cherenkov array and an energy estimator based on the radio amplitude at 100 m measured with Tunka-Rex. The line indicates a linear correlation.

F.G. Schröder et al., JPS Conf. Proc. 9 (2016) 010008

Mass

Properties of primary particle

energy

distance to Xmax

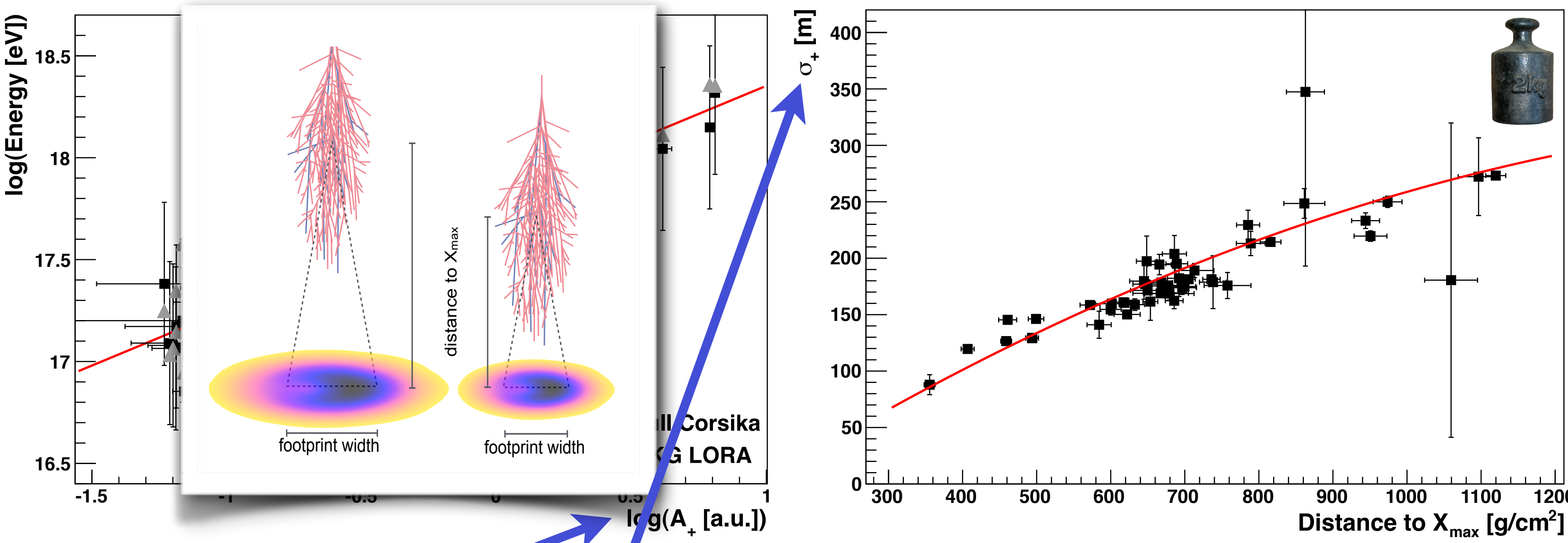

$$P(x', y') = A_+ \cdot \exp\left(\frac{-[(x' - X_+)^2 + (y' - Y_+)^2]}{\sigma_+^2}\right) - A_- \cdot \exp\left(\frac{-[(x' - X_-)^2 + (y' - Y_-)^2]}{\sigma_-^2}\right) + O$$

LOFAR

A. Nelles et al., JCAP 05 (2015) 018

Measurement of particle mass

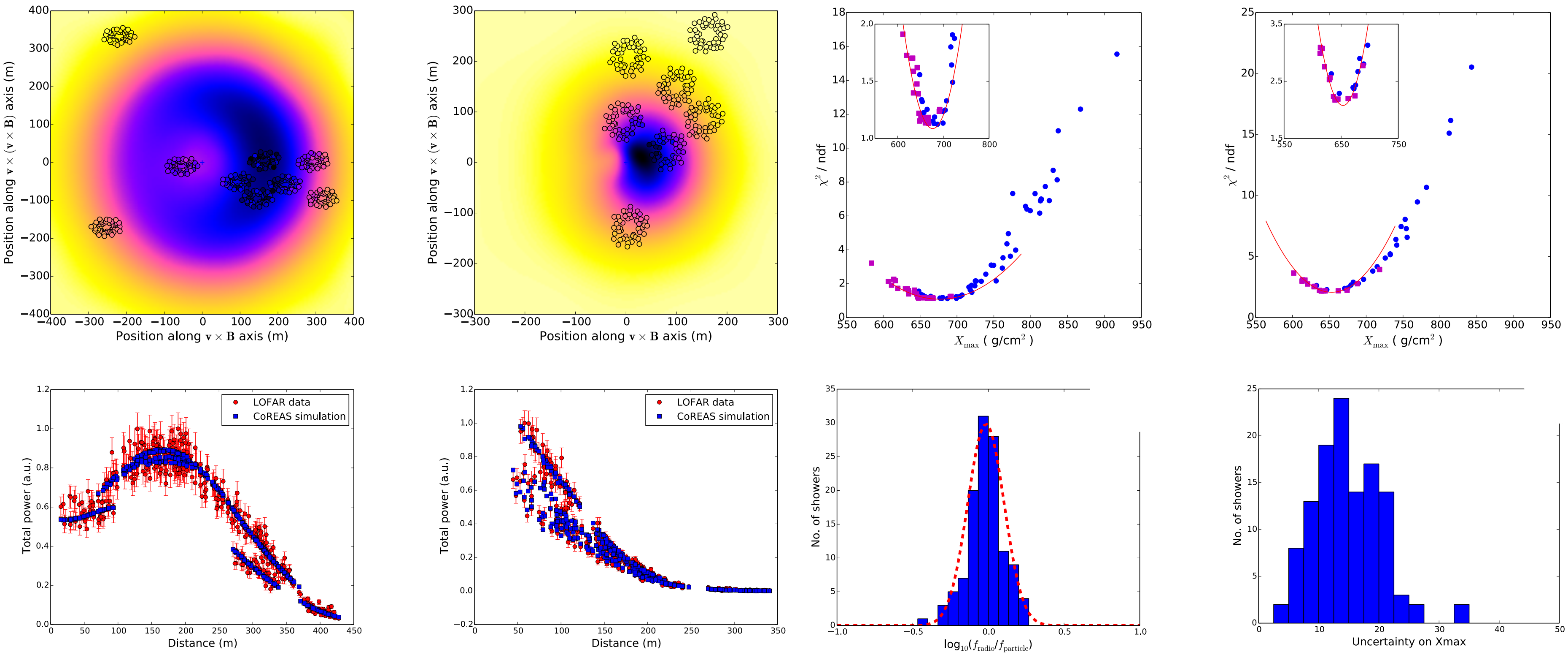

$\sigma_E \approx 32\%$

$\sigma_{X_{max}} \approx 17\ \mathrm{g/cm^2}$

S. Buitink et al., PRD 90 (2014) 082003

Depth of the shower maximum

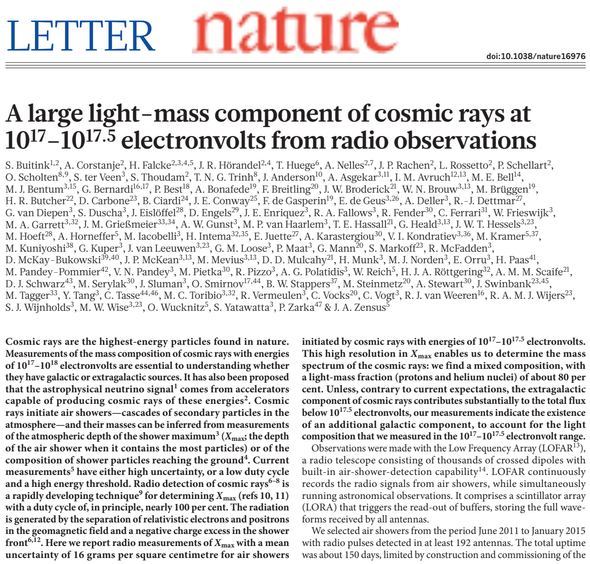

LETTER nature

doi:10.1038/nature16976

A large light-mass component of cosmic rays at 10^{17}–$10^{17.5}$ electronvolts from radio observations

S. Buitink[1,2], A. Corstanje[2], H. Falcke[2,3,4,5], J. R. Hörandel[2,4], T. Huege[6], A. Nelles[2,7], J. P. Rachen[2], L. Rossetto[2], P. Schellart[2], O. Scholten[8,9], S. ter Veen[3], S. Thoudam[2], T. N. G. Trinh[8], J. Anderson[10], A. Asgekar[3,11], I. M. Avruch[12,13], M. E. Bell[14], M. J. Bentum[3,15], G. Bernardi[16,17], P. Best[18], A. Bonafede[19], F. Breitling[20], J. W. Broderick[21], W. N. Brouw[3,13], M. Brüggen[19], H. R. Butcher[22], D. Carbone[23], B. Ciardi[24], J. E. Conway[25], F. de Gasperin[19], E. de Geus[3,26], A. Deller[3], R.-J. Dettmar[27], G. van Diepen[3], S. Duscha[3], J. Eislöffel[28], D. Engels[29], J. E. Enriquez[3], R. A. Fallows[3], R. Fender[30], C. Ferrari[31], W. Frieswijk[3], M. A. Garrett[3,32], J. M. Grießmeier[33,34], A. W. Gunst[3], M. P. van Haarlem[3], T. E. Hassall[21], G. Heald[3,13], J. W. T. Hessels[3,23], M. Hoeft[28], A. Horneffer[5], M. Iacobelli[3], H. Intema[32,35], E. Juette[27], A. Karastergiou[30], V. I. Kondratiev[3,36], M. Kramer[5,37], M. Kuniyoshi[38], G. Kuper[3], J. van Leeuwen[3,23], G. M. Loose[3], P. Maat[3], G. Mann[20], S. Markoff[23], R. McFadden[3], D. McKay-Bukowski[39,40], J. P. McKean[3,13], M. Mevius[3,13], D. D. Mulcahy[21], H. Munk[3], M. J. Norden[3], E. Orru[3], H. Paas[41], M. Pandey-Pommier[42], V. N. Pandey[3], M. Pietka[30], R. Pizzo[3], A. G. Polatidis[3], W. Reich[5], H. J. A. Röttgering[32], A. M. M. Scaife[21], D. J. Schwarz[43], M. Serylak[30], J. Sluman[3], O. Smirnov[17,44], B. W. Stappers[37], M. Steinmetz[20], A. Stewart[30], J. Swinbank[23,45], M. Tagger[33], Y. Tang[3], C. Tasse[44,46], M. C. Toribio[3,32], R. Vermeulen[3], C. Vocks[20], C. Vogt[3], R. J. van Weeren[16], R. A. M. J. Wijers[23], S. J. Wijnholds[3], M. W. Wise[3,23], O. Wucknitz[5], S. Yatawatta[3], P. Zarka[47] & J. A. Zensus[5]

Cosmic rays are the highest-energy particles found in nature. Measurements of the mass composition of cosmic rays with energies of 10^{17}–10^{18} electronvolts are essential to understanding whether they have galactic or extragalactic sources. It has also been proposed that the astrophysical neutrino signal[1] comes from accelerators capable of producing cosmic rays of these energies[2]. Cosmic rays initiate air showers—cascades of secondary particles in the atmosphere—and their masses can be inferred from measurements of the atmospheric depth of the shower maximum[3] (X_{max}; the depth of the air shower when it contains the most particles) or of the composition of shower particles reaching the ground[4]. Current measurements[5] have either high uncertainty, or a low duty cycle and a high energy threshold. Radio detection of cosmic rays[6–8] is a rapidly developing technique[9] for determining X_{max} (refs 10, 11) with a duty cycle of, in principle, nearly 100 per cent. The radiation is generated by the separation of relativistic electrons and positrons in the geomagnetic field and a negative charge excess in the shower front[6,12]. Here we report radio measurements of X_{max} with a mean uncertainty of 16 grams per square centimetre for air showers initiated by cosmic rays with energies of 10^{17}–$10^{17.5}$ electronvolts. This high resolution in X_{max} enables us to determine the mass spectrum of the cosmic rays: we find a mixed composition, with a light-mass fraction (protons and helium nuclei) of about 80 per cent. Unless, contrary to current expectations, the extragalactic component of cosmic rays contributes substantially to the total flux below $10^{17.5}$ electronvolts, our measurements indicate the existence of an additional galactic component, to account for the light composition that we measured in the 10^{17}–$10^{17.5}$ electronvolt range.

Observations were made with the Low Frequency Array (LOFAR[13]), a radio telescope consisting of thousands of crossed dipoles with built-in air-shower-detection capability[14]. LOFAR continuously records the radio signals from air showers, while simultaneously running astronomical observations. It comprises a scintillator array (LORA) that triggers the read-out of buffers, storing the full wave-forms received by all antennas.

We selected air showers from the period June 2011 to January 2015 with radio pulses detected in at least 192 antennas. The total uptime was about 150 days, limited by construction and commissioning of the

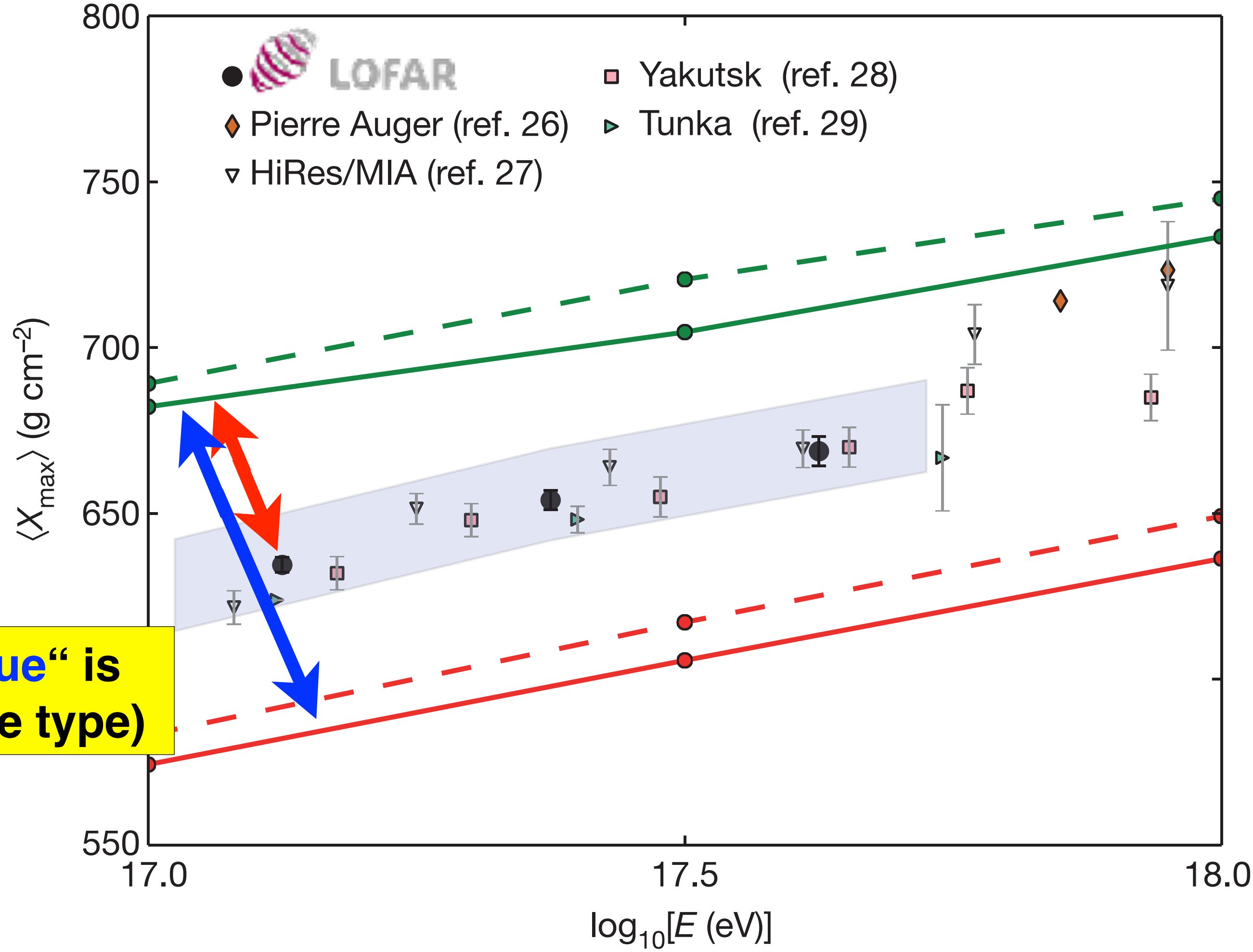

relative distance "red/blue" is measure for ln A (particle type)

S. Buitink et al., Nature 531 (2016) 70

Mean logarithmic mass

$$\ln A = \sum k_i \ln A_i$$

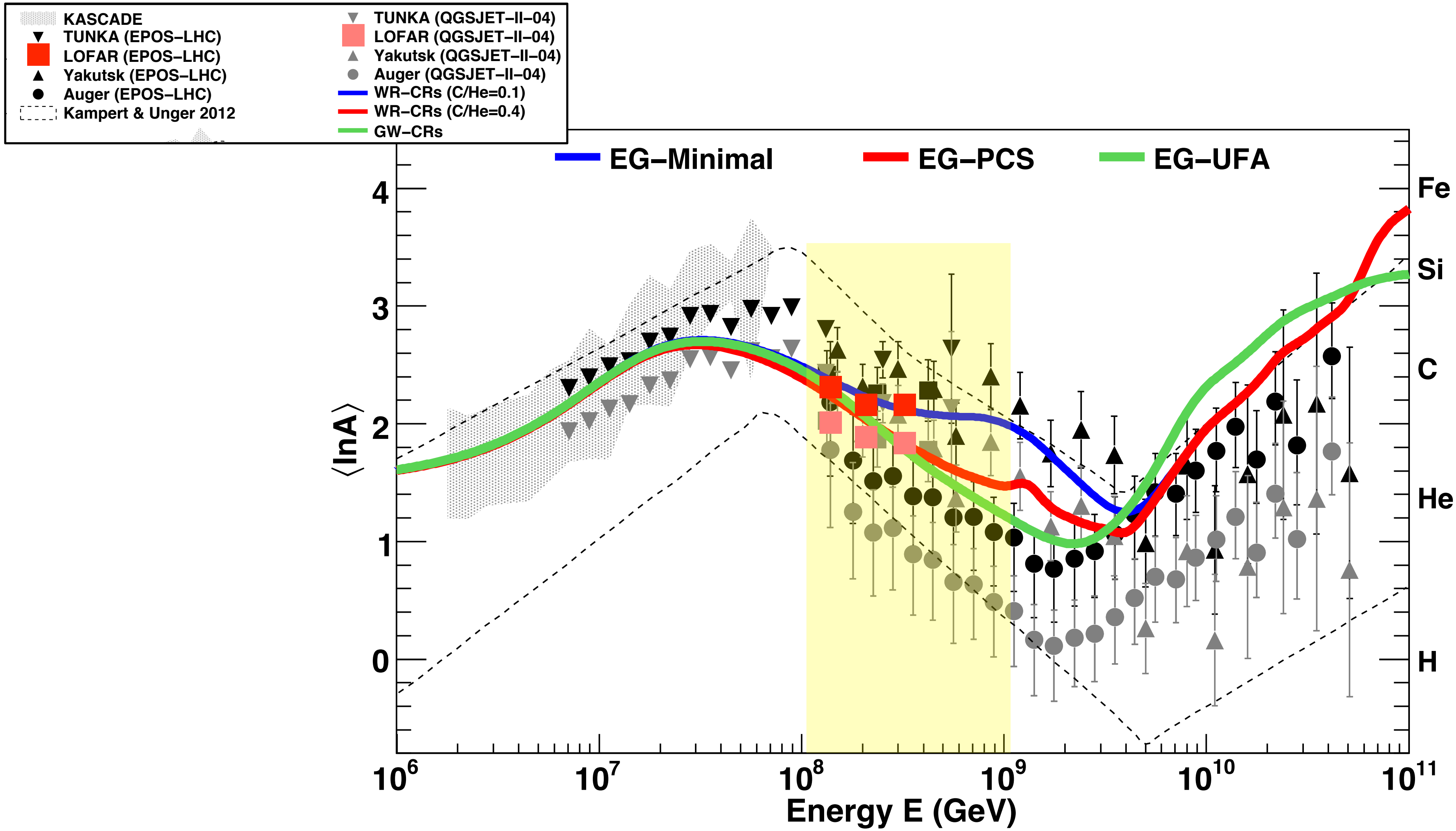

S. Thoudam et al., A&A 595 (2016) A33

Xmax RD vs FD

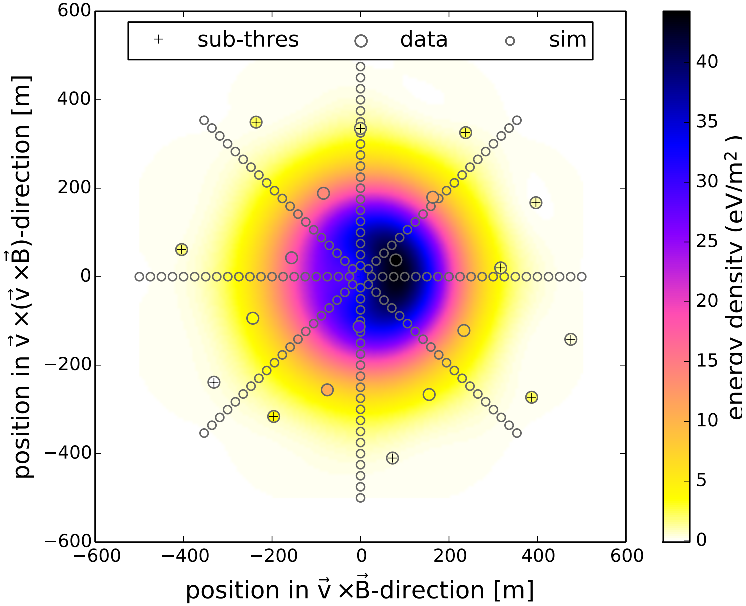

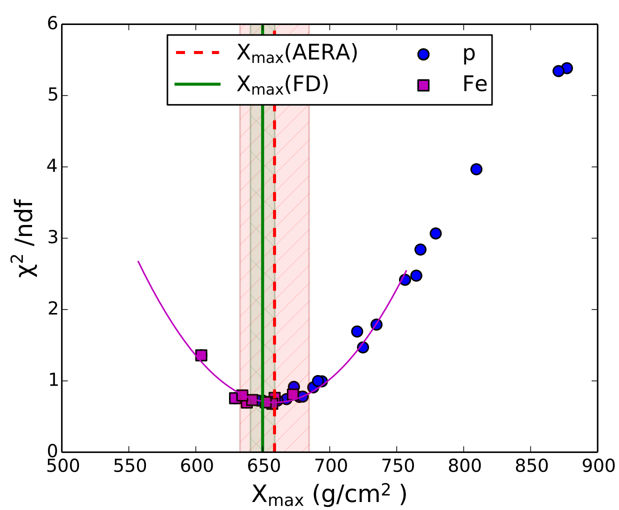

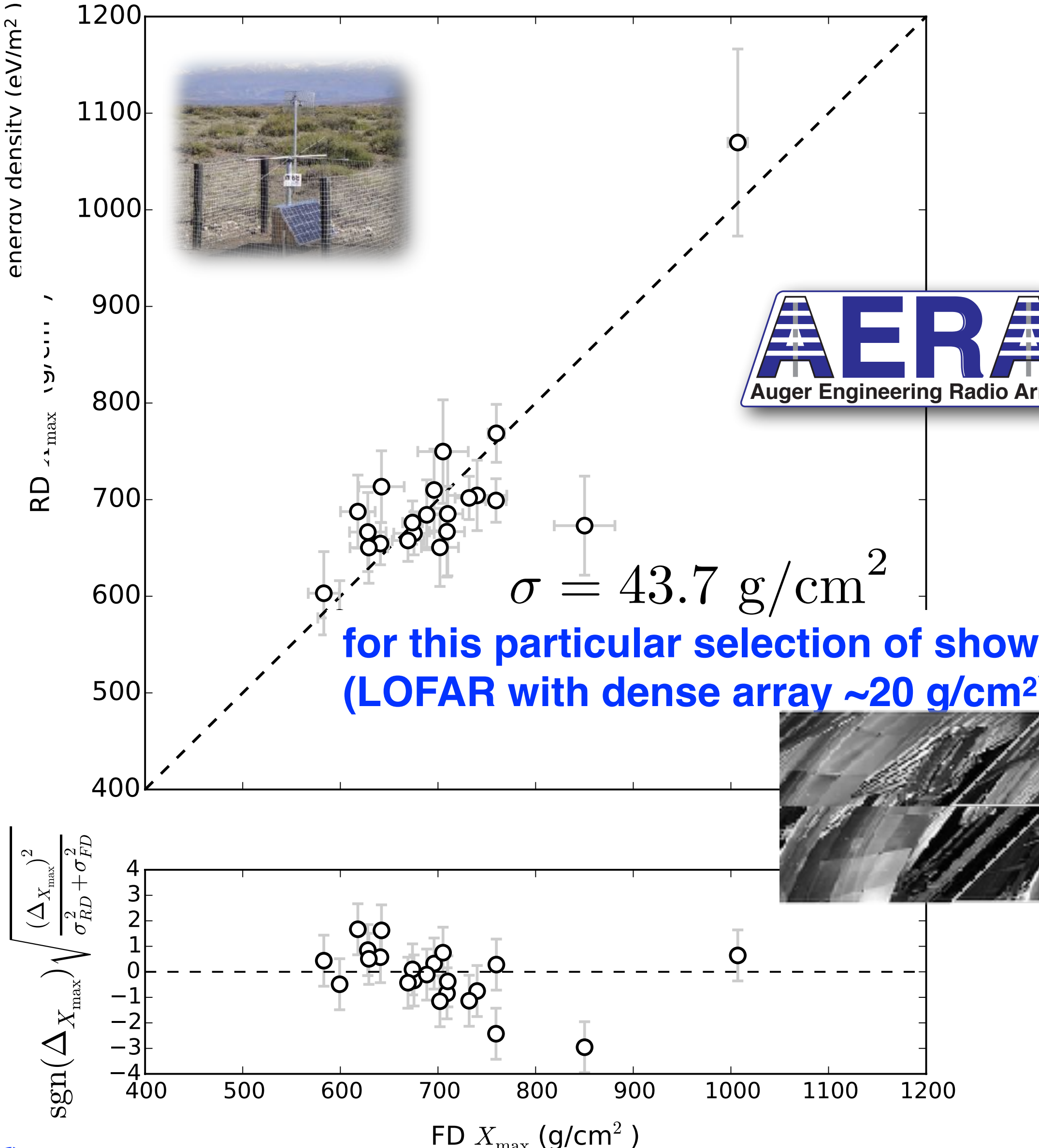

for this particular selection of showers
(LOFAR with dense array ~20 g/cm²)

J. Schulz, PhD thesis RU Nijmegen (2016)

Shower maximum: proof by Tunka-Rex

- One of several methods: slope of lateral distribution

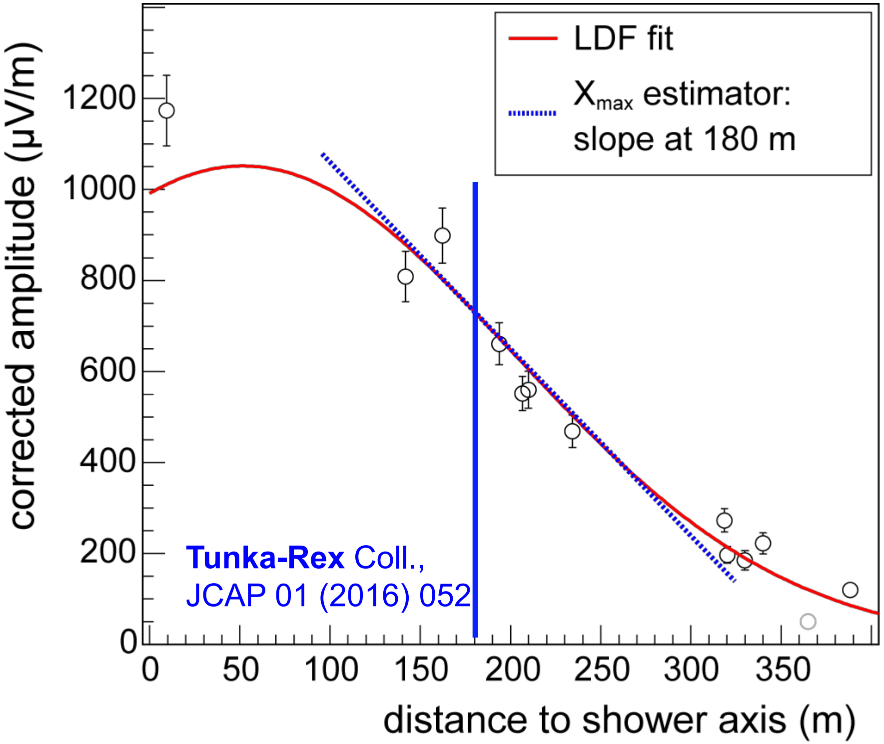

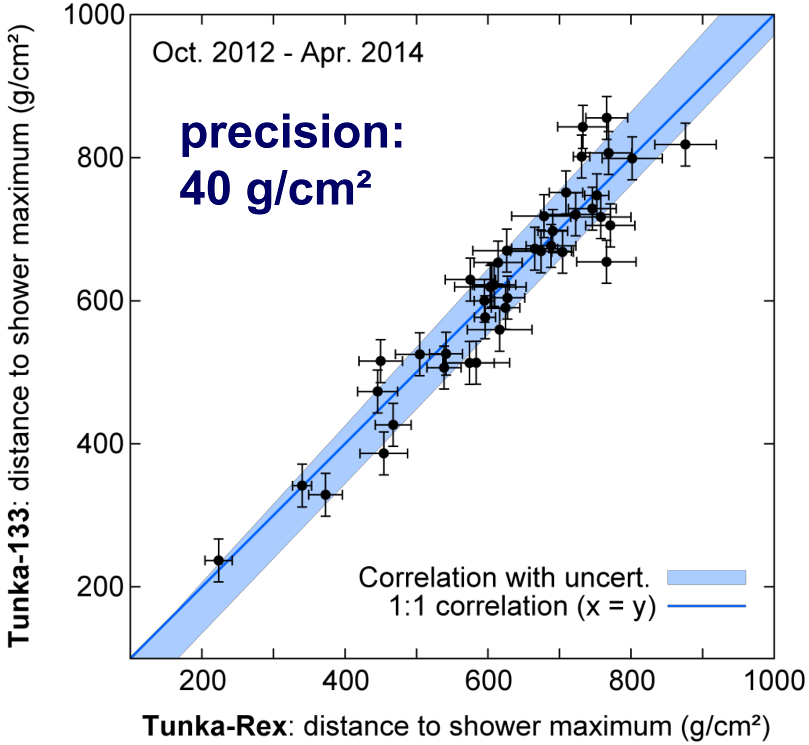

frank.schroeder@kit.edu
Institut für Kernphysik

Determine the properties of the incoming particle with the radio technique

- direction ~ 0.1° - 0.5°
- energy ~ 20% - 30%
- type (X_{max}) ~ 20 - 40 g/cm²

(depending on detector spacing)

—> radio technique is routinely used to measure properties of cosmic rays


The Future
NEXT EXIT

Concept of ARIANNA

- On ice-shelf: **Ice-water boundary** almost perfect reflector for radio emission
- **Independent antenna stations** can be installed at low costs on the surface
- **Real-time data transfer** via satellite
- Solar and wind power possible
- **High gain antennas** (50 - 1000 MHz) can be used to instrument a large volume
- Array of about 1000 antennas needed

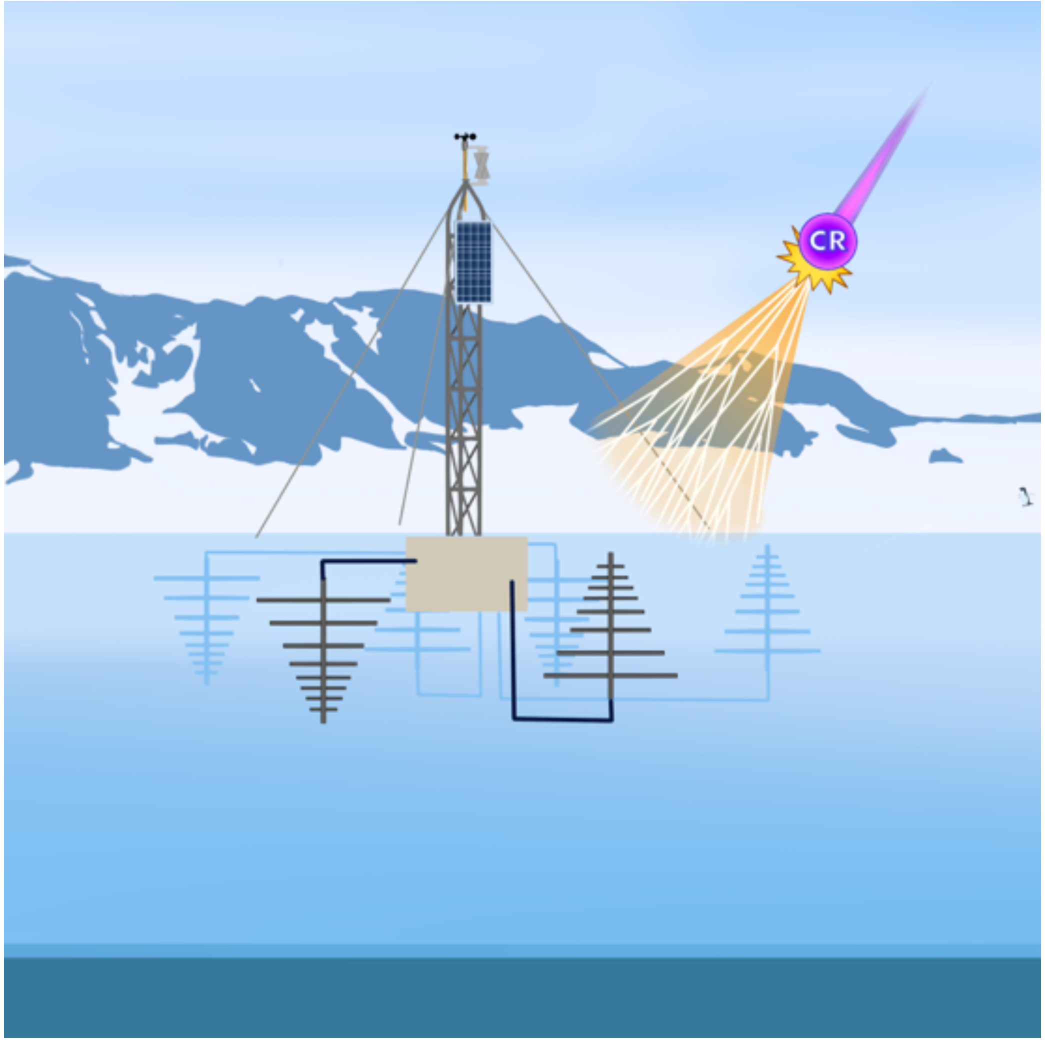

S.W. Barwick et al., Astropart.Phys. 90 (2017) 50

ARIANNA

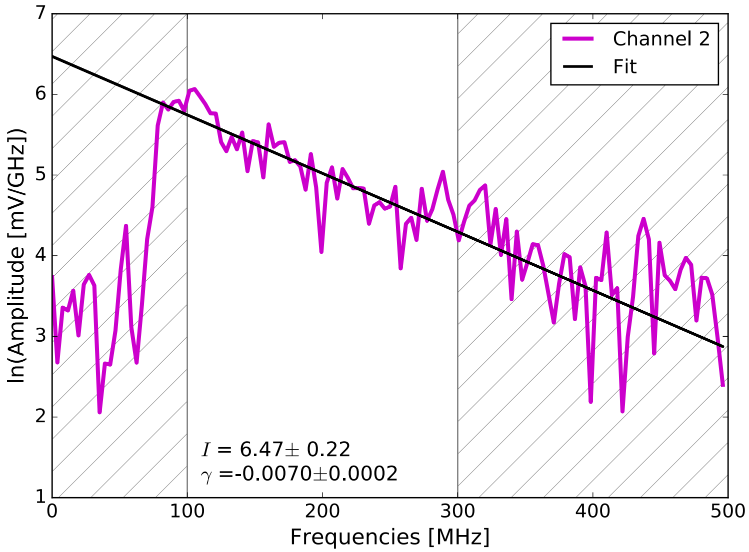

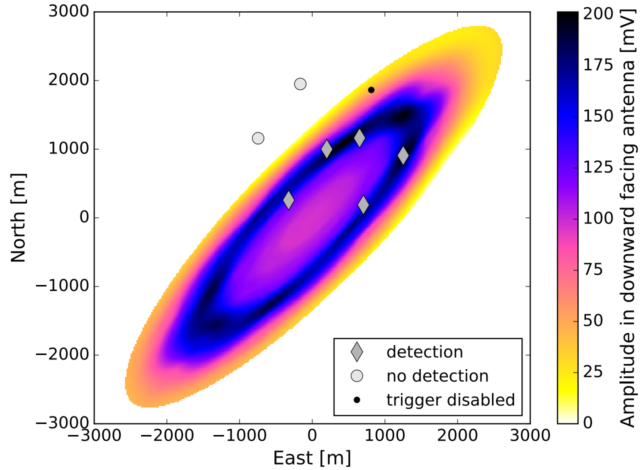

use **slope** **of measured** **frequency spectrum** **to derive** **energy** **and other shower parameters**

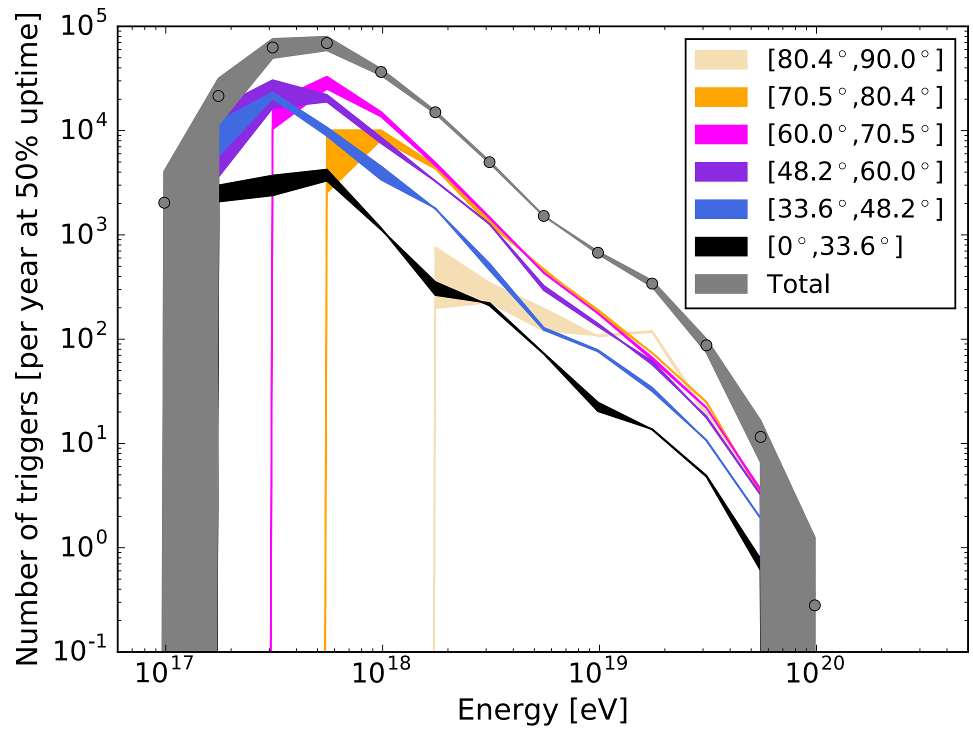

full ARIANNA
36 km² x 36 km²
1296 km²

S.W. Barwick et al., Astropart.Phys. 90 (2017) 50

Extension of scintillator array (LORA)

LOFAR

S. Buitink
K. Mulrey

2.5 km

Existing station
New station

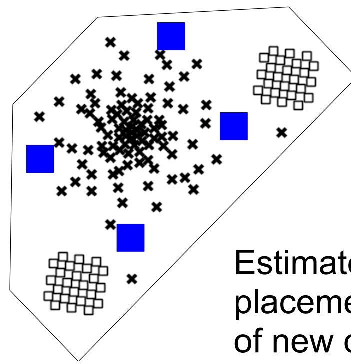

Estimated placement of new detectors

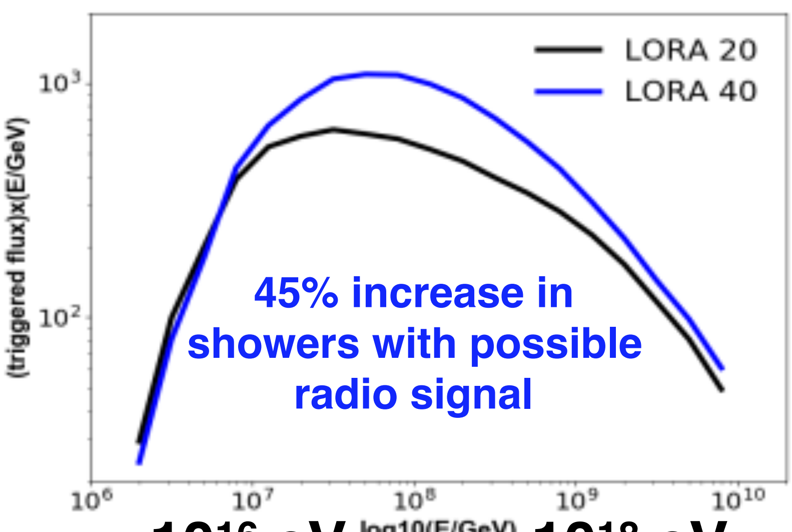

45% increase in showers with possible radio signal

10^{16} eV 10^{18} eV

adding 20 scintillator stations in 2018

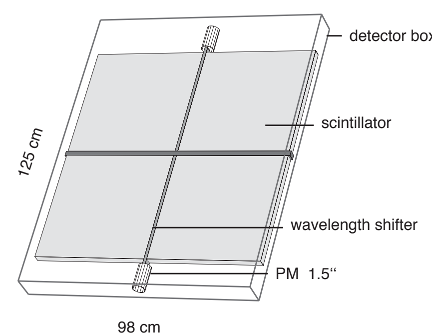

Upgrade of the Pierre Auger Observatory
(astro-)physics of the highest-energy particles in nature

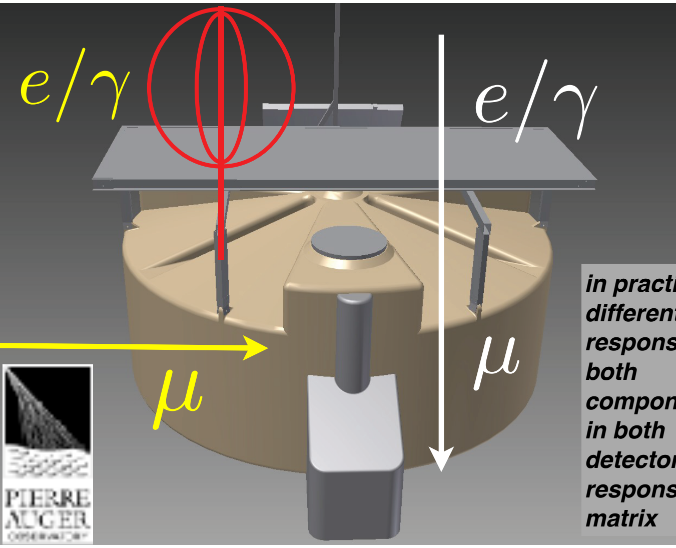

in practice: different response to both components in both detectors: response matrix

upgrade PAO
- electronics
- scintillator layer
- radio detector

Key science questions
- What are the sources and acceleration mechanisms of ultra-high-energy cosmic rays (UHECRs)?
- Do we understand particle acceleration and physics at energies well beyond the LHC (Large Hadron Collider) scale?
- What is the fraction of protons, photons, and neutrinos in cosmic rays at the highest energies?

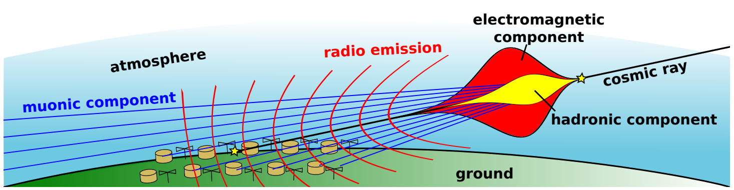

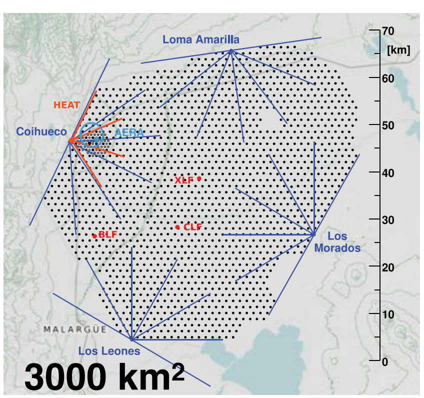

Advanced Grant Hörandel 2018

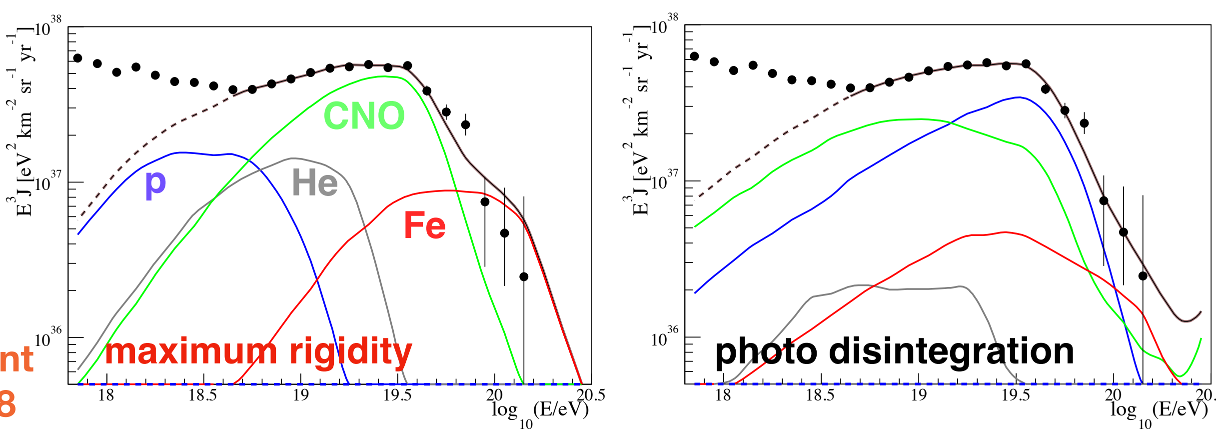

A large radio array the Pierre Auger Observatory

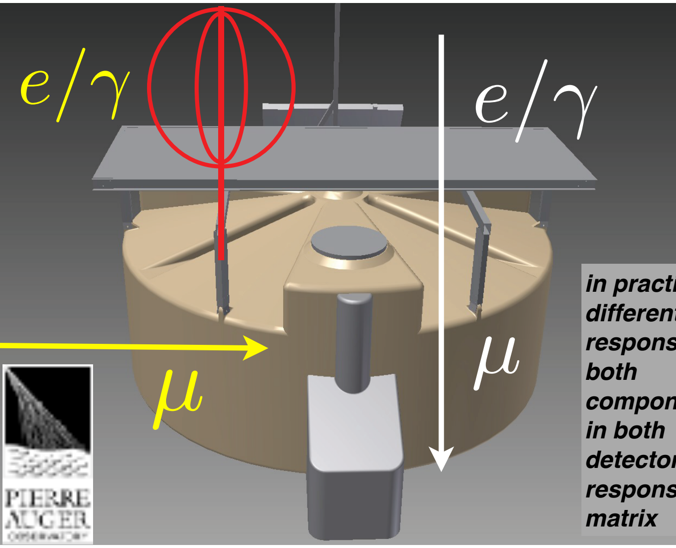

in practice: different response to both components in both detectors: response matrix

objective

- origin of cosmic rays
- type of particle up to highest energies
- isolate protons, photons, neutrinos
- extend e/m-muon separation to high zenith angles
  --> horizontal air showers
  (i.e. increase exposure of SSD analyses)
- increase the sky coverage/overlap with TA
- absolute energy calibration from 1st principles
- independent mass scale
- clean e/m measurement
  --> shower physics

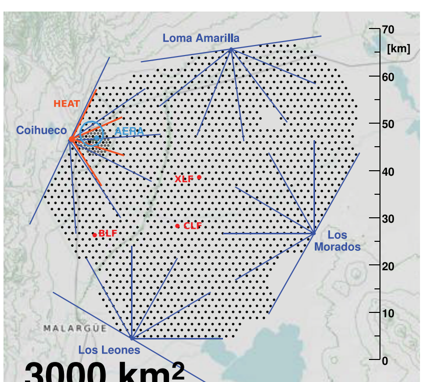

Advanced Grant Hörandel 2018

A large radio array the Pierre Auger Observatory

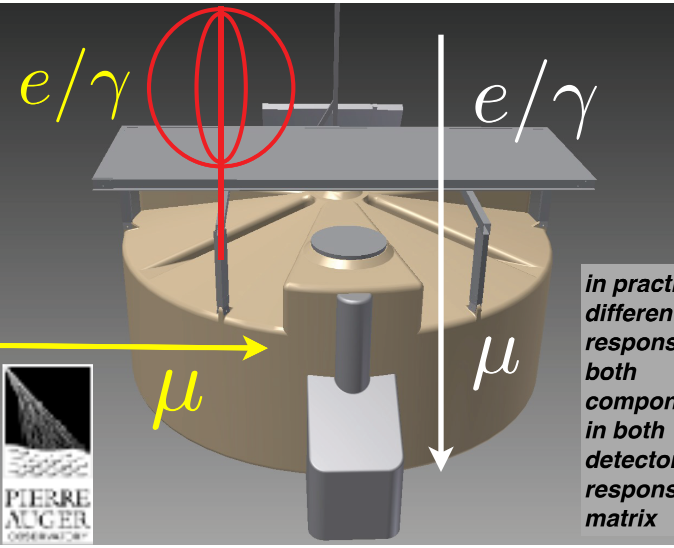

in practice: different response to both components in both detectors: response matrix

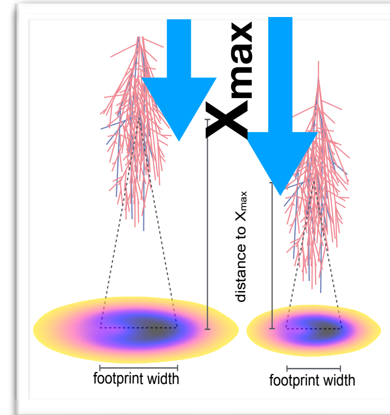

attention:
type of particle determined

for vertical showers:
- size of footprint
- geometrical measurement

for horizontal showers:
- electron/muon ratio
- important: radio emission not absorbed in atmosphere

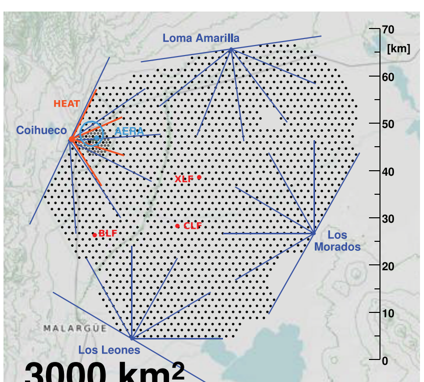

Advanced Grant Hörandel 2018

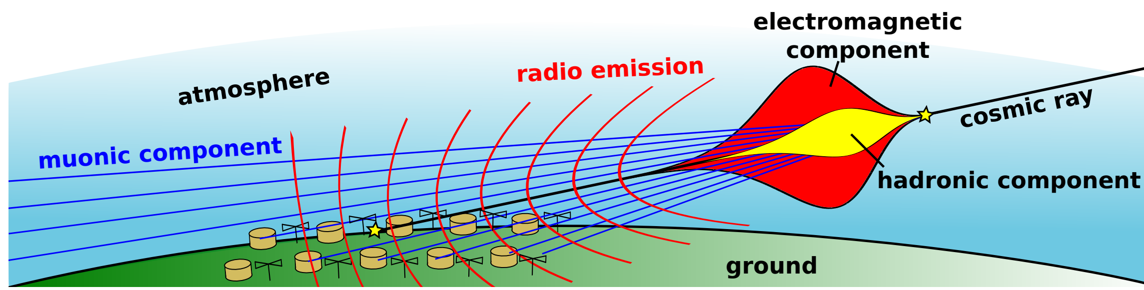

dio detector provides good mass separation

J.R. Hörandel

radio detector (e/m)

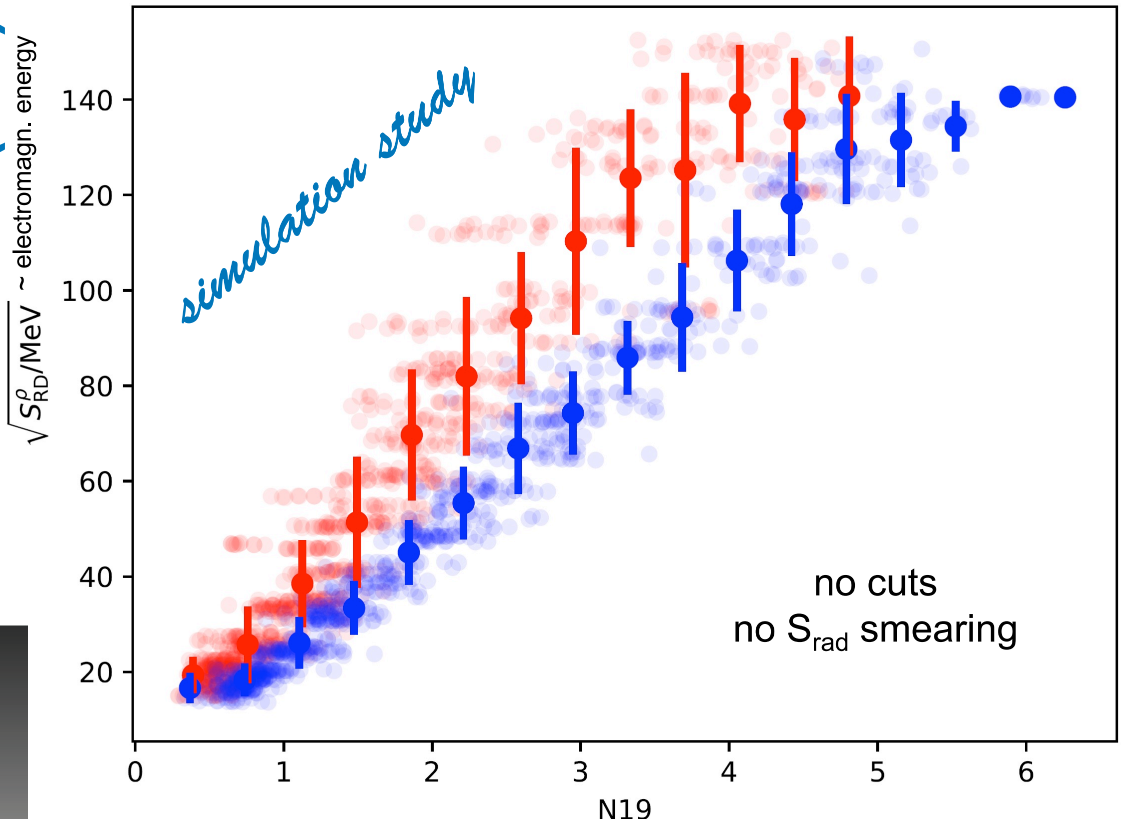

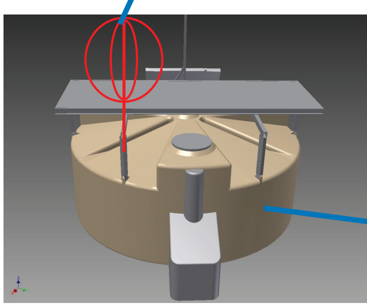

water Cherenkov detector (μ)

- can separate species with S_{rad} and N19
- separation increases with energy
- scaling at highest energies probably artifact of maximum simulated energy

A large radio array at the Pierre Auger Observatory

preparatory work & feasibility

AERA 17 km² --> 3000 km²

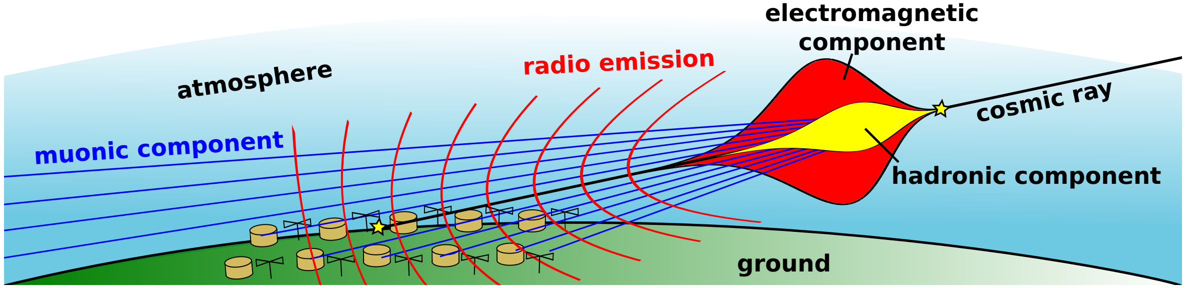

expect large radio footprint from simulations

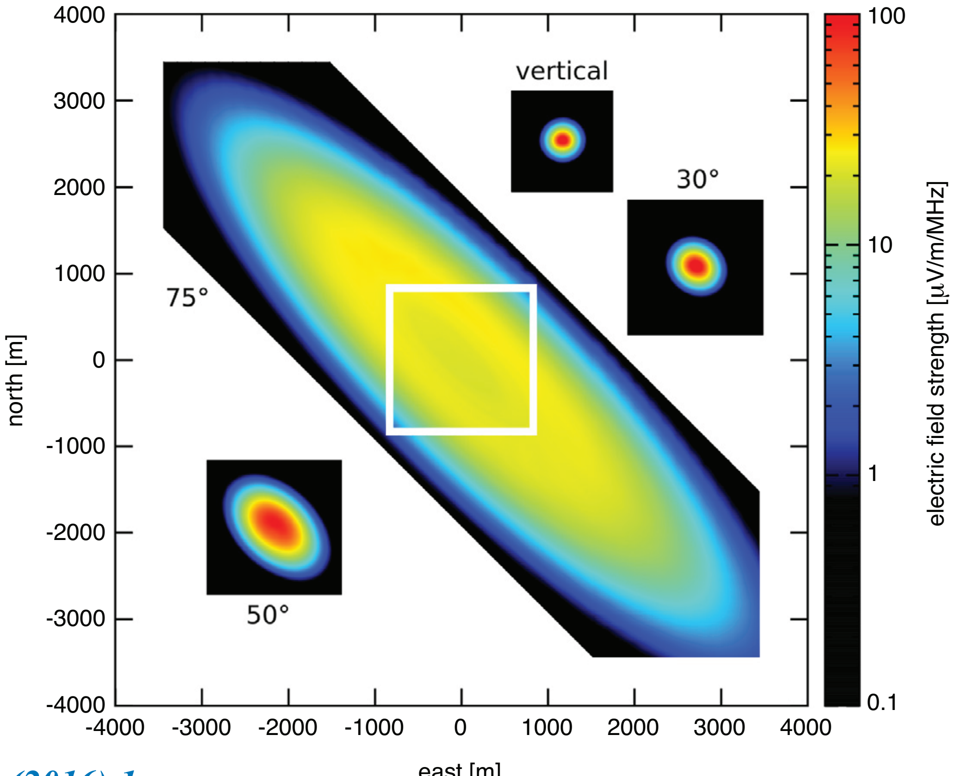

see e.g. T. Huege, Phys. Rep. 620 (2016) 1

A large radio array at the Pierre Auger Observatory

preparatory work & feasibility

AERA 17 km²
--> 3000 km²

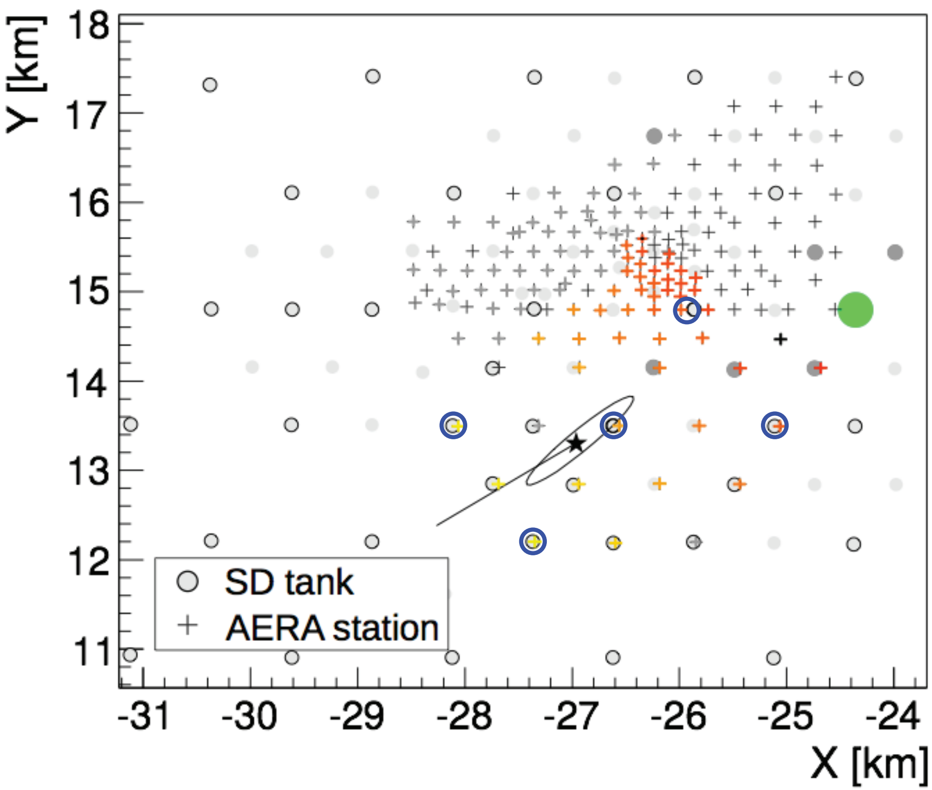

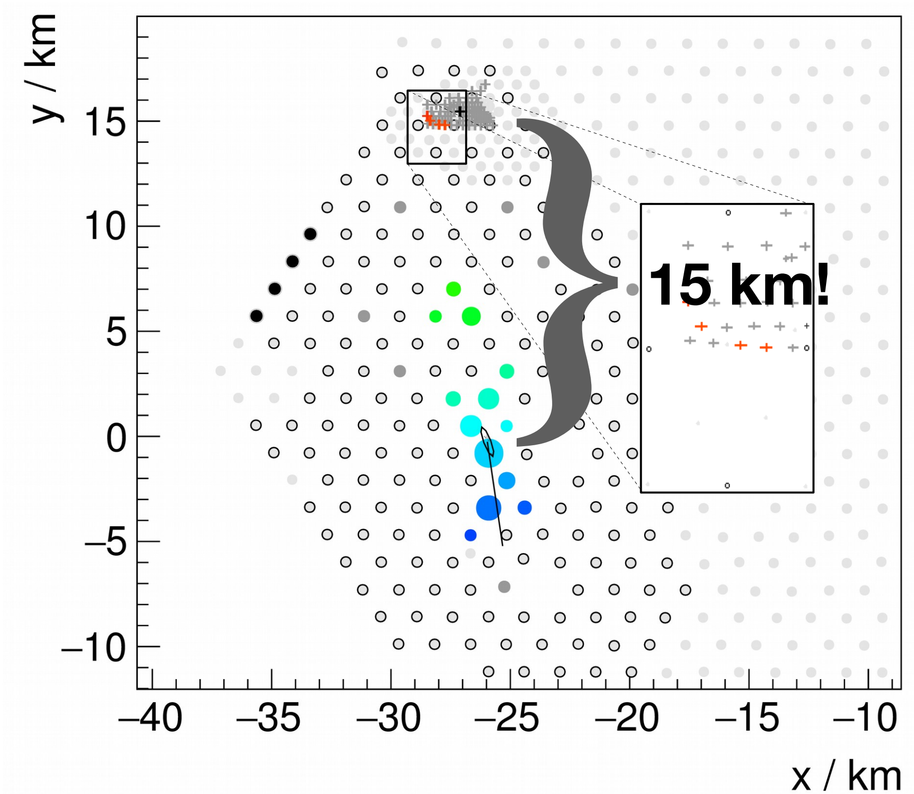

horizontal air showers registered and reconstructed with existing AERA

Pierre Auger coll. submitted (2018) arXiv: 1806.05386

Horizontal air showers have large footprints in radio emission

M. Gottowik

AERA 17 km²
--> 3000 km²

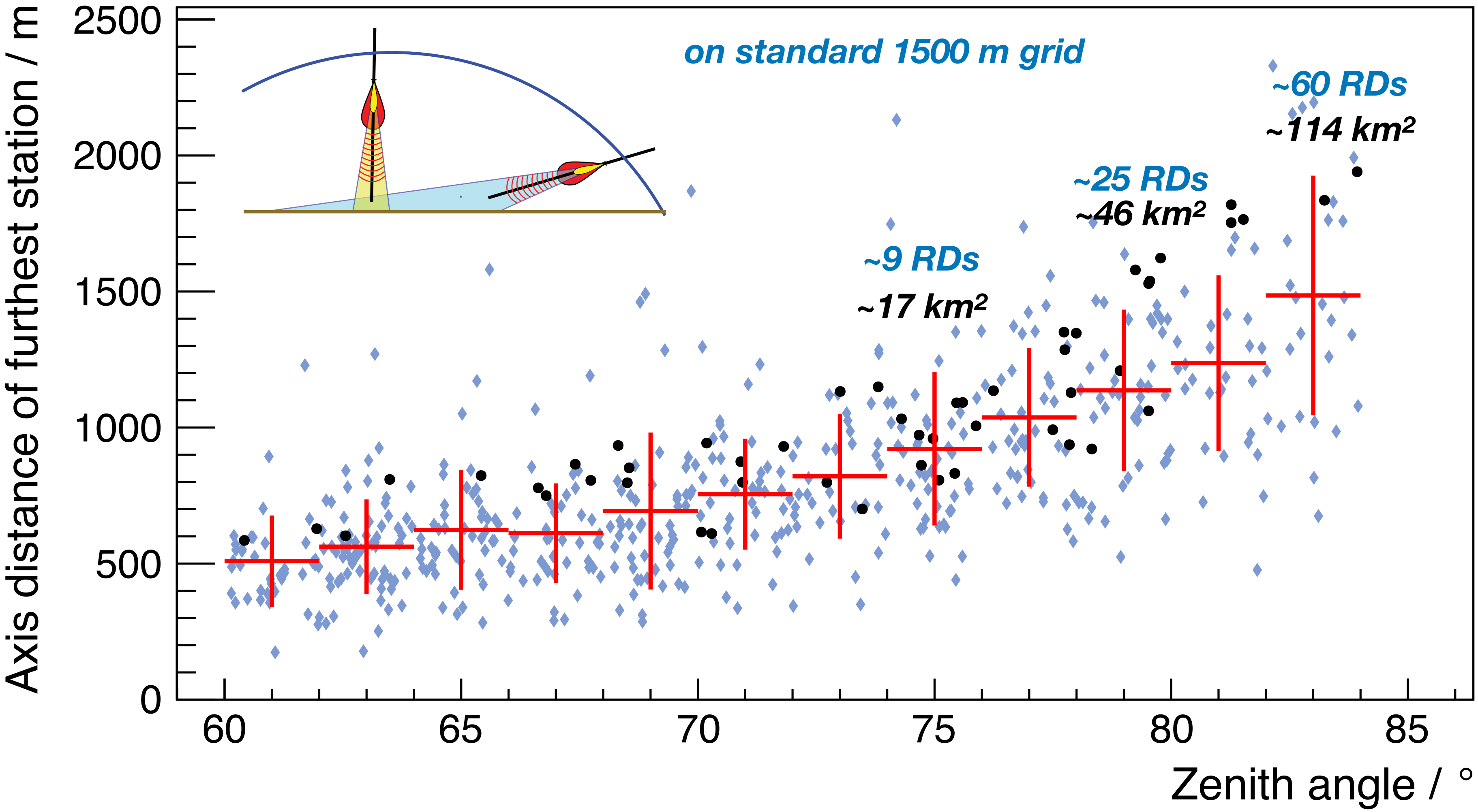

this is MEASURED with the *small* 17km² AERA

Pierre Auger coll. submitted (2018) arXiv: 1806.05386

Radio Antenna - SALLA

Our default antenna is the SALLA antenna.

Well known from Tunka-REX and prototypes at PAO.

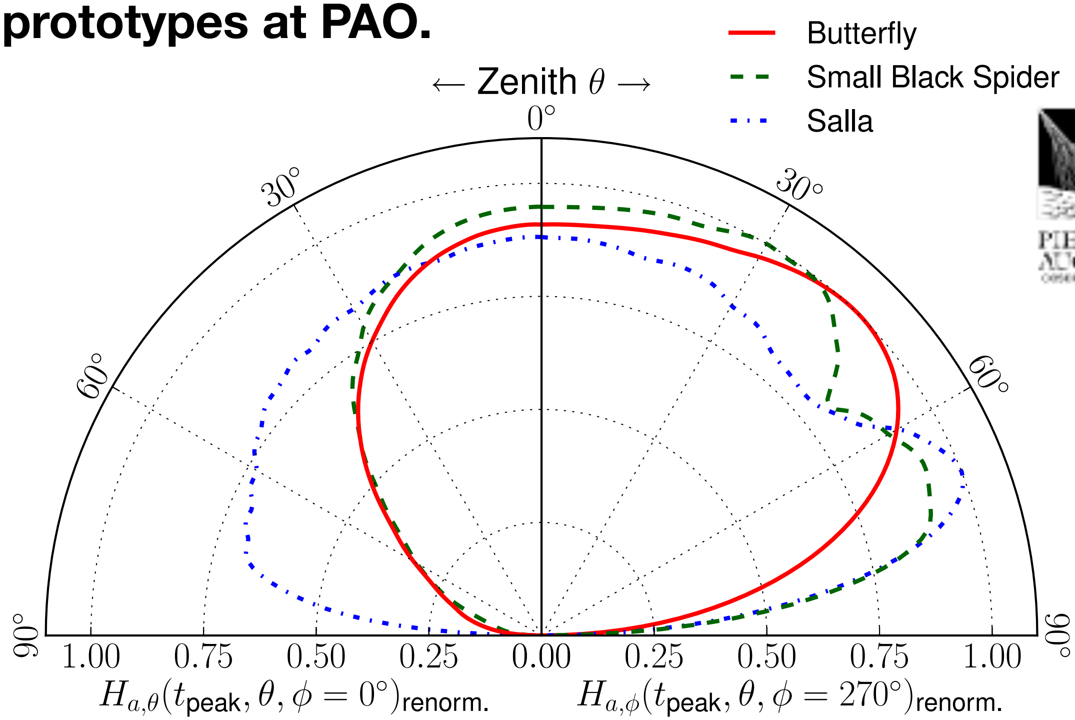

P. Abreu et al., JINST 7 (2012) P10011

measured antenna characteristics

Tunka-REX - 63 stations

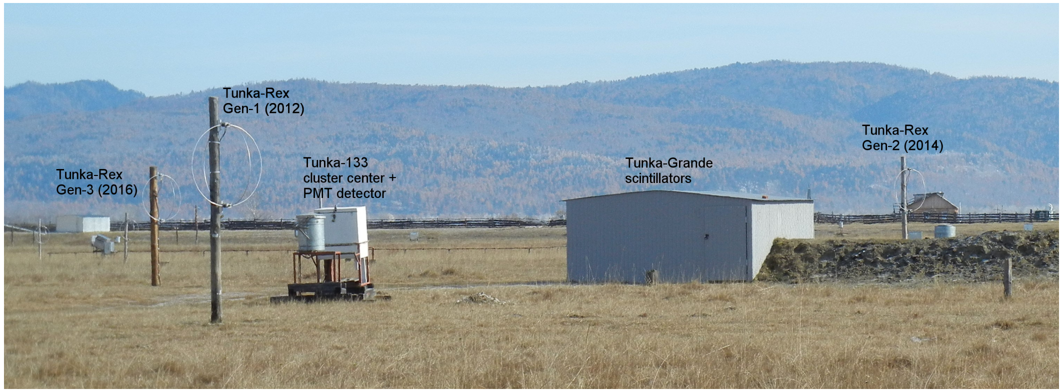

F. Schröder et al, PoS ICRC2017, 459

mechanical mounting: 1st prototype in place